Escola Tècnica Superior d'Enginyeria de Telecomunicació de Barcelona

UNIVERSITAT POLITÈCNICA DE CATALUNYA

Final Research Project

Local Binary Patterns applied to Face Detection and Recognition

Laura Sánchez López

November 2010

Directors: **Francesc Tarrés Ruiz**
Antonio Rama Calvo

Department: **Signal Theory & Communication Department**

Abstract

Nowadays, applications in the field of surveillance, banking and multimedia equipment are becoming more important, but since each application related to face analysis demands different requirements on the analysis process, almost all algorithms and approaches for face analysis are application dependent and a standardization or generalization is quite difficult. For that reason and since many key problems are still not completely solved, the face analysis research community is still trying to cope with face detection and recognition challenges.

Although emulating human vision system would be the ideal solution, it is a heuristic and complicated approach which takes into account multiple clues such as textures, color, motion and even audio information. Therefore, and due to the fast evolution of technology that makes it possible, the recent trend is moving towards multimodal analysis combining multiple approaches to converge to more accurate and satisfactory results.

Contributions to specific face detection and recognition applications are helpful to enable the face analysis research community to continue building more robust systems by concatenating different approaches and combining them. Therefore, the aim of this research is to contribute by exploring the *Local Binary Patterns* operator, motivated by the following reasons. On one hand, it can be applied to face detection and recognition and on the other hand due to its robustness to pose and illumination changes.

Local Binary Patterns were first used in order to describe ordinary textures and, since a face can be seen as a composition of micro textures depending on the local situation, it is also useful for face description. The LBP descriptor consists of a global texture and a local texture representation calculated by dividing the image into blocks and computing the texture histogram for each one. The global is used for discriminating the most non-face objects (blocks), whereas the second provides specific and detailed face information which can be used not only to select faces, but also to provide face information for recognition.

The results will be concatenated in a general descriptor vector, that will be later used to feed an adequate classifier or discriminative scheme to decide the face likeness of the input image or the identity of the input face in case of face recognition. It is in that stage where this research will focus, first evaluating more simple classification methods and then trying to improve face detection and recognition ratios by trying to eliminate features vector redundancy.

Contents

Index of Tables

Index of Figures

Chapter 1

Introduction

Face detection and recognition are playing a very important role in our current society, due to their use for a wide range of applications such as surveillance, banking and multimedia equipment as cameras and video game consoles to name just a few.

Most new digital cameras have a face detection option for focusing faces automatically. Some companies have even gone further, like a well-known brand, which has just released a new functionality not only for detecting faces but also for detecting smiles by analyzing "*happiness*" using facial features like mouth, eye lines or lip separation, providing a new "*smile shutter*" feature which will only take pictures if persons smile.

In addition, most consumer electronic devices such as mobile phones, laptops, video game consoles and even televisions include a small camera enabling a wide range of image processing functionalities including face detection and recognition applications. For instance, a renowned TV manufacturer has built-in a camera to some of their television series to make a new feature called *Intelligent Presence Sensor* possible. The users' presence is perceived by detecting faces, motion, position and even age, in the area in front of the television and after a certain time with no audience, the set turns off automatically, thus saving both energy and TV life.

On the other hand, other demanding applications for face detection and recognition are in the field of automatic video data indexing to cope with the increase of digital data storage. For example, to assist in the indexing of huge television contents databases by automatically labeling all videos containing the presence of a given individual.

In a similar way, face detection and recognition techniques are helpful for *Web Search Engines* or consumers' picture organizing applications in order to perform automatic face image searching and tagging. For instance, *Google's Picasa* digital image organizer has a built-in face recognition system that can associate faces with people, so that queries can be run on pictures to return all images with a specific group of people together. Another example is *iPhoto*, a photo organizer distributed with *iLife* that uses face detection to identify faces of people in photos and face recognition to match faces that look like the same person.

After four decades of research and with today's wide range of applications and new possibilities, researchers are still trying to find the algorithm that best works in different illuminations, environments, over time and with minimum error.

This work pretends to explore the potential of a texture descriptor proposed by researches from the *University of Oulu* in Finland [1]-[7]. This texture face descriptor is called *Local Binary Patterns* (LBP) and the main motivations to study it in this work are:

- Low computation complexity of the LBP operator.
- It can be applied for both detection and recognition.
- Robustness to pose and illumination changes.

Local Binary Patterns were first used in order to describe ordinary textures where the spatial relation was not as significant as it is for face images. A face can be seen as a composition of micro textures depending on the local situation. The LBP is basically divided into two different descriptors: a global and a local. The global is used for discriminating the most non-face objects (blocks), whereas the second provides specific and detailed face information which can be used not only to select faces, but also to provide face information for recognition.

So the whole descriptor consists of a global texture and a local texture representation calculated by dividing the image into blocks and computing the texture histogram for each one. The results will be concatenated in a general descriptor vector. In such representation, the texture of facial regions is encoded by the LBP while the shape is recovered by the concatenation of different local histograms.

Afterwards, the feature vector will be used to feed an adequate classifier or discriminative scheme to decide the faceness (a measure to determine the similarity of an object to a human face) of the input image or the identity of the input face in case of face recognition.

In the following chapters, a complete system using *Local Binary Patterns* in both face detection and recognition stages will be detailed, implemented and evaluated.

Chapter 2 provides an overview of current *Face Detection* and *Recognition* methods and the most important challenges to better understand the research motivations. *Chapter 3* deals with the *Local Binary Patterns* operator, detailing how to compute it, interpret it and why it is useful for face description.

In *Chapter 4* and *5* the theory for *LBP* application to *Face Detection* and *Recognition* respectively is discussed. The fourth chapter exposes the detection scheme proposal, different classification methods and finally some system improvements such as the use of skin segmentation pre-stage for detection algorithm optimization. In a similar way, the fifth chapter describes the image pre-processing phase for face recognition and the proposed identification scheme.

Before beginning with the empirical phase, *Chapter 6* is dedicated to presenting the face databases used and their adaptation to the research experiments. *Chapter 7* then describes the experiments conducted, beginning with an initial section dedicated to skin segmentation, followed by a face detection section and finalized by the face recognition section.

The development tools to obtain the implementation of the proposed classification schemes for the empirical phase, resulting in a complete *Face Processing Tool* application in C++ are presented in *Chapter 8*.

Chapter 9 details the research conclusions providing an overview of the complete proposal, the improvements achieved, problems found during the research and future lines of work.

Finally, the *Appendix* section contains useful additional information to complete and to better understand this research work, such as more detailed information about the image databases, results tables and a description of the used algorithms.

Chapter 2

Face Detection and Recognition: a broad classification

Since over 40 years, facial analysis has been an important research field due its wide range of applications like: law enforcement, surveillance, entertainment like video games and virtual reality, information security, banking, human computer interface, etc.

The original interest in facial analysis relied on face recognition, but later on the interest in the field was extended and research efforts where focused in the appearance of model-based image, video coding, face tracking, pose estimation, facial expression, emotion analysis and video indexing, as it has been shown in the previous chapter.

Currently, face detection and recognition are still a very difficult challenge and there is no unique method that provides a robust and efficient solution to all situations face processing may encounter. In some controlled conditions, face detection and recognition are almost solved or at least present a high accuracy rate but in some others applications, where the acquisition conditions are not controlled, face analysis still represents a big challenge. In this section, a brief overview of the main algorithms together with the most representative challenges for face detection and recognition are presented.

2.1. Face Detection

In most cases, these research areas presume that faces in an image or video sequence have been already identified and localized. Therefore, in order to build a fully automated system a robust and efficient face detection method is required, being an essential step for having success in any face processing application.

Face detection is a specific case of object-class detection, which main task is to find the position and size of objects in an image belonging to a given class. Face detection algorithms were firstly focused in the detection of frontal human faces, but nowadays they attempt to be more general trying to solve face multi-view detection: in-plane rotation and out-of-plane rotation. However, face detection is still a very difficult challenge due to the high variability in size, shape, color and texture of human faces.

Generally, face detection algorithms implement face detection as a binary pattern classification task. That means, that given an input image, it is divided in blocks and each block is transformed into a feature. Features from class face and non face are used to train a certain classifier. Then given a new input image, the classifier will be able to decide if the sample is a face or not.

Going deeply, face detection methods can be classified in the following categories:

- **Knowledge-based methods**: these techniques are based in rules that codify human knowledge about the relationship between facial features (*Yang [15]*).

- **Feature invariant techniques** (e.g. facial features (*Yow & Cipolla* [16]), texture and multiple features): they consist of finding structural features that remain invariant regardless of pose variations and lighting condition.
- **Template matching methods** (e.g. predefined templates and deformable templates (*Yuille* [17])): these approaches are based in the use of a standard face pattern that can be either manually predefined or parameterized by means of a function. Then, face detection consists of computing the correlations between the input image and the pattern.
- **Appearance-based methods** (e.g. Neural Networks (*Juell* [18]), Support Vector Machine (*Schulze* [20]), Hidden Markov Models *(Rabiner* [21]) and Eigenfaces (*Turk & Pentland* [22])): contrary to models searching techniques, appearance-based models or templates are generated training a collection of images containing the representative variations of face class.
- **Color-based methods**: these techniques are based on the detection of pixels which have similar color to human skin. For this propose, different color spaces can be used (*Zarit* [23]): RGB, normalized RGB, HSV, CIE-xyz, CIE-LUV, etc.
- **AdaBoost face detector**: the Adaptive Boosting (*Viola & Jones* [24]) method consists of creating a strong face detector by forming an ensemble of weak classifiers for local contrast features found in specific positions of the face.
- **Video-based approaches** (e.g. color-based, edge-based, feature-based, optical flow-based (*Lee* [25]), template-based and Kalman filtering-based face tracking (*Qian* [26])): this kind of face detectors exploits the temporal relationship between frames by integrating detection and tracking in a unified framework. Then, human faces are detected in the video sequence, instead of using a frame-by-frame detection.

Obviously, these categories are interrelated between them and they can be combined in order to improve face detection ratios. The compromise consists of using as much uncorrelated elements as possible without penalizing computing time.

In order to compare different methods, different parameters can be used in face detection systems. Normally, the algorithm performance is compared by means of the *detection ratio* and *false alarm ratio*. Then, general errors in face detection schemes are:

- *False negative*: face not correctly detected, due to a *low detection ratio*.
- *False positive*: non face detected as face, due to a *high false alarm ratio*.

This project analyses a face detection method based on *Local Binary Patterns* which can be considered as an *appearance-based method.* This kind of methods normally obtain good results, due to the fact that depending on the variability of the images/samples collection the face detection and false alarm ratios can be adjusted. Moreover, these methods are efficient in the detection and the computing cost is lower compared with other techniques.

2.2. Face Recognition

Nowadays, automatic people's face recognition is a challenging task which receives much attention as a result of its many applications in fields such as security applications, banking, law enforcement or video indexing.

The task of face recognition in still images consists of identifying persons in a set of test images with a system that has been previously trained with a collection of face images labeled with each person identity.

Face recognition can be divided in following basic applications, although the used techniques are basically the same:

- **Identification**: an unknown input face is to be recognized matching it against faces of different known individuals database. It is assumed that the person is in the database.
- **Verification**: an input face claims an identity and the system must confirm or rejects it. The person is also a member of the database.
- **Watch List**: an input face, presented to the system with no claim of identity, is matched against all individuals in database and ranked by similarity. The individual identity is detected if a given threshold is surpassed and if not is rejected.

Different strategies and schemes try to solve face recognition problem. The classification of these approaches into different categories is not easy because different criteria can be taken into account. But one of the most popular and general classification schemes is the following one:

- **Holistic methods**: based in face overall information, this kind of methods try to recognize faces in an image using the whole face region as an input, treating the face as a whole. For instance, statistical approaches use statistical parameters to create a specific face model or space to be used for the recognition stage. The training data is used to create a face space where the test faces can be mapped and classified.
- **Feature-based methods**: non-holistic methods based in identifying structural face features such as the eyes, mouth and nose, and the relations between them to make the final decision. First feature matching strategies were based on the manually definition of facial points and the computation of the geometric distances between them, resulting in a feature grid for people identification. Recent evolved algorithms place the facial points automatically and create an elastic graph (*Elastic Graph Matching, Lades [27]*) in order to resolve previous algorithms' insensitivity to pose variations.
- **Hybrid methods**: hybrid approaches try to take advantage of both techniques.
- **Neural network algorithms:** this technique (*Viennet* [19]) can be considered as statistical approach (holistic method), because the training procedure scheme usually searches for statistical structures in the input patterns. However, due to the fact that it is based on human brain biological understanding, a conceptually different principle, neural networks can be classified as separately approach.

2.3. Challenges

In order to better understand the face detection and recognition task and its difficulties, the following factors must be taken into account, because they can cause serious performance degradation in face detection and recognition systems:

- Pose: face images vary due to relative position between camera and face and some facial features like the eyes or the nose can be partially o totally hidden.
- Illumination and other image acquisition conditions: face aspect in an image can be affected by factors such as illumination variations, in its source distribution and intensity, and camera features such as sensor response and lenses. Differences produced by these factors can be greater than differences between individuals.
- Occlusions: faces can be partially occluded by other objects (beards, moustaches and glasses) and even by faces from other people.
- Facial expressions: facial appearance can be directly affected by the facial expression of the individual.

Moreover, the following factors are specific from **face detection** task and basically related to computational efficiency that demands, for example, to spend as shortest time as possible exploring non-face image areas.

- Faces per image: normally faces rarely appear in images. 0 to 10 faces are to be found in an image.
- Scanning areas: the sliding window for image exploration evaluates a huge number of location and scale combinations and directly depends on the selected:
    - scanning step (for location exploration)
    - downsampling ratio (for scale exploration)

On the other hand, **face recognition** specific challenges:

- Images taken years apart: facial appearance can considerably change over the years, driving to *False Reject* errors that can provoke the access deny of legitimate users.
- Similar identities: biometric recognition systems are susceptible of *False Accept* errors where an impostor with a similar identity can be accepted as a legitimate user.

In some case, the training data used for face detection and recognition systems are frontal view face images, but obviously, some difficulties appear when trying to analyze faces with different pose angles. Therefore, some processing schemes introduce rotated images in their training data set and other try to identify particular features of the face such as the eyes, mouth and nose, in order to improve positive ratios.

After giving a general overview of the different methods, this work has been focused on a technique based in the use of the LBP operator which can be used for both face detection and recognition, motivated by its robustness to pose and illumination changes and due to its low computation complexity. Next chapter will explain in detail how LBP can be used for both tasks.

Chapter 3

Local Binary Patterns

This chapter introduces a discriminative feature space that can be applied for both face detection and recognition challenges, motivated by its invariance with respect to monotonic gray scale transformations (i.e. as long as the order of the gray values remains the same, the LBP operator output continues constant, see [37]) and the fact that it can be extracted in a single scan trough the whole image.

Local Binary Patterns (LBP) is a texture descriptor that can be also used to represent faces, since a face image can be seen as a composition of micro-texture-patterns.

Briefly, the procedure consists of dividing a facial image in several regions where the LBP features are extracted and concatenated into a feature vector that will be later used as facial descriptor.

3.1. Texture Descriptor

The LBP originally appeared as a generic texture descriptor. The operator assigns a label to each pixel of an image by thresholding a 3x3 neighborhood with the centre pixel value and considering the result as a binary number. In different publications, the circular 0 and 1 resulting values are read either clockwise or counter clockwise. In this research, the binary result will be obtained by reading the values clockwise, starting from the top left neighbor, as can be seen in the following figure.

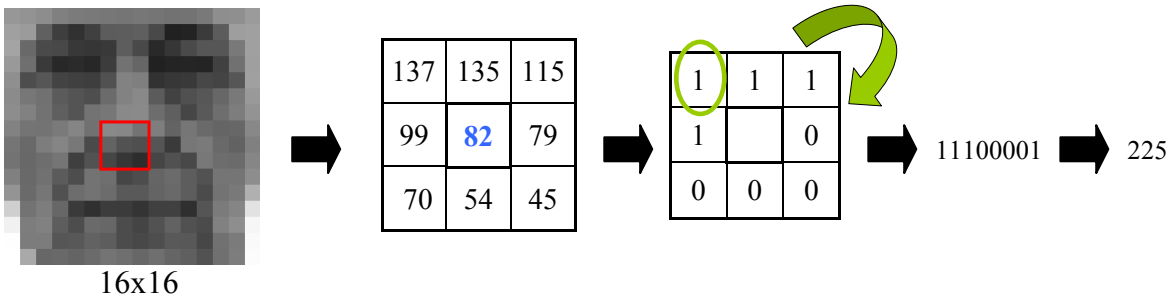

Figure 1. *LBP labeling: binary label is read clockwise starting from top left neighbor.*

In other words, given a pixel position (x_c, y_c), LBP is defined as an ordered set of binary comparisons of pixel intensities between the central pixel and its surrounding pixels. The resulting decimal label value of the 8-bit word can be expressed as follows:

$$LBP(x_c, y_c) = \sum_{n=0}^{7} s(l_n - l_c)2^n \tag{1}$$

where l_c corresponds to the grey value of the centre pixel (x_c, y_c), l_n to the grey values of the 8 surrounding pixels, and function *s(k)* is defined as:

$$s(k) = \begin{cases} 1 & if \quad k \geq 0 \\ 0 & if \quad k < 0 \end{cases} \tag{2}$$

3.2. Local Binary Patterns Extension

In order to treat textures at different scales, the LBP operator was extended to make use of neighborhoods at different sizes. Using circular neighborhoods and bilinear interpolation of the pixel values, any radius and number of samples in the neighborhood can be handled. Therefore, the following notation is defined:

(P, R) which means ***P*** sampling points on a circle of ***R*** radius.

The following figure shows some examples of different sampling points and radius:

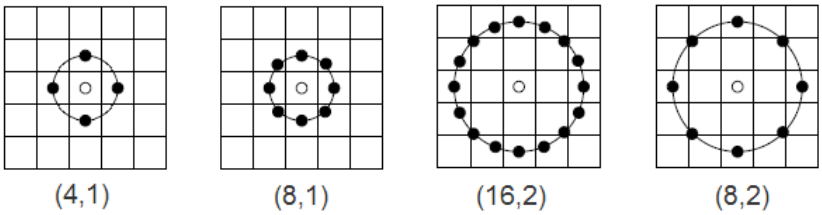

Figure 2. *LBP different sampling point and radius examples.*

In $LBP_{(4,1)}$ case, the reason why the four points selected correspond to vertical and horizontal ones, is that faces contain more horizontal and vertical edges than diagonal ones.

When computing pixel operations taking into account *NxN* neighborhoods at the boundary of an image, a portion of the *NxN* mask is off the edge of the image. In such situations, different padding techniques are typically used such as zero-padding, repeating border elements or applying a mirror reflection to define the image boarders. Nevertheless, in LBP operator case, the critical boundary, defined by the radius R of the circular operation, is not solved by using a padding technique, instead of that, the operation is started at image pixel (R, R). The advantage is that the final LBP labels histogram will be not influenced by the borders, although the resulting LBP labels image size will be reduced to (Width-R)x(Height-R) pixels.

3.3. Uniform Patterns

Ojala [7], in his work *Multiresolution gray-scale and rotation invariant texture classification with Local Binary Patterns,* reveals that it is possible to use only a subset of the 2^P local binary patterns to describe textured images. This subset is called **uniform patterns** or **fundamental patterns**.

A LBP is called uniform if the circular binary pattern (clockwise) contains maximal 2 transitions from 0 to 1 and vice versa.

Circular Binary Pattern	# of bitwise transitions	Uniform pattern?
11111111	0	Yes
00001111	1	Yes
01110000	2	Yes
11001110	3	No
11001001	4	No

Table 1. *Example of uniform and non uniform Local Binary Patterns*

Each of these patterns has its own bin in the LBP histogram. The rest of the patterns with more than 2 transitions will be accumulated into a single bin. In our experiments the non uniform patterns are accumulated into bin 0.

This type of LBP histogram is denoted $LBP^{u2}_{(P,R)}$, containing less than 2^P bins.

Considering the case of having a LBP histogram with P=8 and u2, 8 bit binary labels are obtained with only 58 uniform values from a total of 256 different values. Taking into account that one more bin is needed in order to represent the non uniform patterns, a final 59-bin histogram represents the $LBP^{u2}_{(8,R)}$ histogram. Consequently, a 76.95% reduction in the features vector is achieved.

This reduction is possible due to the fact that the uniform patterns are enough to describe a textured image, as *Ojala* [7] pointed out in his research and as it can be observed in the following three tables showing the total uniform patterns present in different textured images cases.

At a glance, it can be clearly observed that textured images are mainly composed by uniform patterns (~80%), therefore in the LBP histogram it makes sense to assign individual bins to the uniform patterns and to group less representative pattern (non-uniform) in one unique bin.

Following values stand for $LBP^{u2}_{(8,1)}$ extracted from 16x16 images collected from Internet.

16x16 Images	Number of samples	% Uniform patterns in the image
Faces	6650	81,29 %
Non Faces	4444432	82,49 %

Table 2. *Percentage of uniform patterns in $LBP_{(8,1)}^{u2}$ case using 16x16 images*

Above results are very similar to the ones obtained by ***Ojala*** **[7]** in his experiments with textured images:

LBP case	% Uniform patterns in the image
(8, 1)	90%
(16,2)	70%

Table 3. *Percentage of uniform patterns for different LBP cases: Ojala[7] results*

And also similar to the ones reached by **T.Ahonen [1]** using FERET database and 19x19 images:

LBP case	% Uniform patterns in the image
(8, 1)	90.6%
(8,2)	85.2%

Table 4. *Percentage of uniform patterns for different LBP cases: T.Ahonen [1] results with FERET DB*

The example below is intended to clarify the LBP histogram computation procedure by detailing the $LBP^{u2}_{(8,1)}$ histogram extraction of a 16x16 Internet face image:

1. For each pixel in the image the $LBP_{(8,1)}$ operator is extracted. Notice that image borders are ignored due to the fact that a 3x3 neighborhood is required. Therefore, a

resulting 14x14 $LBP_{(8,1)}$ labels image is obtained. Observe that black values (0 grey level) correspond to non uniform label and white values (255 grey level) to the 0 bitwise transitions label ('11111111' or '00000000')

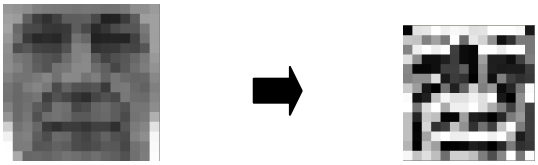

Figure 3. *$LBP_{(8,1)}$ extraction from 16x16 face image results in 14x14 labels image*

2. Then 59-bin $LBP^{u2}_{(8,1)}$ histogram is computed by accumulating all non uniform patterns with more than 2 transitions in bin 0, then, the rest of uniform patterns are accumulated in a dedicated bin. See *Figure 4* to have an overview of how the uniform patterns are placed in the labels histogram

Uniform Label (decimal)	Uniform Label (binary)	Number of Transitions	$LBP^{u2}_{(8,R)}$ histogram bin
non uniform patterns	non uniform patterns	>2	0
0	00000000	0	1
1	00000001	1	2
2	00000010	2	3
3	00000011	1	4
4	00000100	2	5
⋮	⋮	⋮	⋮
251	11111011	2	54
252	11111100	1	55
253	11111101	2	56
254	11111110	1	57
255	11111111	0	58

Figure 4. *LBP labels and their corresponding bin in the final 59-bin $LBP^{u2}_{(8,R)}$ histogram*

Next *Figure 5* shows the resulting 59-bin $LBP^{u2}_{(8,1)}$ histogram, where the highest pick (bin 0, the first one) that corresponds to the non uniform patterns is the 18.75% of values of the 14x14 total labels. Consequently, the 81.25% stands for uniform values. Moreover, it is interesting to notice that the second important pick in the histogram (bin 58, the last one) is the 5.85% of histogram labels and corresponds to the 255 label with 0 bitwise transitions ('11111111').

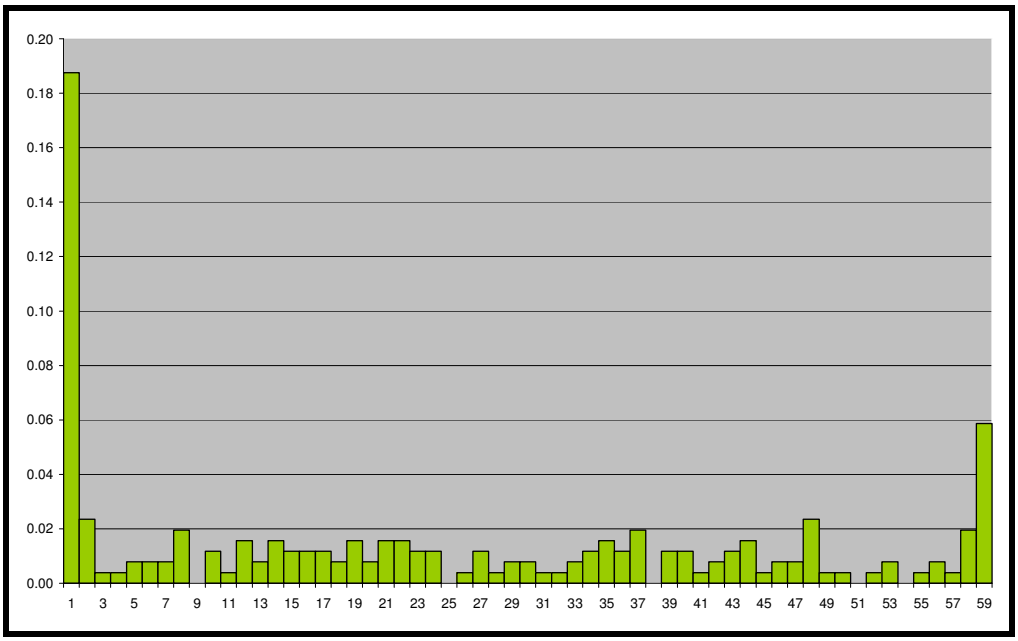

Figure 5. *59-bin $LBP_{(8,1)}^{u2}$ histogram from a 16x16 Internet face image.*

Chapter 4

Local Binary Patterns applied to Face Detection

In this chapter, *Local Binary Patterns* application to face detection is considered, as the facial representation in a face detection system.

In order to improve algorithm efficiency and speed, two stages face detection scheme will be introduced in next *section 4.2*: a first coarse stage to preselect face candidates and a second fine stage to finally determinate the faceness of the input image.

Following *Figure 6* introduces the generic face detection scheme proposed for this research project, including:

- **Training stage** (top box): faces and non-faces training samples are introduce in the system, and feature vectors for 1st coarse and 2nd fine stages are calculated in parallel and later concatenated in a unique *Enhanced Features Vector* of 203-bin to describe each face and non-face image sample. Then, all these results will be used to generate a mean value model for each class.
- **Test stage** (bottom box): for each new test image, skin segmentation pre-processing is firstly applied to improve face detection efficiency. Then the result will feed 1st coarse classification stage and only face candidates will go through 2nd fine classification stage. Just test images with positive results in both stages will be classified as faces.

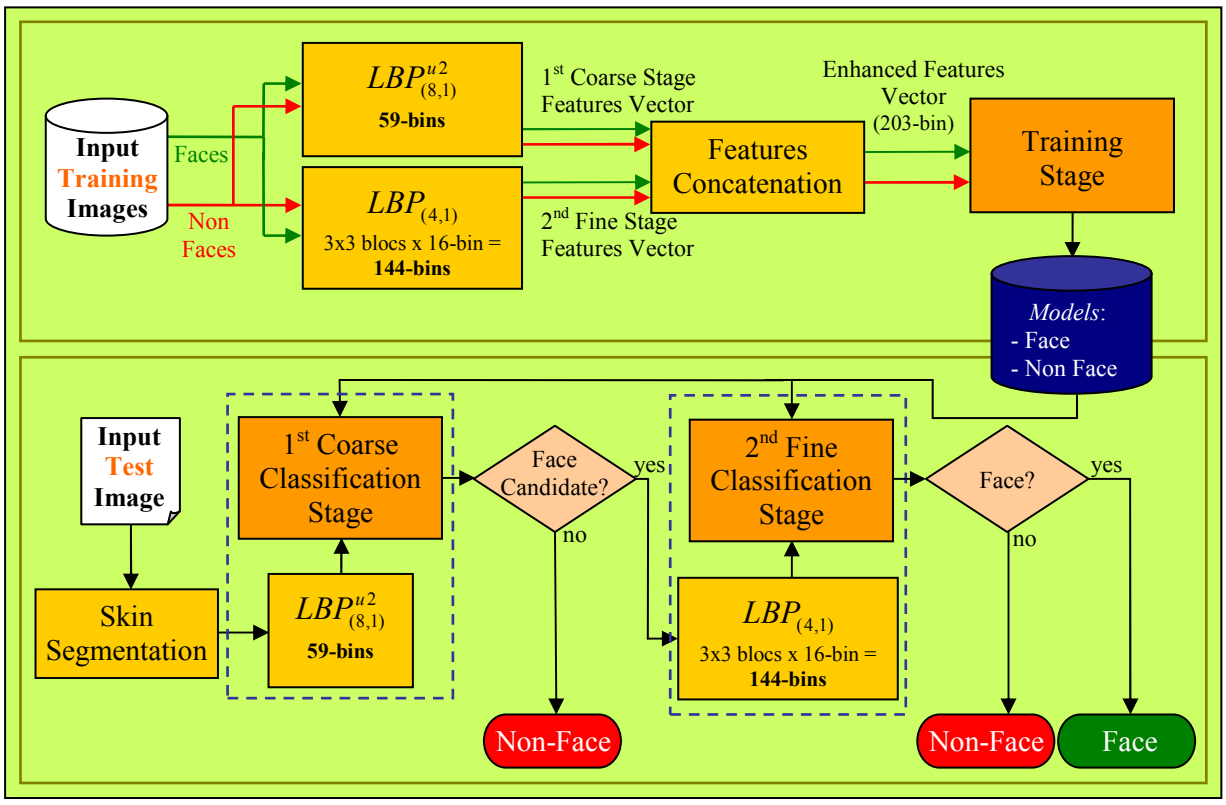

Figure 6. *Face Detection Scheme*

Above block diagram is intended to give an overview of the face detection system, although some processes has been overlooked to simplify it, such as the input image scanning and down-sampling (see section *4.1* and the final overlapping detection removal process (see section *4.4.2.2*).

In each stage, a different part of a 203-bin LBP feature vector is used together with an appropriate classifier. This chapter also introduces different classification methods in order to study LBP face representation potential.

4.1. Image block scanning method

Input image exploration for face candidate searching is done by means of a window-sliding technique applied at a different image scales. As a result, faces can be detected at a different image locations and resolutions.

The following parameters describe the scanning method and have to be decided as a trade-off between face detector resolution and algorithm speed:

- Block size: square or rectangular block that determinates the resolution of the face detector.
- Moving scan step: number of pixels that defines the window-sliding step to get each next block to be analyzed.
- Down-sampling rate: down scale factor for the scaling technique to reach all locations and scales in an image.

Notice that when searching in high resolution images, using a small down-sampling rate and a small moving scan step can considerably slow down the face detection algorithm. The influence of theses parameters are evaluated in more detail in *Appendix III.1.1 Face Detection Computational Cost Analysis*.

4.2. Feature Extraction for Two Stages Face Detection Scheme

Considering the work of *A.Hadid* [5][6] about face detection using LBP, a face detector based on 2 stages is implemented. The main reason to select such a scheme is to improve speed and efficiency detection. Only face candidates extracted from first coarse stage will go through second fine stage (see *Figure 6*).

As it will be explained later in more detail, instead of using NxN pixel values (image size) to describe an image, this new facial representation is proposed to achieve:

1. Dimensionality reduction: only 203 values needed and it is more efficient for low-resolution.
2. Efficiency in the representation of the face towards different challenges like illumination or pose variations.

Image size cases	Number of pixels	Reduction using 203 values
16x16	256	20,70 %
18x21	378	46,29 %
19x19	361	43,76 %

Table 5. *Face descriptor length reduction for the image sizes used in this research*

4.2.1. Coarse Stage Features Extraction

The first stage verifies if the global image appearance can be a face candidate. Therefore, $LBP^{u2}_{(8,1)}$ is extracted from the whole image obtaining a 59-bin labels histogram to have an accurate description of the global image.

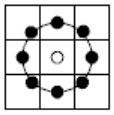

Figure 7. $LBP_{(8,1)}$

4.2.2. Fine Stage Features Extraction

Only positive results from previous step will be evaluated by means of a fine second stage that checks the spatial distribution of texture descriptors.

In this case, $LBP_{(4,1)}$ operator is applied to the whole 16x16 pixel image and a 14x14 result image is obtained.

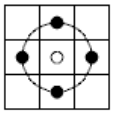

Figure 8. $LBP_{(4,1)}$

Then the resulting image is divided in 3x3 blocks of size 6x6 pixels with 2 pixels overlapping, as shown in *Figure 9*, where the grey block represents the first 6x6 pixel block and the green lines indicate the rest of overlapped blocks (2 pixels overlap).

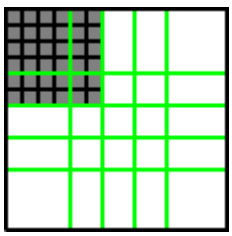

Figure 9. *Face detection – 2nd fine stage – 3x3 blocks division with 2 pixels overlapping*

Using 3x3 blocks division, each block gives a brief description of the local region by means of its 16-bin labels histogram. As a result, an amount of 144 (3x3 x 16-bin) features vector is

obtained from this second fine stage. As it can be later seen, a different weight can be applied to each region in the classification phase to emphasize most important face regions.

In training stage, these 2 resulting labels histograms are concatenated in an enhanced feature vector, resulting in a face representation histogram of:

$$59\text{-bin} + (3\text{x}3 \text{ blocks x } 16\text{-bin}) = 59\text{-bin} + 144\text{-bin} = \mathbf{203\text{-bin}}$$

Next *Figure 10* images show the result of applying local binary patterns in 1st coarse and 2nd fine stages. In result images *(a)* and *(b)*, it can be clearly observed why *LBP*s are called a texture descriptor.

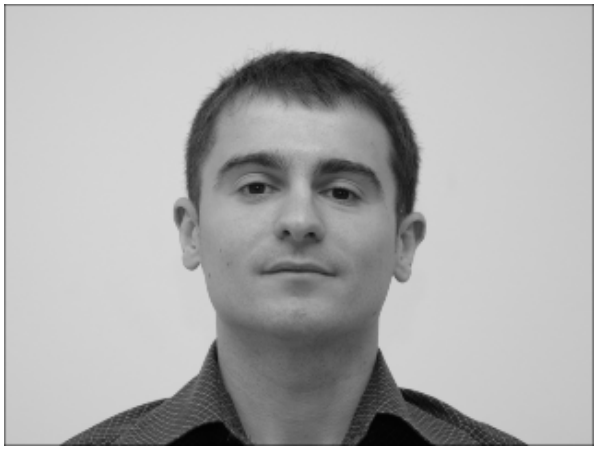

(a) Original image

(b) 1st Stg: $LBP_{(8,1)}$ labels image

(c) 2nd Stg: $LBP_{(4,1)}$ labels image rescaled to 0...255

Figure 10. *Image labeling example*[1]

As shown in *Figure 10*, the contours of the facial features (eyes, mouth, nose, kin, eyebrows…) are clearly remarked. In 1st stage labels image, contours are strongly highlighted giving a general overview of the image faceness being useful to discriminate non-face images in first fast stage. On the other hand, in 2nd stage labels image, local texture information is more detailed being useful for final stage decision where the image faceness is locally evaluated.

[1] Some post processing is applied to $LBP_{(4,1)}$ image in order to enable image visualization: each pixel value (label) is multiplied per 15 to change range from 0…15 to 0…225.

Notice that in 1st stage image, totally uniform textures are represented in white ('11111111') and black ('00000000'), confirming that uniform patterns give essential information when describing face images texture information, as seen in previous *section 3.3*.

Following figures are intended to compare faces and non-faces labels histograms of both stages. *Figure 11* shows in *(a)* a 16x16 pixels face image sample, in *(b)* the result $LBP_{(8,1)}$ labels image and in *(c)* its corresponding histogram with non-uniform patterns accumulated in first bin. Last plot *(d)* represents the 2nd stage labels histogram showing the concatenated 3x3 blocks x 16-bin $LBP_{(4,1)}$ histograms. *Figure 12* shows the same information but calculated for a non-face image sample.

Notice that in case of 1st coarse stage, non-uniform patterns are accumulated in the first bin of the 59-bin labels histogram and in the 2nd fine stage, one bin is dedicated for each possible pattern as uniform and non-uniform are treated equally to obtain more accurate local information.

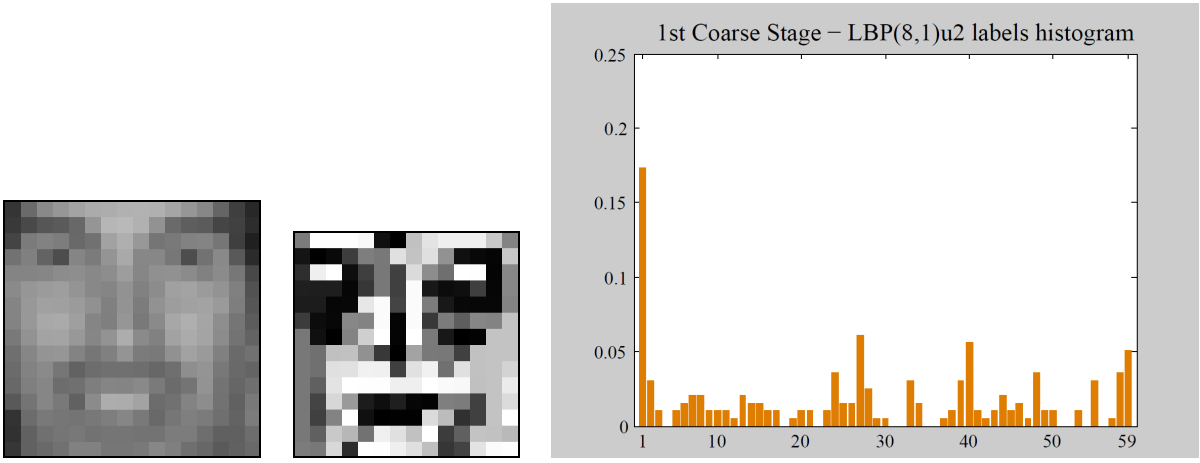

(a) Face sample *(b) 1st Stage $LBP_{(8,1)}$ labels image* *(c) 1st Stage $LBP^{u2}_{(8,1)}$ labels histogram*

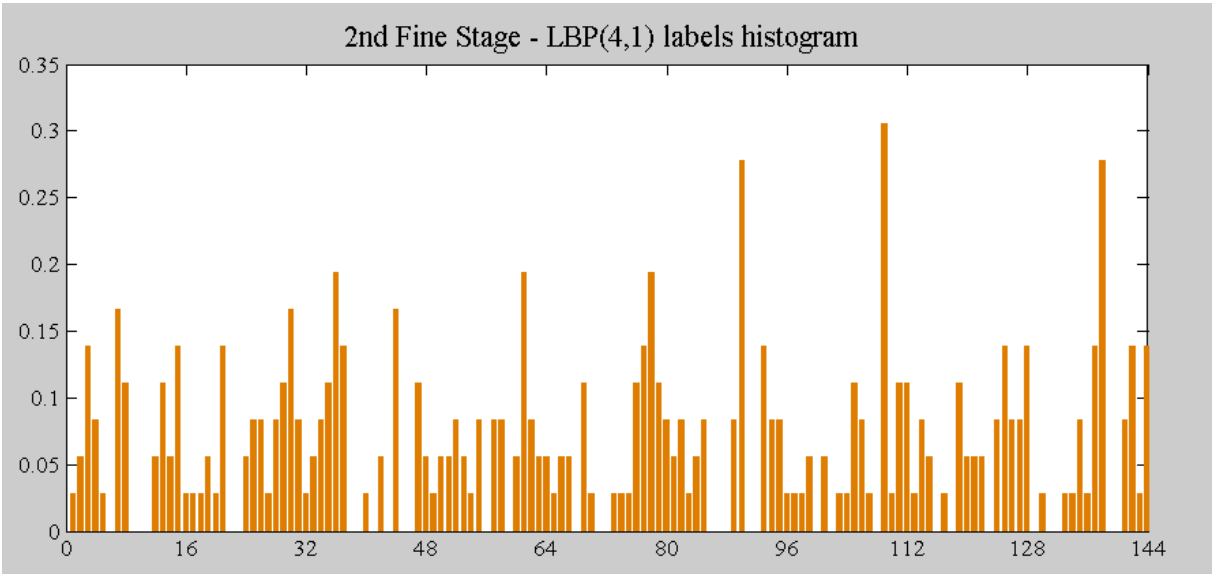

(d) 2nd Stage $LBP_{(4,1)}$ labels histogram

Figure 11. *Face image - Labels histogram example*

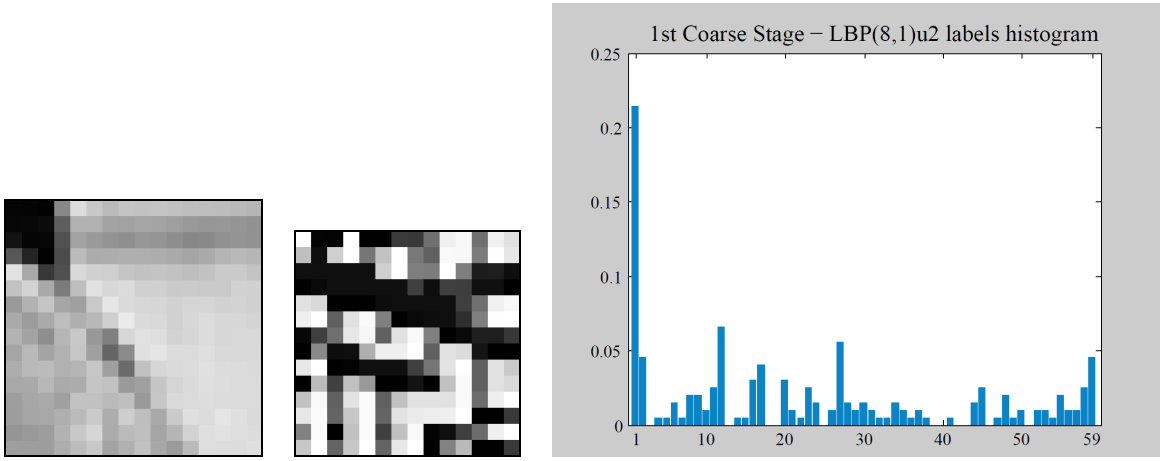

(a) Non-face sample *(b) 1st Stage $LBP^{2}_{(8,1)}$ labels image* *(c) 1st Stage $LBP^{u2}_{(8,1)}$ labels histogram*

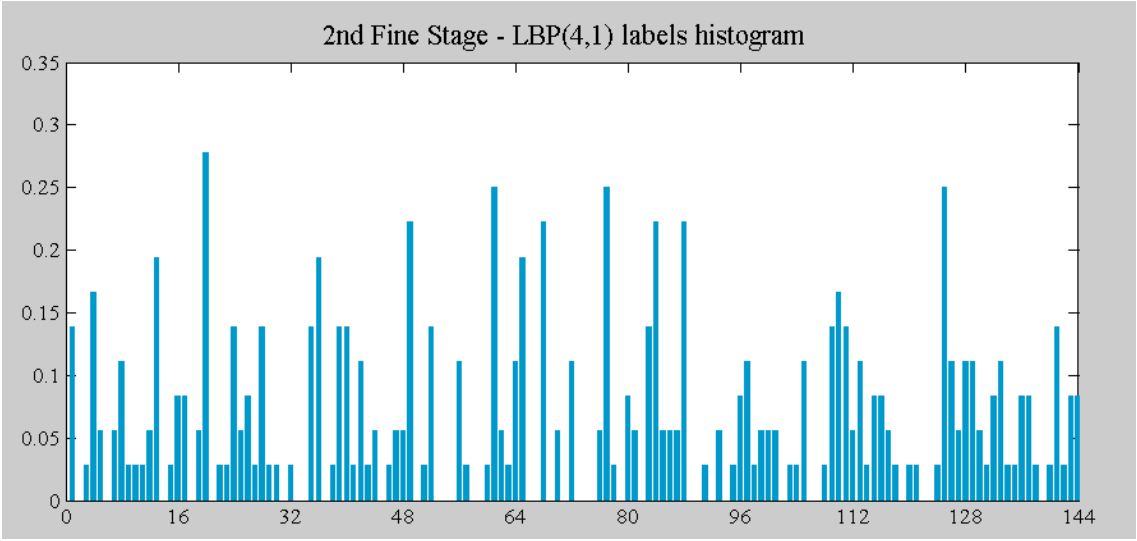

(d) 2nd Stage $LBP_{(4,1)}$ labels histogram

Figure 12. *Non-face image - Labels histogram example*

Comparing both examples, once again it can be confirmed that most important labels in $LBP_{(8,1)}$ case corresponds to uniform patters, as it can be observed in 1st stage $LBP^{u2}_{(8,1)}$ labels histograms where the first bin contains the percentage of non-uniform patterns. In *Figure 11* only 18% of the pattern are non-uniform and in *Figure 12* only the 22%.

At first glance, it is very difficult to highlight the main differences between both samples histograms that make possible that the resulting enhanced features vectors are useful in the task of faces and non-faces class discrimination. Therefore, some how it is noticeable that some noise, i.e., information not useful to discriminate between both classes, is mixed with the useful information. Consequently, it can be assumed that a technique to extract the uncorrelated components can be helpful to remove irrelevant information and moreover to reduce features vector dimensionality. For that reason, *Principal Component Analysis* (PCA) will be introduced in next section as a method for this purpose.

4.3. Face Detection Classification

Following *Face Detection Scheme* (*Figure 6*), once the enhanced feature vectors are obtained for the training samples, some kind of faces and non-faces models are needed in order to complete training stage and to be used in classification stage.

In *A.Hadid* publications, the proposed face detection classification method is the ***Support Vector Machine (SVM)***, see [5][6], which will be exposed in section *4.3.3*.

One of the contributions of this work is the study of the LBP by decreasing the computational cost. Thus, in a first stage more simple classifiers have been used in order to investigate its potential as face descriptor.

The first one is ***Chi Square*** dissimilarly metric due to the fact that it is easy to implement and that it is a good technique for histogram comparison, as it will be explained in more detail in *Face Recognition* chapters.

The second one is the ***Principal Component Analysis (PCA)*** based on the idea of minimizing the features vector size.

And the last contribution is presented after ***SVM*** introduction, a combination of ***SVM and PCA*** is proposed as an approach to reduce data dimensionality for SVM scheme.

Figure 13 gives an overview of this research proposed methods for face detection task:

- **Skin segmentation** pre-processing will be introduced in section *4.4.2.1* as a part of the *4.4 Face Detection System Improvements* chapter.
- **Feature Extraction** was already explained in previous section *4.2 Feature Extraction for Two Stages Face Detection Scheme*.
- **Feature Space Dimensionality Reduction** will be later detailed in section *4.3.3.2* and also in this section, where PCA and SVM are going to be introduced.
- **Classifier** block is the main target of this current section.

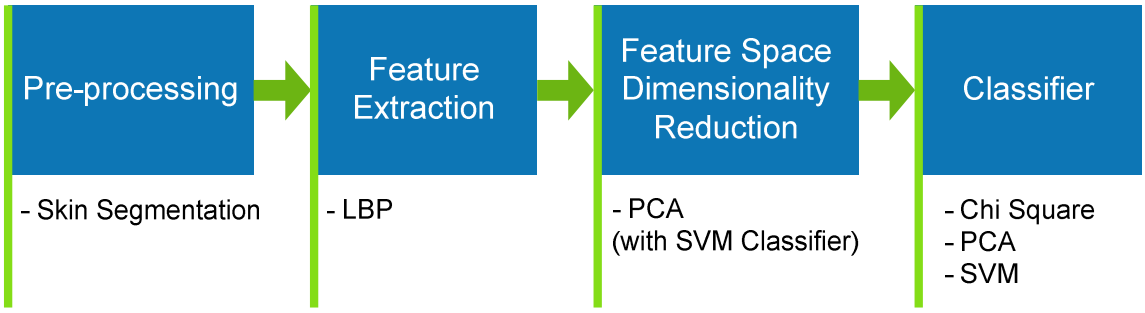

Figure 13. *Face Detection Block Diagram – Proposed Methods Overview*

4.3.1. Chi Square Classification

After features extraction step, a mean model of the *Enhanced Feature Vectors* for faces and non-faces, respectively, is calculated: M_{face} and $M_{non\text{-}face}$. Then, as a first approach to be able to compare a new input sample $\boldsymbol{S}$ with these models, *Chi Square* is proposed as a simple dissimilarly metric to compare this sample with both classes, faces and non-faces.

This classification technique is the one selected for face recognition. Later it will be explained in more detail in chapter *5.6. Face identification*.

The main idea consists of finding the minimum quadratic difference normalized between samples in the feature vector to be evaluated, $\boldsymbol{S}$, with samples of a given model features vector, $\boldsymbol{M}$:

$$\chi^2(S,M) = \sum_i \frac{(S_i - M_i)^2}{|S_i + M_i|} \tag{3}$$

In this case, two models exist: faces (M_{face}) and non-faces ($M_{non\text{-}face}$); and each model is calculated as the mean value of its training feature vectors:

$$\begin{aligned} M_{face_i} &= \sum_{j=1}^{Numfaces} \frac{S_{face_i,j}}{Numfaces} \\ M_{non-face_i} &= \sum_{k=1}^{NumNonfaces} \frac{S_{non-face_i,k}}{NumNonfaces} \end{aligned} \tag{4}$$

where:

- $M_{face\ i}$ is the *i*-sample of the face model feature vector, M_{face}.
- $M_{non\text{-}face\ i}$ is the *i*-sample of the non-face model feature vector, $M_{non\text{-}face}$.
- $S_{face\ i,j}$ is the i-sample of face number j feature vector.
- $S_{face\ i,j}$ is the i-sample of non-face number j feature vector.
- *i* is the feature vector sample out of a total of 203.
- *j* is a sample of the face training set.
- *k* is a sample of the non-face training set.
- *NumFaces* can be different from *NumNonFaces*.

Figure 14. *Face Detection Block Diagram - Chi Square Classifier*

4.3.1.1. Non Weighted

Extending this notation to the two face detection stages:

$$\chi^2_{1st\_stage}(S,M) = \sum_{i=1}^{NumFeatCoarse} \frac{(S_i - M_i)^2}{S_i + M_i} \tag{5}$$

$$\chi^2_{2nd\_stage}(S,M) = \sum_{j=1}^{NumBlocks}\left(\sum_{i=1}^{NumFeatFine}\frac{(S_{i,j}-M_{i,j})^2}{S_{i,j}+M_{i,j}}\right) \quad (6)$$

where:

- *NumFeatCoarse* is the number of features in the 1st coarse stage, in this case 59 bins result from $LBP_{8,2}^{u2}$.
- *NumFeatFine* is the number of features in the 2nd fine stage, in this case 16 bins result from $LBP_{4,1}$.
- *NumBlocks* is the total number of regions, in this case 3x3 overlapped regions for the 2nd fine stage.

4.3.1.2. Weighted

Another interesting experiment consists of weighting the different face regions to investigate whether there are more important blocks than others in face description:

$$\chi^2_{2nd\_stage_w}(S,M) = \sum_{j=1}^{NumBlocks} w_j\left(\sum_{i=1}^{NumFeatFine}\frac{(S_{i,j}-M_{i,j})^2}{S_{i,j}+M_{i,j}}\right) \quad (7)$$

where w_j is the weight for region j.

As a first approach in order to decide block weights, it is important to notice that nose, mouth and eyes regions are likely to provide more important information in face description task, than bottom left and right blocks where normally background areas, hair and even cloth can be present.

Taking into account these assumptions, different sets of block weights can be firstly defined in order to later decide, in a empirically way, the combination to produce best classification results.

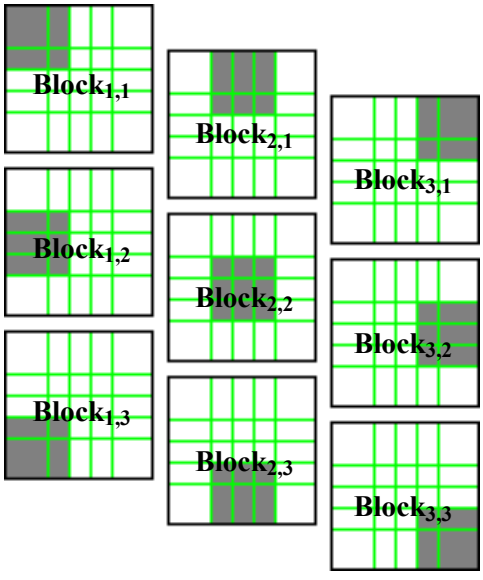

Figure 15. *Step by step, in grey, the nine overlapping blocks of 2nd classification stage*

In section *7.2.1* in results chapter, the blocks weights are empirically found out and classification results using *Chi Square* as classification technique are presented (about 85% true positive and 96% true negative), concluding that although this method is not enough to obtain best classification ratios is good enough to perceive the LBP descriptor potential.

4.3.2. Principal Component Analysis

Principal Component Analysis (PCA), also known as *Karhunen-Loéve* transform (KLT), is a very useful statistical technique in the field of face processing, image compression, etc…, due to its capability of reducing data set dimensionality by means of extracting its essential components.

PCA is a powerful tool for high dimensional data sets, because it is a way of identifying patterns in data, and converting them so as to emphasize their similarities and differences. By representing the *D* dimensional data in a lower dimensional space, the degrees of freedom, as well as space and time complexities, are reduced. The goal is to represent data in a space that best describes the variation while taking into account the squared error.

Moreover, another advantage of PCA is that once data patterns are found the data can be compressed by reducing the number of dimensions, without much loss of information. This technique is very useful in image compression field.

Basis

PCA procedure is conceptually quite simple. For a given *D* dimensional data set ***X***:

1. First, the mean vector $\mu[d]$ of dimensions *Dx1* is computed, where *N* is the number of samples in the data set:

$$\mu[d] = \frac{1}{N}\sum_{n=1}^{N} X[d,n] \tag{8}$$

2. Then, *DxD* covariance matrix ***C*** for the full data set is calculated as follows:
    a. The mean vector $\mu[d]$ is subtracted from each column of the data matrix **X** resulting in matrix ***B*** of *DxN* dimension.

$$\mathbf{B} = \mathbf{X} - \boldsymbol{\mu} \cdot \mathbf{1} \tag{9}$$

    b. Then, covariance matrix ***C*** of *DxD* dimension is computed:

$$\mathbf{C} = \frac{1}{N}\mathbf{B} \cdot \mathbf{B}^{*} \tag{10}$$

3. Next step consists of extracting the eigenvectors ($\boldsymbol{e_d}$) and eigenvalues ($\boldsymbol{\lambda_d}$) as follows:
    a. Eigenvectors: compute matrix **V**, formed by *D* columns vectors of *D* length each, which diagonalizes the covariance matrix ***C***.

$$\mathbf{V}^{-1}\mathbf{C}\mathbf{V} = \boldsymbol{\Lambda} \tag{11}$$

$$\mathbf{V} = \begin{bmatrix} \mathbf{e}_1 & \cdots & \mathbf{e}_D \end{bmatrix} \tag{12}$$

    b. Eigenvalues: the diagonal values of *DxD* matrix $\boldsymbol{\Lambda}$:

$$\mathbf{\Lambda} = \begin{bmatrix} \lambda_1 & 0 & \dots & 0 & 0 \\ 0 & \lambda_2 & \dots & 0 & 0 \\ \vdots & \vdots & \ddots & \vdots & \vdots \\ 0 & 0 & \dots & \lambda_{D-1} & 0 \\ 0 & 0 & \dots & 0 & \lambda_D \end{bmatrix} \tag{13}$$

4. Eigenvalues have to be order decreasingly in order to have the components in order of significance. The eigenvectors with the largest eigenvalues correspond to the directions of maximum variance.
5. Then, the *L* largest eigenvalues and their corresponding eigenvectors have to be chosen, assuming that the rest of the dimension space, *D-L*, is irrelevant information. Some information will be lost, but the smaller the eigenvalues, the smaller the lost.
6. Once the components (eigenvectors) have been selected, an *LxL* matrix **A** with the *L* eigenvectors as columns has to be formed.
7. Finally, the transpose of matrix **A** has to be taken and multiplied by the original data set, having previously extracted its mean value. It can be demonstrated that this process minimizes squared error criterion. In results section, *Chapter 7*, the obtained **x′** dimension is only 25% of the original **x** dimension.:

$$\mathbf{x}' = \mathbf{A}^t \cdot (\mathbf{x} - \boldsymbol{\mu}) \tag{14}$$

8. The inverse transform to get the original data back can be achieved by applying the following back-projection. Only if all eigenvectors with $\lambda_d \neq 0$ are used in the inverse transformation the original data will be exactly recovered. When using reduced number of eigenvectors, the retrieved data will have some lost of information.

$$\mathbf{x}'' = \mathbf{A} \cdot \mathbf{x}' + \boldsymbol{\mu} \tag{15}$$

Following *Figure 16* is intended to give an overview of the PCA transformation with a two dimension example, where it can be observed that eigenvectors describe the principal directions, and the eigenvalues represent the variance of the data along each principal direction.

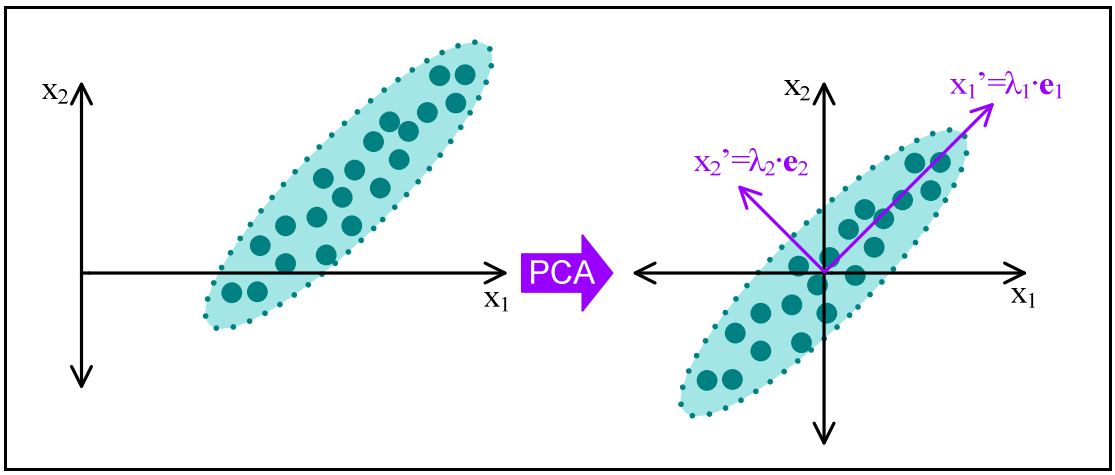

Figure 16. *PCA transformation applied to a two dimensions example*

Then, *Figure 17* show the result of reducing data dimensionality (setting $\lambda_2=0$) and back-projecting to the initial space. The result is an approximation of the original data without redundant information and the lower the eigenvalue λ_2 the better the estimation.

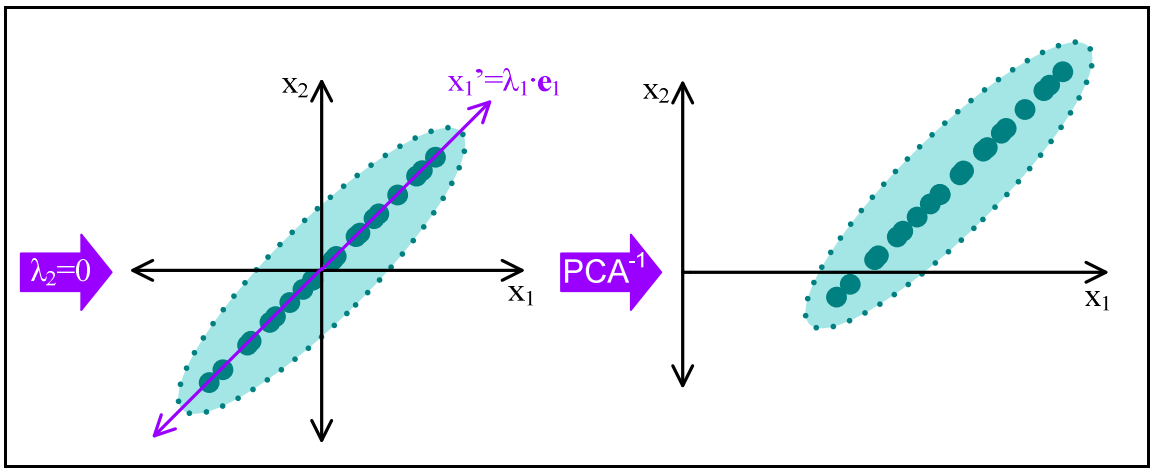

Figure 17. *Dimension reduction and PCA back-projection*

Application to face detection

In this research, LBP enhanced feature vectors for 1st and 2nd stages have dimensions 59 and 144 respectively. Therefore, PCA is an interesting technique that can help to reduce data dimensionality by avoiding irrelevant information.

When comparing faces and non faces mean values, the difference between them is not obvious due to the high dimensionality of the data. Therefore, the goal by using this method is to extract the *"Principal Components"* so as to achieve a better comparison.

In the training stage, faces and non faces samples will generate one unique eigenvectors matrix that will represent the feature space (LBP space). Then for each class (faces and non-faces) one representative model is selected (e.g. the mean of all training samples of each class). These both models are projected to the LBP space.

In the test stage, given a new input test sample, its feature vector will be projected to the orthonormal basis. Then, comparing, this projected version of the input sample with the two projected models, faces and non-faces, the minimum distance will provide the faceness of the input vector. In experimental results *Chapter 7*, it will also be discussed the possibility of performing this comparison in the original space after back-projecting.

Following sections introduces how to use PCA as classifier using both face and non-face models or just by taking into account face class.

Figure 18. *Face Detection Block Diagram - PCA Classifier*

For more information about PCA algorithms, see *Appendix V. OpenCV Functions Reference*.

4.3.2.1. Face/Non Face Models & Relative Difference Normalized

Once the projected input vector is obtained, a method to compare it to both models is needed. *Figure 19* represents the PCA projection space, where S_1 and S_2 are the projected input samples to be evaluated and M_{face} and M_{non_face} are respectively face and non-face class models, which are obtained as the mean value of the training samples. The minimum distance to the models will indicate the faceness of the input samples. As a result, S_1 will be classified as face and S_2 as non-face. This method is called *Nearest Neighbour*.

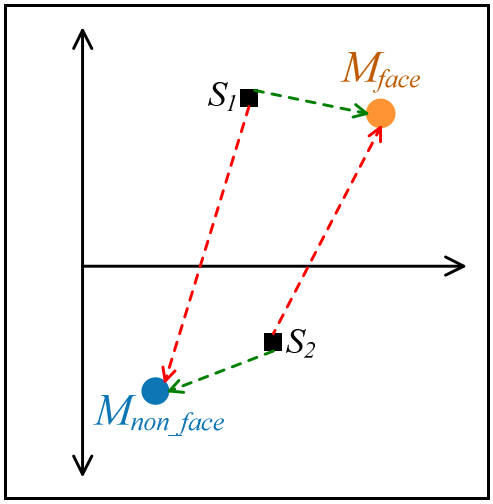

Figure 19. *PCA projected space – Min. distance of input samples to both class models*

Applied to our two stage classification scheme, the minimum distance will show the faceness of the image in the first coarse classification stage and only face candidates will go through second fine classification stage.

As seen in previous chapters, *Local Binary Patterns* histogram representation, taking into account *uniform patterns*, contains some bins with higher value than the others. For instance, in the first stage feature vector the first bin (0) is the highest one and stands for non uniform values, and the second most important pick is the last bin (58), that corresponds to totally uniform patterns.

Therefore, in order to give a homogeneous weight for all labels histogram bins the *Relative Difference Normalized* is proposed as the best comparison tool for PCA results.

$$\begin{aligned} \textit{Relative Difference Normalized}_{face} &= \sqrt{\sum_{i=1}^{n} \frac{\left(M_{face_i} - S_i\right)^2}{S_i^2}} \\ \textit{Relative Difference Normalized}_{non\text{-}face} &= \sqrt{\sum_{i=1}^{n} \frac{\left(M_{non\_face_i} - S_i\right)^2}{S_i^2}} \end{aligned} \tag{16}$$

Where:

- S is the projected input vector.
- M_{face} is the projected faces mean model.
- M_{non_face} is the projected non-faces mean model.

- *n* is the length of the feature vector: 59 in the first stage and 144 in the second one.
- If *Relative Difference Normalized* $_{face}$ < *Relative Difference Normalized* $_{non\_face}$, then the input vector will be classified as a face. Otherwise, it will be classified as non-face.

4.3.2.2. Only Faces & Threshold

Since one of the most important problems faced in this research is the complexity of representing the non faces class, the following experiment pretends to classify faces only taking into account a face space, by means of its eigenvectors matrix and an appropriate threshold.

The method is different from the previous one, each input vector is projected in an orthonormal matrix only for faces class and if the reconstructed vector is "enough close to" the original one then this input image will be classified as a face. An empirical threshold will be used to indicate this minimum distance to the original vector as it can be observed in *Figure 20*.

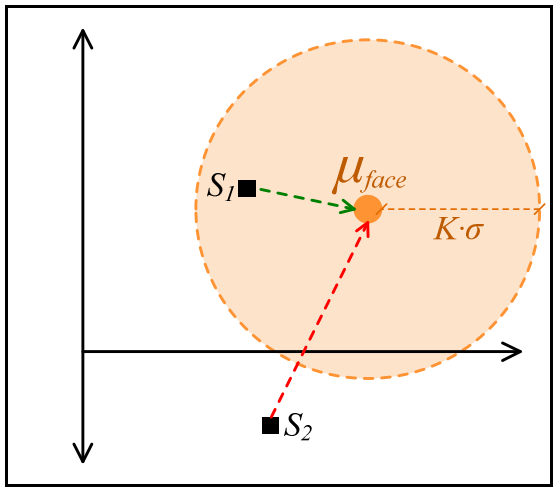

Figure 20. *PCA projected space - Distance of input samples to face class model*

This threshold is extracted from faces training set. The relative difference normalized, (16), between original training sample and reconstructed is calculated for each face sample. Then the mean value and the standard deviation is calculated and later used in classification stages as threshold:

$$1stStg\_FaceCandidate(S) = \begin{cases} true, & if \;\; S \le Threshold_{1stStg} \\ false & if \;\; S > Threshold_{1stStg} \end{cases} \tag{17}$$

Only face candidates will go trough second stage:

$$2ndStg\_FaceClassified(S') = \begin{cases} true, & if \;\; S' \le Threshold_{2ndStg} \\ false & if \;\; S' > Threshold_{2ndStg} \end{cases} \tag{18}$$

where:

- S is input sample.
- S' is S face candidate resulting from 1st stage coarse classification.
- 1st Stage Threshold: $Threshold_{1stStg} = (\mu_{1stStg} + K_{1stStg} \cdot \sigma_{1stStg})$
- 2nd Stage Threshold: $Threshold_{2ndStg} = (\mu_{2ndStg} + K_{2ndStg} \cdot \sigma_{2ndStg})$

- K_{1stStg} and K_{2ndStg} values enable a better adjustment of the thresholds by weighting the deviation. These parameters can be different in order to be more restrictive in one stage than in the other one.
- μ_{1stStg} and μ_{2ndStg} are relative difference normalized distance mean values from 1st and 2nd stage respectively.
- σ_{1stStg} and σ_{2ndStg} are relative difference normalized distance standard deviation values from 1st and 2nd stage respectively.

In section *7.3.2* in results chapter, the different parameters are adjusted: the number of eigenvectors to eliminate and, in the case of using only faces model, the *K* values to adjust the detection threshold. After evaluating detection mean ratios (about 85% true positive and 95% true negative), which are very similar to the obtained with *Chi Square*, it can be concluded that the fine-tuning of the parameters in order to maximize detection ratios is a difficult task and no remarkable benefits are achieved. Nevertheless, it is interesting to remark that only by using faces class better results are obtained, about a 84% true positive and 98 true negative.

4.3.3. Support Vector Machines

Based on A.Hadid experiments using LBP for face detection, see [5][6], a *Support Vector Machines (SVM)* classifier is selected in order to train and detect frontal faces. This classifier is selected due to its well standing in statistical theory and since it has been successfully applied to various detection tasks in computer vision.

In this chapter, a brief introduction to *Support Vector Machines (SVM)* is presented based on the following literature: [11], [30] and [31].

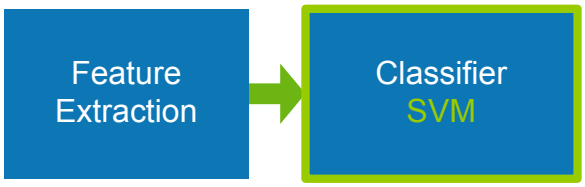

Figure 21. *Face Detection Block Diagram - SVM Classifier*

SVM is a learning technique developed by *V.Vapnik* and his team (*AT&T Bell Labs*). It is a set of related supervised learning methods used for classification and regression and it belongs to the family of generalized linear classifiers.

SVM can be seen as a way of training polynomial, neural networks or radial basis functions [31]. While most of the techniques used to train this kind of classifiers are based on the idea of minimizing the training error, usually called *empirical risk*, SVM operates on another principle called *structural risk minimization*, which minimizes an upper bound of the generalization error.

Empirical risk is defined as the measured mean error rate on training, namely the training error and s*tructural risk minimization* is an inductive principle intended to find the best model as a trade-off between lowest complexity in terms of order and the quality of fitting the training data (see s*tructural risk minimization* section in [41] from *Vapnik* and *Chervonenkis*).

A special property of SVM is that it simultaneously minimizes the empirical classification error and maximizes the geometric margin. Therefore, it is also known as *maximum margin classifiers*.

Viewing the input data as two sets of vectors in an *n*-dimensional space, a SVM will construct a separating hyperplane in that space maximizing the margin between the two data sets. Training a SVM consists of finding the optimal hyperplane, that is, the one with the maximum distance from the nearest training patterns, called support vectors.

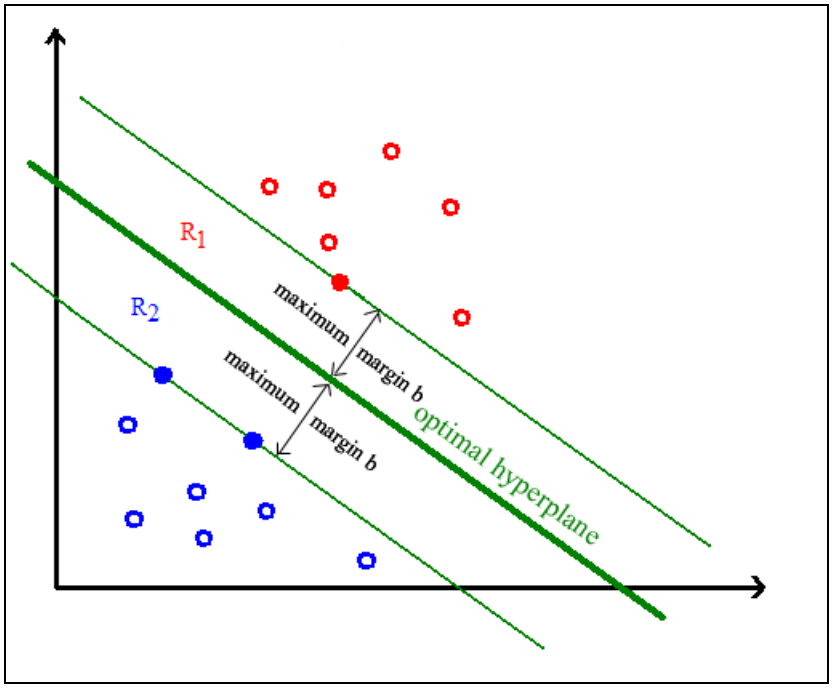

Figure 22. *SVM Optimal hyperplane*

Above *Figure 22* shows that SVM optimal hyperplane is the one with the maximum distance from the nearest training patterns. The support vectors (*solid dots*) are those nearest patterns, a distance ***b*** from the hyperplane.

To calculate the margin, two parallel hyperplanes are constructed, one on each side of the dividing one, which are pushed up against the two data sets. Intuitively, a good separation is achieved by the hyperplane that has the largest distance to the neighboring data points of both classes. **The larger the margin or distance between these parallel hyperplanes, the better the generalization error** of the classifier will be.

If the two classes are non-separable, the optimal hyperplane will be the one that maximizing the margin and that minimizes the number of misclassification errors. **The trade off between margin and misclassification error is controlled by a positive constant C** that has to be chosen beforehand. In this case, it can be shown that the solution to this problem is a linear classifier:

$$f(\mathbf{x}) = sign(\sum_{i=1}^{l} \alpha_i y_i \mathbf{x}^T \mathbf{x}_i + b) \tag{19}$$

whose coefficients α_i are the solution of the following quadratic programming problem:

$$Minimize\ \boldsymbol{\Lambda} \qquad W(\boldsymbol{\Lambda}) = -\boldsymbol{\Lambda}^T 1 + \frac{1}{2}\boldsymbol{\Lambda}^T D\boldsymbol{\Lambda}$$

$$subject\ to \begin{cases} \boldsymbol{\Lambda}^T y & = 0 \\ \boldsymbol{\Lambda} - C\mathbf{1} & \le 0 \\ -\boldsymbol{\Lambda} & \le 0 \end{cases} \tag{20}$$

where:
$$\begin{aligned} (\Lambda)_i &= \alpha_i \\ (1)_i &= 1 \\ D_{ij} &= \alpha_i y_i \mathrm{x}^T \mathrm{x}_i \end{aligned} \tag{21}$$

then only a small number of coefficients α_i are different from zero, and since every coefficient corresponds to a particular data point, this means that the solution is determined by the data points associated to the non-zero coefficients. These data points, called *support vectors*, are the only ones relevant for the solution of the problem. That means the rest could be deleted from the data set and the same result would be achieved.

Intuitively, the *support vectors* are the data points that lie at the border between the two classes. Their number is usually small, and *Vapnik* demonstrated that it is proportional to the generalization error of the classifier.

Since it is unlikely that any real life problem can actually be solved by a linear classifier, the technique has to be extended in order to allow non-linear decisions surfaces. Then, the original set of variables ***x*** is projected in a higher dimensional *feature space:*

$$\mathbf{x} \in \mathbf{R^d} \Rightarrow z(\mathbf{x}) \equiv (\phi_1(\mathbf{x}),...,\phi_n(\mathbf{x})) \in \mathbf{R^n} \tag{22}$$

By formulating the linear classification problem in this feature space, the solution will have the following form:

$$f(\mathbf{x}) = sign(\sum_{i=1}^{l} \alpha_i y_i \mathbf{z}^T(\mathbf{x})\mathbf{z}_i(\mathbf{x}_i) + b) \tag{23}$$

Two problems are met at that point: $\phi_i(\mathbf{x})$ features selection in order to lead to a rich class decision surfaces and the computation complexity of the scalar product $\mathbf{z}^T(\mathbf{x})\mathbf{z}_i(\mathbf{x}_i)$ for very large number of features *n*.

A possible solution to these problems consists of letting $n \to \infty$ and making the following choice:

$$z(\mathbf{x}) \equiv (\sqrt{\lambda_1}\psi_1(\mathbf{x}),..,\sqrt{\lambda_i}\psi_i(\mathbf{x}),...) \tag{24}$$

Where λ_i and ψ_i are the *eigenvalues* and *eigenfunctions* of an integral operator whose kernel ***K(x,y)*** is a positive definite symmetric function. With this choice the scalar product in the feature space becomes particularly simple because:

$$\mathbf{z}^T(\mathbf{x})\mathbf{z}_i(\mathbf{x}_i) = \sum_{i=1}^{\infty} \lambda_i \psi_i(\mathbf{x})\psi_i(\mathbf{x}) = K(\mathbf{x},\mathbf{y}) \tag{25}$$

where the last equality comes from the *Mercer-Hilbert-Schmidt* theorem for positive definite functions.

The quadratic programming problem that has to be solved now is exactly the same as in equation (21), except for the matrix D elements, which now are the following ones:

$$D_{ij} = \alpha_i y_i K(\mathbf{x}, \mathbf{x}_i) \tag{26}$$

As a result of this choice, the SVM classifier has the following form:

$$f(\mathbf{x}) = sign(\sum_{i=1}^{l} \alpha_i y_i K(\mathbf{x}, \mathbf{x}_i) + b) \tag{27}$$

In the literature, some of the kernel functions proposed and the type of decision surface they define are:

Kernel Function	Type of Classifier
$K(\mathbf{x},\mathbf{x}_i)=exp(-\|\|\mathbf{x}-\mathbf{x}_i\|\|^2)$	Gaussian Radial Basis Functions
$K(\mathbf{x},\mathbf{x}_i)=(\mathbf{x}^T\mathbf{x}_i + 1)^d$	Polynomial of degree d
$K(\mathbf{x},\mathbf{x}_i)=tanh(\mathbf{x}^T\mathbf{x}_i - \Theta)$	Multi Layer Perceptron

Table 6. *Kernel functions and their corresponding decision surface type.*

An important benefit of the *Support Vector Machine* approach is that the complexity of the resulting classifier is characterized by the number of support vectors, independent of the dimensionality of the transformed space.

In order to solve the training problem efficiently and taking into account the expectation that the number of support vectors will be very small and therefore many of the components of $\mathbf{\Lambda}$ will be zero, one can think in iterative algorithm keeping to zero those components α_i associated with data points that are not support vectors, then only optimizing over a reduced set of variables.

The problem of minimizing the magnitude of the weight vector constrained by the separation can be seen as an unconstrained problem by the method of *Lagrange* undetermined multipliers and by means of the *Kuhn-Tucker* construction can be reformulated as maximizing:

$$L(\boldsymbol{\alpha}) = \sum_{i=1}^{l} \alpha_i - \frac{1}{2} \sum_{i,j=1}^{l} \alpha_i \alpha_j y_i y_j K(\mathbf{x}, \mathbf{x}_i) \tag{28}$$

subject to the constraints:

$$\sum_{i=1}^{l} \alpha_i y_i = 0, \qquad \alpha_i \geq 0 \tag{29}$$

For further information, in the literature [11], [30] and [31], a more detailed explanation of *Support Vector Machines* can be found.

4.3.3.1. SVM applied to face detection classification

Going back to the purpose of this work, let apply this theory to the face detection particular case. Based in *A.Hadid* experiments, [6], a second degree polynomial kernel function is selected as decision surface type. The LBP is computed at each iteration, LBP_x, from the subwindow and fed to the SVM classifier to determine whether it is a face or not. The classifier decides on the faceness of the subwindow according to the sign of the following function:

$$f(LBP) = sign(\sum_{i=1}^{l} \alpha_i y_i K(LBP_x, LBP_{ti}) + b) \quad (30)$$

where:

- ***LBP**ti*** is the LBP representation of the training sample *ti*.
- ***yi*** is 1 or -1 depending on whether *ti* is a positive or negative sample (face or non-face).
- ***l*** is the number of samples.
- ***b*** is a scalar (bias).
- ***K*** is the second degree polynomial kernel function defined by:
  $K(LBP_x, LBP_{ti}) = (1 + LBP_x \cdot LBP_{ti})^2$
- ***αi*** are the parameters of the SVM classifier, recovered by solving the following quadratic programming problem:

$$Max(\sum_{i=1}^{l} \alpha_i - \frac{1}{2} \sum_{i,j=1}^{l} \alpha_i \alpha_j y_i y_j K(LBP_{ti}, LBP_{tj}) \quad (31)$$
$$Subject \quad to: \begin{cases} \sum_{i=1}^{l} \alpha_i y_i = 0, \quad 0 \le \alpha_i \le C \end{cases}$$

- ***C*** is the cost of constrain violation during the training process which is fixed to 5 in *A.Hadid* experiments.

The cost of constrain violation during the training process, *C*, has to be empirically calculated and controls the trade off between training errors and model complexity. If C is too large, then the system may overfit[2] and if it is too small, then it may underfit[3] (see [41]).

In section *7.2.3* in results chapter, the SVM parameters will be adjusted for both 1st coarse and 2nd fine classification stages. Then, the face detection classification ratios will be presented showing best results compared to the previous classification proposals: *Chi Square* and *PCA*. In addition, an extra 3rd classification stage will be proposed, as a contribution of this research project, to improve final results.

For further information about SVM algorithms used, see *Appendix V. OpenCV Functions Reference*.

4.3.3.2. PCA before applying SVM

As seen in previous sections, *PCA* is an interesting technique that can help to reduce data dimensionality by avoiding irrelevant information. Therefore, this section proposes the use of *Principal Component Analysis* as post processing of the *Features Extraction* stage and previous to the *SVM* classifier, as it can be seen in *Figure 23*.

[2] Overfitting (machine learning): consists of fitting training data but predicting new examples inaccurately.
[3] Underfitting (machine learning): consists of obtaining prediction errors due to mathematical model inaccuracy.

Figure 23. *Face Detection Block Diagram - PCA Feature Space Reduction*

The methodology is the same as the already explained in PCA section *4.3.2*. In the training stage, faces and non faces samples will generate one unique eigenvectors matrix that will represent *LBP* space. Then, each training sample will be projected to the orthonormal basis, then back-projected and directly used to train the *SVM* classifier.

In the test stage, the input vector under study will be projected and back-projected to the PCA matrix before entering the SVM classification stage.

In section *7.2.3.2* in results chapter, for simplicity, as it is very hard to fine-tuning all the parameters involved in the system, the same values calculated in *PCA* classification (*7.2.2*) and *SVM* classification (*7.2.3*) sections will be used. Only the 3rd threshold stage will be adapted to the new system. Final results will be presented showing also satisfactory face detection ratios, although maybe by finding again the optimal number of eigenvectors could improve the system.

Summarizing this section and taking into account experimental results *Chapter 7*, first classification method *Chi Square* serves to have a first perception of the *LBP* descriptor potential (about 85% true positive and 96% true negative). Then, *PCA* classification technique shows that redundant information reduction can be performed with also similar results (about 85% true positive and 95% true negative). After that, *SVM* classifier together with a 3rd threshold stage contribution will provide the best results of the face detection section (about 95% true positive and 99% true negative). And the last classification proposal, the redundancy reduction using *PCA* before *SVM* classification presents also good results but very similar than using only *SVM*.

4.4. Face Detection System Improvements

Following section is intended to illustrate the improvements applied in the face detection scheme, starting with *Bootstrap Strategy* to reduce false face detection in training stage, and following with classification optimizations such as *Skin Segmentation* and *Overlapped Detections Removal*.

4.4.1. Training Stage

4.4.1.1. Bootstrap strategy to non-face pattern recollection

As proposed by *A.Hadid* in [6] and *K.-K. Sung* in [14], in face detection training stage, the negative examples are collected by means of a bootstrap strategy consisting of reentering false detections into the training set in a iterative way.

Applying such an approach, the difficult task of manually selecting representative non-face training samples is avoided just by weighting useful patterns from among redundant ones. At the end of each bootstrap iteration, the non-faces set is enlarged with new non-faces patterns that the current system has wrongly classified.

Such a strategy is applied in our experiments in order to collect the non-face patterns. Therefore, firstly, between 6000-7000 non-face patterns are randomly extracted from a set of natural images from Internet which do not contain faces.

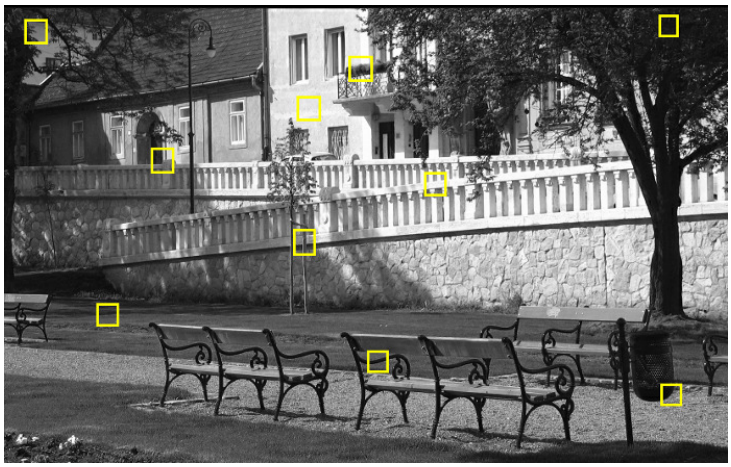

Figure 24. *Natural image from which negative training samples are extracted*

Then the following scheme is iterated several times until the number of false alarms (non-faces classified as faces) is minimized:

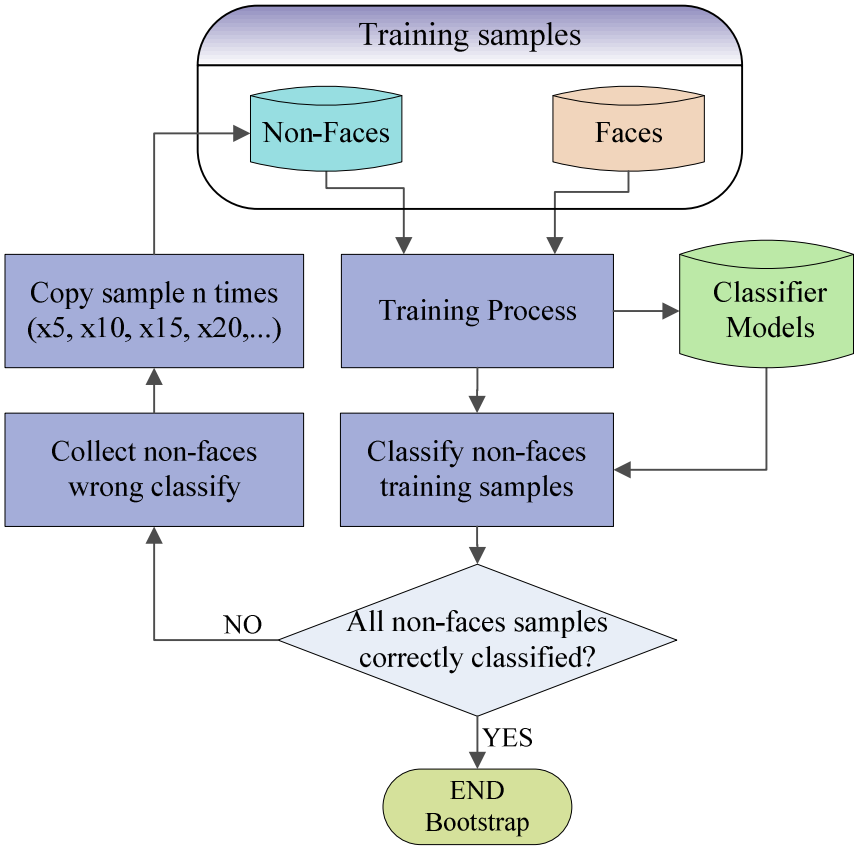

Figure 25. *Bootstrap strategy flow chart*

As it will be later verified in experimental results chapter, sometimes it is not possible to converge to point of no false detections and a commitment between detection ratio drop and false alarm ratio improvement is required.

4.4.2. Classification Stage

Following section deals with classification stage improvements, as it can be *Skin Segmentation* to speed face detection task and *Overlapping Detection Removal* for false detection reduction.

4.4.2.1. Skin Segmentation

As demonstrated in the computational cost analysis (*Appendix III.1.1*), the huge number of iterations[4] required to explore whole image will result in a high computational effort. Thus, a preprocessing step to reduce the computational cost without affecting the efficiency is proposed.

Figure 26. *Face Detection Block Diagram with Skin Segmentation Pre-processing*

Based on *A. Hadid* and *M.Pietikäinen* experiments, see [5], a skin detector is proposed to preprocess images to find the potential face regions, avoiding scanning the whole image and therefore speeding the classification process. The method they propose and the one used in this research are conceptually the same, a part from some differences in the pre and post processing.

After skin segmentation, the two stages LBP face detection method is applied only in the resulting regions. Depending on the image type, the processing time can be significantly reduced. Notice that such a reduction will always depend on the image color itself.

In the literature, different skin segmentation procedures can be found. The most widely used due to its robustness against intensity and illumination variations is the based on skin chromaticity (see *Appendix II. Skin Chromaticity*).

Skin Segmentation Procedure

The training stage consists of manually select skin areas from different images, in order to collect several skin images with different skin tones, illumination conditions and camera calibrations.

[4] The number of blocks and required iterations can be calculated using formula (69) and (70) from *Appendix III.1.1*.

Then, the images are converted from RGB to chromaticity space, obtaining the intensity and two chromaticity coordinates. Only *u* and *v* components are considered to obtain robustness against luminance and to describe the different skin colors.

A.Hadid defines the skin model using two quadratic functions which determine the upper and lower bounds. After skin segmentation, they apply morphological operations, basically dilations followed by erosions until the image no longer changes, with the intention of eliminate isolated pixels.

In this research, the skin segmentation procedure is detailed in the following points:

a) Image preprocessing (training / test)

Before calculating the LUV components a preprocessing is applied to the original image to smooth the image and avoid compression noise (JPEG cases) and other artifacts. A 3x3 simple blur filter is used, consisting of the sum over a pixel 3×3 neighborhood with subsequent scaling by 1/(3x3).

1/9	1/9	1/9
1/9		1/9
1/9	1/9	1/9

Figure 27. *Smooth filter*

b) LUV conversion (training / test)

Then, LUV conversion is applied and the 3 components are split:

- RGB image is converted to floating-point format and scaled to fit 0..1 range
- Then is converted to CIE XYZ by means of the following formula:

$$\begin{bmatrix} X \\ Y \\ Z \end{bmatrix} = \begin{bmatrix} 0.412453 & 0.357580 & 0.180423 \\ 0.212671 & 0.715160 & 0.072169 \\ 0.019334 & 0.119193 & 0.950227 \end{bmatrix} \begin{bmatrix} R \\ G \\ B \end{bmatrix} \tag{32}$$

- Then CIE LUV (*Perceptual Uniformity*) is calculated as follows:

$$\begin{aligned} L &= \begin{cases} 116 \cdot Y^{1/3} - 16 & for \quad Y > 0.008856 \\ 903.3 \cdot Y & for \quad Y \le 0.008856 \end{cases} \\ u' &= \frac{4X}{X + 15Y + 3Z} \\ v' &= \frac{9Y}{X + 15Y + 3Z} \end{aligned} \tag{33}$$

- And then CIE UCS (*Uniform Chromaticity Scale*) is calculated as shown:

$$\begin{aligned} u &= 13 \cdot L \cdot (u' - u_n), \quad where\ u_n = 0.19793943 \\ v &= 13 \cdot L \cdot (v' - v_n), \quad where\ v_n = 0.46831096 \end{aligned} \tag{34}$$

where:

$$0 \le L \le 100$$
$$-134 \le u \le 220$$
$$-140 \le v \le 122$$

- The values are then converted to the destination data type, 8-bit image in this case:

$$\begin{aligned} L &= L \cdot 255/100 \\ u &= (u + 134) \cdot 255/354 \\ v &= (v + 140) \cdot 255/262 \end{aligned} \tag{35}$$

c) Skin model definition (training)

After color conversion, for each pixel and taking into account a neighborhood of following number of pixels, the *u* and *v* components mean value is calculated for each box:

$$SkinDetBoxSize\_Training = \left\lfloor \frac{imageWidth}{10} \right\rfloor x \left\lfloor \frac{imageHeight}{10} \right\rfloor \tag{36}$$

Independently from training image dimension, with this box size, it is ensure that from each skin sample image, 100 blocks are taking into account.

For simplicity, once all *u* and *v* components mean values are extracted from whole training data set, the *uv* skin model bounds are defined by means of a rectangle area, with the following coordinates:

- top-left = (*u_min*, *v_max*)
- bottom-right = (*u_max*, *v_min*)

where *u_min*, *u_max*, *v_min* and *v_max* are the skin samples coordinates with maximum and minimum *u* and *v* values.

d) Skin segmentation (test)

Given an image to be segmented, steps **a)** and **b)** are applied. Afterwards, exploring pixel by pixel and taking into account a defined box size (37), the *u* and *v* components mean values are calculated as in training stage.

$$SkinDetBoxSize\_Test = \left\lfloor \frac{IMG\_MIN\_WIDTH\_DET}{4} \right\rfloor x \left\lfloor \frac{IMG\_MIN\_HEIGHT\_DET}{4} \right\rfloor \tag{37}$$

This box size is selected in order to avoid image artifacts and to smooth possible region containing an eye or mouth that can create undesirable holes in the final skin mask. If the expected face size is *IMG_MIN_WIDTH_DET x IMG_MIN_HEIGHT_DET*, then a mouth or an eye is supposed to be approximately a quarter of the face height and a quarter of the face width.

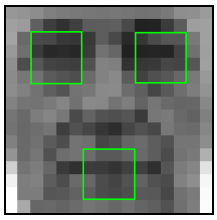

Figure 28. *16x16 image size.*

Then, skin model thresholds are applied to determinate if the box region is skin or not.

The resulting mask (called ***pre-mask*** in experimental results chapter), before applying morphological operations (see [12]), is calculated only once before down-sampling (see section *4.1*) and then, down-sampled together with the original image in order to save processing time.

In order to better understand the proposed advanced morphological operations, the base ones should be presented:

- Dilation consists of dilating the source image x[n] using a specified structuring element b[n] that determines the shape of a pixel neighborhood over which the maximum is taken.

$$y[n] = x[n] \oplus b[n] \tag{38}$$

- Erosion consists of eroding the source image x[n] using a specified structuring element b[n] that determines the shape of a pixel neighborhood over which the minimum is taken.

$$y[n] = x[n] \Theta b[n] \tag{39}$$

Morphological operations are performed with the intention of eliminating isolated pixels after each down-sampling step:

1st) ***Closing*** (dilation followed by erosion): used to eliminate dark and small elements like the eyes and mouth in a face. Therefore, the structuring element selected is 3x5 pixels ellipse.

$$y[n] = (x[n] \oplus b[n]) \Theta b[n] \tag{40}$$

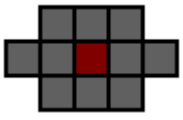

Figure 29. *Closing structuring element: 3x5 pixels ellipse*

2nd) ***Opening*** (erosion followed by dilation): used to eliminate faces regions smaller than the face image. Therefore, the structuring element selected is a circle with 11 pixels radius.

$$y[n] = (x[n] \Theta b[n]) \oplus b[n] \tag{41}$$

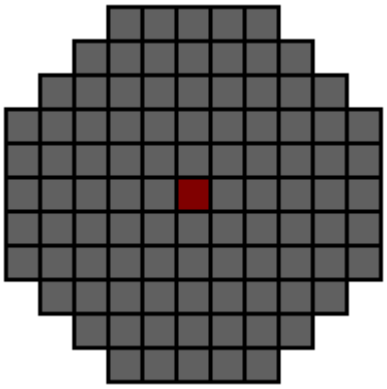

Figure 30. *Opening structuring element: 3x5 pixels ellipse*

Notice that the structuring element used in both morphological operation must be larger than the object to be removed.

Before applying face detection to each *IMG_MIN_WIDTH_DET x IMG_MIN_HEIGHT_DET* block, it is checked if **95%** (***Face Skin Threshold***) of the pixels in the block are classified as skin.

To summarize, next *Figure 31* gives an overview of the skin detection block diagram:

Figure 31. *Skin detection block diagram*

In the experimental results section *7.1*, *uv* values for skin and non-skin training samples will be calculated in order to defined *uv* minimum and maximum thresholds. Then detection ratios will be presented (~98%) using a skin database for testing purposes (see section *6.1.3*) and after that, a justification of the used morphological operations will be introduced showing some examples of how they are able to improve the efficiency of the proposed face detection scheme, e.g. eliminating skin candidates smaller than the minimum face resolution.

4.4.2.2. Overlapping Detections Removal

Following with classification stage improvements, this section exposes a post processing approach to eliminate overlapping detections.

In face detection procedure, the input image is explored (see section *4.1*) by means of a scanning method defined by a square or rectangular box which determines the face detector resolution, a window-sliding moving scan step to get each next block to be analyzed and a down-sampling rate to allow image exploration in different scales.

As a result of this image scanning procedure, most faces are detected at multiple near positions and scales, leading into false detection that worsens face detector reliability.

In the literature, the most common strategies to resolve overlapping detections around a single face are the following ones:

- **Overlapping Detection Removal**: the block with higher classification score is considered the correct face detection and all other detection locations which overlap it are likely to be errors, and can therefore be eliminated.

- **Overlapping Detection Merge**:
  - The centroid of the near detections defines the location of the detection result.
  - Overlapping windows are approximated with one big box that contains all overlapped boxes.

Computationally speaking, the most adequate method is removal one, because it saves up the centroid or container box calculation. Therefore, in this research removal algorithm was first implemented to evaluate its performance and as the results were very satisfactory, no extension to merge methods was required.

Overlapping Detection Removal

The technique consists of sorting all detection boxes, including different scales, in decreasing order taking into account classification score. Then, the first box with highest faceness score is compared to the rest of the bounding boxes. Each box that overlaps it in more than a given percentage (threshold) is deleted from the boxes array.

Empirically, 30% is decides as overlapping threshold achieving best results. Only in case of real face overlapping, one face partially occluding another one, can lead to undesired results.

Next figure shows the result of applying overlapping detection removal algorithm. In yellow all face candidates and in red the result of applying overlapping discrimination:

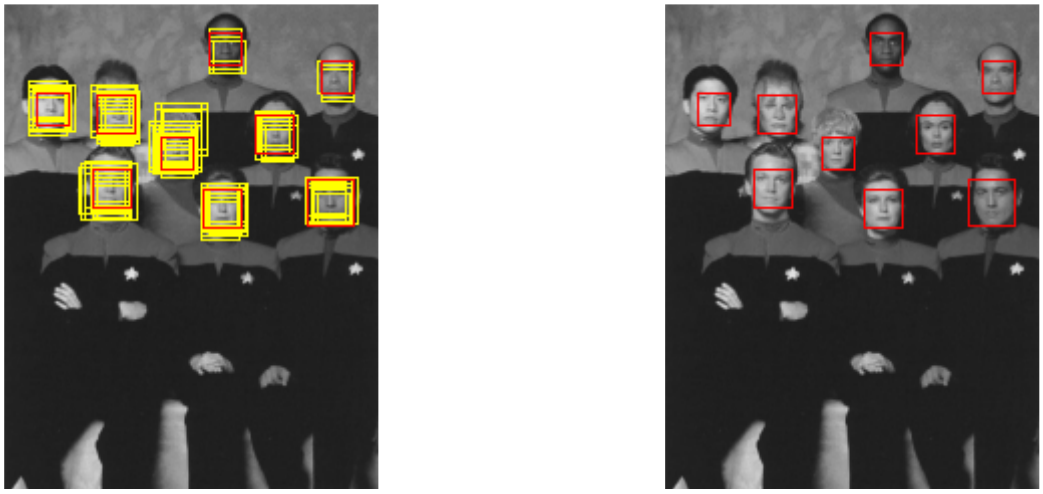

(a) In yellow all face detection and in red result face with higher SVM faceness score.

(b) Result after overlapping boxes removal.

Figure 32. *Overlapping detection removal example (CMU Test-Voyager2.bmp30% scale)*

Chapter 5

Local Binary Patterns applied to Face Recognition

Local Binary Patterns descriptor is not only an efficient discriminative feature for face detection scenarios, but also for face recognition task.

This work pretends not only explore face detection approach but also face recognition method. Once *LBP* extraction is implemented, face recognition implementation based in the *University of Oulu* proposed methods (see [1][2][4]) is a straightforward task.

The *LBP* based face recognition approach consists of extracting the *LBP* features histograms from the whole face (59-bin histogram), divide the face image into 7x7 blocks and concatenate the blocks histograms into a unique vector (7x7 blocks x 59-bin/block = 2891 features). These features are calculated for each individual sample and a mean model is computed for each ID subset.

In face identification step, given a new input face image, the 2891 features vector is extracted and compared to all available models by means of a dissimilarly metric. The input face will be identified with the minimum ID model distance.

Following *Figure 33* introduces the generic face recognition scheme proposed for this research project:

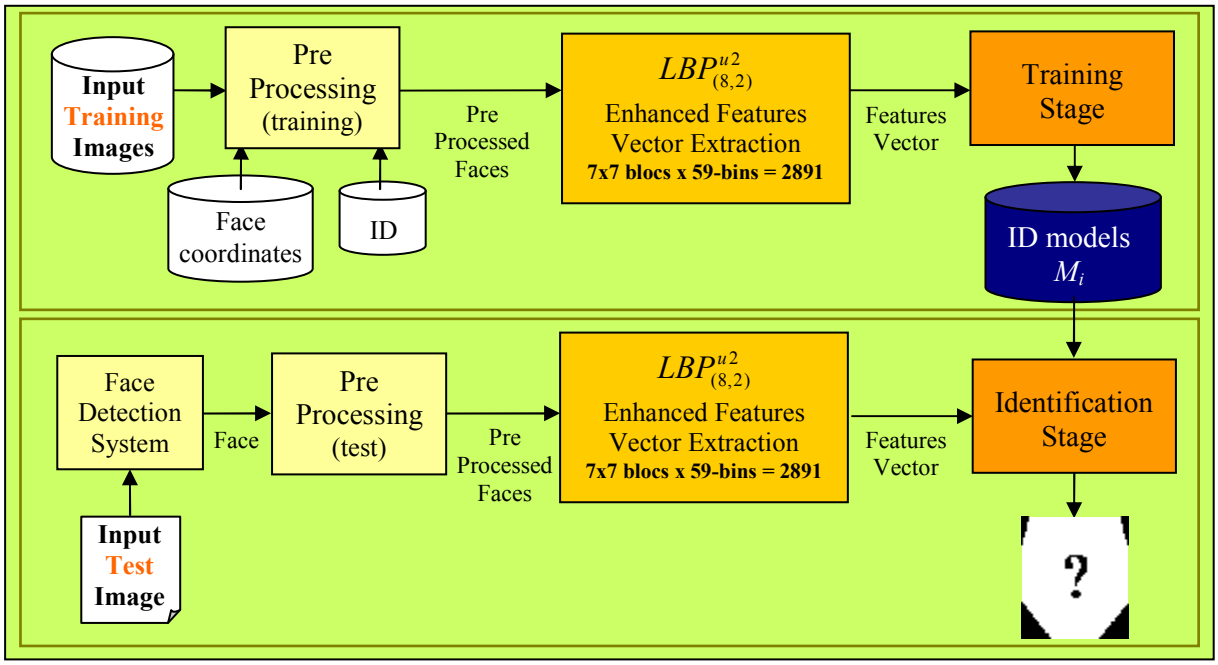

Figure 33. *Face Recognition Scheme*

- **Training stage** (top box): input face samples are introduced in the pre-processing block together with an face-coordinates file and an ID label to crop faces from input image and resize them, if necessary. Then $LBP^{u2}_{(8,2)}$ *Enhanced Features Vector*

is extracted and used to feed the training block that will output a mean value model for each ID in the training database.

- **Test stage** (bottom box): for each new test image, face detection block will output the cropped and resized face that will go through pre-processing stage for image quality improvement. Then $LBP^{u2}_{(8,2)}$ *Enhanced Features Vector* will be extracted and compared to the available ID models in the identification stage.

As it will be seen in more detail, this chapter not only pretends to explain and test *University of Oulu* method, but also to improve it by means of using *Principal Component Analysis* to extract data redundancy simplifying features vector dimensionality.

5.1. Image preprocessing

Before the classification, input images should be adapted and enhanced to the face recognition system, either in training or test stage. The following steps describe image preprocessing stages:

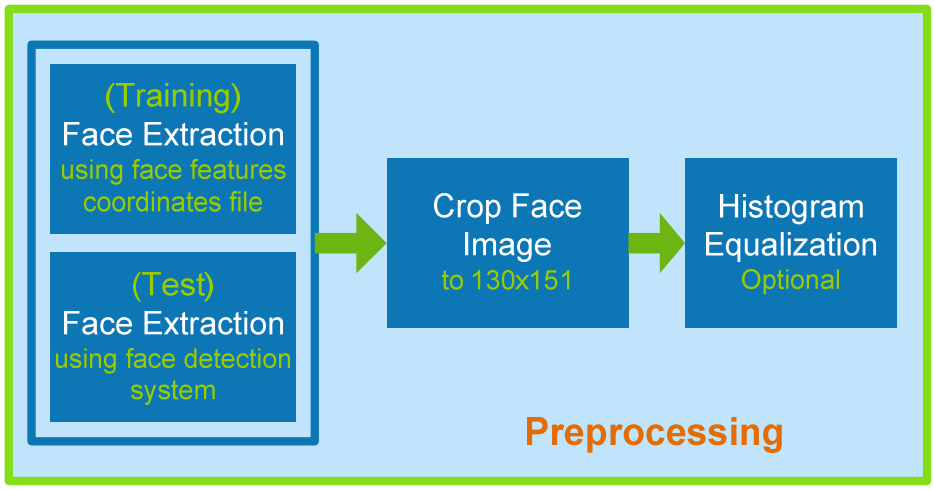

Figure 34. *Face Recognition – Preprocessing Block Diagram*

- **Face Extraction**

Faces are extracted from images by means of:

- Training case: a face features coordinates files provided for each image in the training dataset (see face recognition database information in section *6.3*).
- Test case: a face detection pre-stage.

- **Crop extracted faces images**

In the literature [1], *7x7 blocks* of size *18x21 pixels* are recommended as a good trade-off between recognition performance and feature vector length. Therefore, and taking into account that 2 pixels margin is needed to apply $LBP^{u2}_{(8,2)}$ operator (see section *3.2*), face images need to be cropped to the following size:

$$\textbf{\textit{Width}} = (7 \text{ blocks} \times 18 \text{ pixels}) + (2 \text{ margins} \times 2 \text{ pixels/margin}) = \textbf{130 pixels}$$
$$\textbf{\textit{Height}} = (7 \text{ blocks} \times 21 \text{ pixels}) + (2 \text{ margins} \times 2 \text{ pixels/margin}) = \textbf{151 pixels}$$

- **Histogram Equalization**

Histogram equalization is a method of contrast adjustment using image's histogram, [12].

The image histogram represents the relative frequency occurrence of grey levels:

$$\begin{aligned} h(l_k) &= \#\text{ pixels with level } l_k \\ k &= 0\ldots L\text{-}1 = \#\text{ levels} \end{aligned} \tag{42}$$

Then the probability of level k, l_k, is:

$$p_r(l_k) \cong \frac{h(l_k)}{\sum_{k=0}^{L-1} h(l_k)},\ k=0\ldots L\text{-}1 \tag{43}$$

Histogram equalization is a pixel-based operator that consists of applying to each pixel an equalization mapping operation, independently from the value of its neighboring pixels. This mapping function is the cumulative density function of the grey levels l of the image:

$$m_k = \sum_{k=0}^{k} p_r(l_k) \tag{44}$$

Then to quantify the result is needed to be able to use it as a mapping function:

$$m_k^* = \left\lfloor \frac{m_k - m_{\min}}{1 - m_{\min}}(L-1) + \frac{1}{2} \right\rfloor \tag{45}$$

where: m_{min} is the smallest value of m_k.
m_k^* is the resulting mapping function that produces a new image with approximately uniform histogram, namely an equalized image.

After above two steps, the resulting images have same size and equalized histogram to avoid illumination influence.

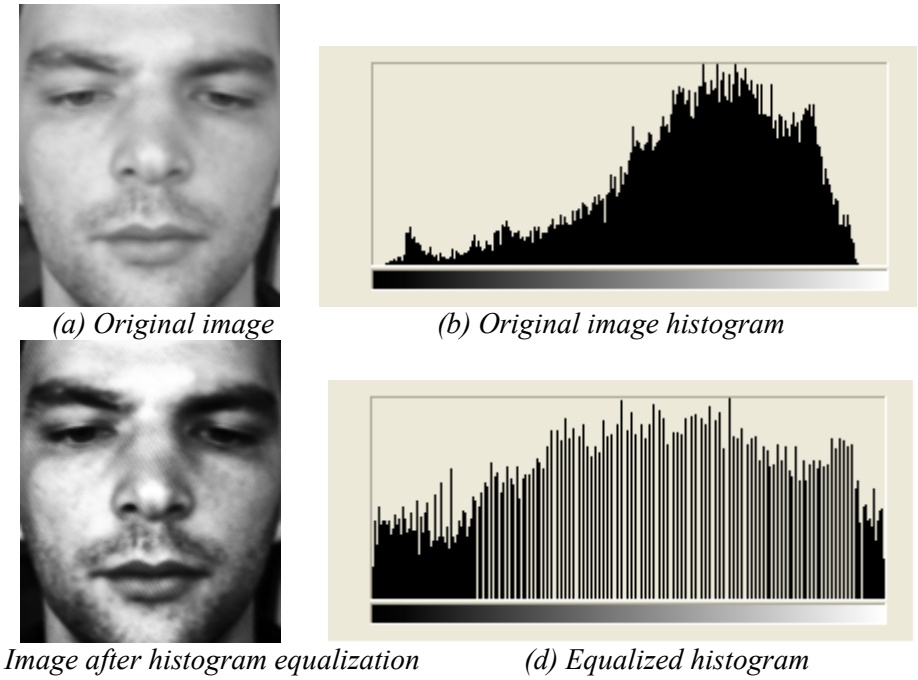

(a) Original image *(b) Original image histogram*

(c) Image after histogram equalization *(d) Equalized histogram*

Figure 35. *Histogram Equalization example*

As it can be observed in *(d)*, sometimes it is impossible to achieve a completely equalize histogram due to the fact that in this equalization process:

- A bin can be moved to a new grey level value bin.
- Bins with different values can result in a same grey value, then various bins can be accumulated into one.
- But a bin can never be divided in different grey level values.

Face images are very sensitive to illumination variations and small changes in light conditions can produce large changes in face appearance making face recognition task more difficult to handle. Therefore, histogram equalization is a useful preprocessing stage to face recognition task in order to not only enhance contrast but also edges and face details.

On the other hand, in some cases, for example, where the left side and right side of the face has a different illumination or a shadow, the result of applying global histogram equalization can cause image degradation. In those cases, the use of local histogram equalization could be more suitable. However, in experimental results chapter (see section *7.3*), only global histogram equalization will be used to verify if results can be improved by using this image preprocessing.

5.2. Face descriptor extraction

Just like in face detection, in face recognition a signature or a description of the face is required. This description will represent each individual in our database. A good face descriptor should retain all the specific features of each individual while compacting all this discriminant information in a few values or coefficients.

In this work, the approach of *A.Hadid* and *T.Ahonen* ([3][4]) has been selected. The authors proposed to use a LBP face descriptor. First, the original face descriptor will be explained. Second, the improvements proposed in this work will be presented in more detail.

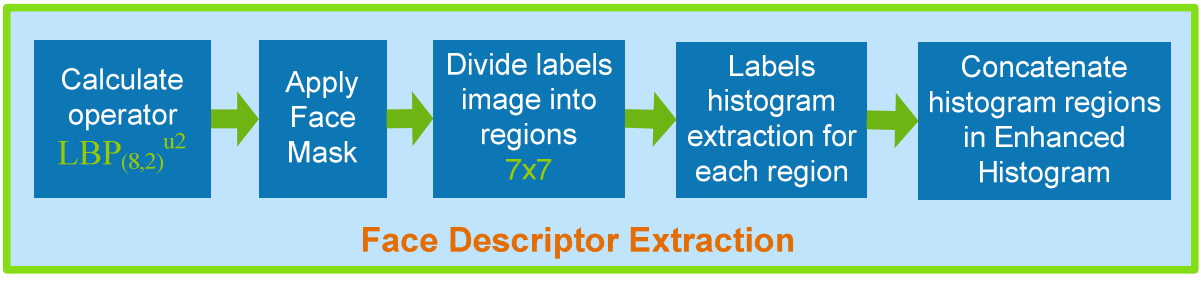

Figure 36. *Face Recognition – Face Description Extraction Block Diagram*

- **Calculate $LBP^{u2}_{(8,2)}$ operator from whole face image**

As a consequence of applying $LBP^{u2}_{(8,2)}$ to the 130x151 image, a resulting image of 126x147 pixels is obtained, due to the fact that 2 pixels frame is required in order to be able to apply LBP of radius 2 (see section *3.2*).

- **Apply face mask**

The above mentioned researchers propose the application of a mask (see *Figure 37*) in order to avoid non face parts in the image. As it will be explained in later experimental results chapter *7.3*, if the image is later divided in blocks and an appropriate weight value w_i is applied to each one, then the same effect can be achieved, at the same time that this extra step can be saved. Nevertheless, in face recognition experiments this mask will be used to verify the effect of using it.

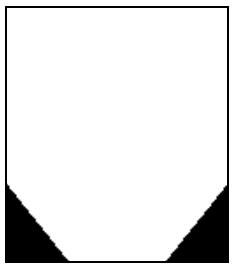

Figure 37. *Image mask example*

- **Divide labels image into several regions (7x7 block of 18x21 pixels)**

As a good compromise between face image description and resulting feature vector length (7x7 blocks x 59-bin/block = 2891), a 7x7 window division is proposed as a best choice for image recognition in *T.Ahonen* [1].

Figure 38. *$LBP_{(8,2)}^{u2}$ image example of size 126x147: 7x7 blocks of 18x21 pixels*

- **Labels histogram extraction for each region**

Considering m facial regions $R_0, R_1, ..., R_{m-1}$, the LBP labels histogram is computed for each region. In our case m is 7x7 regions.

The histogram of each block in the labeled image $f_l(x, y)$ can be defined as

$$H_i = \sum_{x,y} I\{f_l(x, y) = i\}, \quad i = 0,...,n-1 \tag{46}$$

in which n is the number of different labels produced by the LBP operator and

$$I\{A\} = \begin{cases} 1, & A \text{ is true} \\ 0, & A \text{ is false} \end{cases} \tag{47}$$

Region's histogram provides information about the distribution of the local textures, such as edges, spots and flat areas, over the whole image. For this reason, an efficient face representation is achieved because spatial information is kept.

- **Concatenate labels histogram of each region**

Finally, each region histogram is concatenated in a spatially enhanced histogram defined as:

$$H_{i,j} = \sum_{x,y} I\{f_l(x,y) = i\} I\{(x,y) \in R_j\}, \quad i = 0,...,n-1, \quad j = 0,...,m-1 \tag{48}$$

This vector will be used as a face descriptor for face recognition and in our particular case; its length will be 2891 samples (7x7 blocks x 59-bin/block).

In experimental results chapter (see section *7.3*), a combination of experiments is proposed in order to decide the use of the different optional processings*: histogram equalization*, *mask* and *blocks weights*. After them, the use of a mask is discarded, as the blocks weights are able to perform the same functionality.

5.3. Face identification

Once the database is prepared and the spatially enhanced histograms are extracted from each identity face, *T.Ahonen* and *A.Hadid,* in [3] and [4], proposed *Chi Square* algorithm as a basic dissimilarly metric in order to compare each incoming face with the available database identities.

As it will be later exposed in experimental results chapter, this method provides satisfactory results, but as a contribution to this research work, it can be improved at the same time that face descriptor dimensionality is reduced by eliminating redundant information using *Principal Component Analysis* approach.

Before exposing these dissimilarly metrics, next section gives an overview of face regions analysis to take advantage of human face recognition system to improve artificial recognition systems.

5.3.1. Face Regions Analysis

As already exposed in face detection chapter, section *4.3.1.2*, dividing the face image in different regions can help to emphasize face features with essential information for face description and to remove irrelevant information by using an adequate weight value.

Obviously, nose, mouth and eyes regions are likely to provide more important information in face description task, than bottom left and right blocks where normally background areas, hair and even cloth can be present. Moreover, neurophysiologic studies based on face recognition human system evidence that most important face features are eyes and eyebrows, followed by mouth and nose (see [28][29]).

Therefore, and taking into account human system knowledge, *Figure 39* shows a possible good choice for weighting face areas in face recognition procedure.

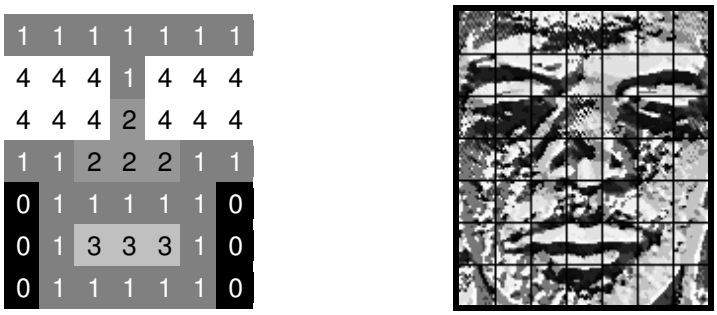

(a) Face regions weights *(b) $LBP_{(8,2)}^{u2}$ image with 7x7 regions*

Figure 39. *Face regions weights sample taking into account human recognition system*

In experimental results chapter, different sets of block weights are defined taking into account above assumptions in order to later decide, in a empirically way, the combination to produce best classification results.

5.3.2. Dissimilarly Metrics

5.3.2.1. Chi Square

For face identification task, first a model for each identity, $\boldsymbol{M_i}$, is required and the simplest way is to calculate the mean value of the $\boldsymbol{N}$ enhanced histograms of each identity. Another possibility is to choose one image under each different illumination for each individual. Doing this way the illumination problems can be reduced at the expense of a higher computational cost. On the other hand, the simplest option is to select just one image as a representative model of the individuals, although the problem will be to find out the best image of the ID dataset that can represent the whole dataset.

Once the models are obtained, training stage is finished and a dissimilarly metrics for histograms is required to compare input samples with the $\boldsymbol{M_i}$ models. In [4], the following methods are proposed:

- Histogram Intersection:

$$D(S,M) = \sum_i \min(S_i, M_i) \tag{49}$$

- Log-Likelihood Statistic:

$$L(S,M) = -\sum_i S_i \log M_i \tag{50}$$

- Chi Square Statistic:

$$\chi^2(S,M) = \sum_i \frac{(S_i - M_i)^2}{|S_i + M_i|} \tag{51}$$

Where $\boldsymbol{S}$ is the current feature vector sample, $\boldsymbol{M}$ is one identity model.

All these measures can be extended to the spatially enhanced histogram by summing up over each face region. Taking *Chi Square Statistic* as the best option for this face recognition application (proposed by *A.Hadid* and *T.Ahonen*), it can be extended for each region and also a different weight can be given for each image block.

$$\chi_w^2(S,M) = \sum_{i,j} w_j \frac{(S_{i,j} - M_{i,j})^2}{|S_{i,j} + M_{i,j}|} \tag{52}$$

where w_j is the weight for region j.

As already exposed in section *5.3.1*, in experimental results chapter will be empirically found out the most suitable w_j weight value for each j region that will enable to achieve a notable identification ratio of 98.74%.

5.3.2.2. Principal Component Analysis

Chi Square Statistic is an adequate method to compare input 2891-bin feature vector to each ID model and experimental results chapter will show the satisfactory (more than 98%) identification ratios achieved. Nevertheless, by experimenting with block weights, it comes the idea that some of the blocks seem to be more important than others, in terms of face description, and that some feature elements may be correlated or simply not given enough significant information to the identification task.

Therefore, it is decided to use the already implemented *Principal Component Analysis*, tested in Face Detection task, to remove redundant information from enhanced face recognition feature vector.

Application to face recognition

Following *Face Detection* section *4.3.2 Principal Component Analysis* and focusing in face recognition application, the method consists of computing the eigenvectors of the input 2891-bin feature vectors taking into account all available samples of all individuals participating in the identification scheme or at least a representative sample of length equal to input vector length.

Enhanced feature vector in face recognition task contains 2891 elements, a quite huge number of elements. For that reason, PCA is an interesting technique to reduce data dimensionality by avoiding irrelevant information.

In order to decide the L significant eigenvectors, a commitment between data dimensionality reduction and relevant information (% Info) preservation is required. Therefore, the most suitable L number is empirically decided by maximizing the positive identification ratio of the particular system.

Then, in the training stage not only the mean model $\boldsymbol{M_i}$ of each individual is calculated but also the *PCA* matrix using input individual samples. The mean models will be stored after projecting them to the orthonormal basis in order to reduce models number of elements from D to L elements.

In the identification task:

- The stored $\boldsymbol{M_i}$ models are back-projected (see *Figure 17*).
- For each input face, the enhanced feature vector is computed.
- Then, the enhanced feature vector is projected and back-projected to the L eigenvectors of the *PCA* transformation matrix to remove irrelevant information.
- Finally, the minimum distance to $\boldsymbol{M_i}$ will identify the individual face under study.

The comparison between the input sample, $\boldsymbol{S_i}$, and the model, $\boldsymbol{M_i}$, could be also done in the projected space but it is done in the back-projected (original space) in order to be able to use face region weights.

As it will be demonstrated in experimental results, after adjusting the optimal number of eigenvectors to be discarded, this method is able to improve identification ratio from 98.74% to 99.14%.

Chapter 6

Image Databases

Before starting with the *Experimental Results* chapter, a briefly presentation of the databases used in the different tests (face detection, face recognition and skin detection) needs to be introduced. In ***Appendix II. Face Databases*** a more detailed explanation can be found and also about other databases mentioned in the literature used for this research, as the *FERET* and the *CMU* databases.

Notice that in order to double the number of face samples available in face detection and recognition face databases, a flipped version is created for each single face image. Therefore, in the following tables, when talking about number of faces, the corresponding flipped versions are included. That means that the original database contains the half of face images.

(a) warp_130x151_BioID_0489.bmp

(b) flip_warp_130x151_BioID_0489.bmp

Figure 40. *BioID image sample and its flipped version*

6.1. Brief Description

6.1.1. GTAV Internet Faces & Non-Faces & Skin Database

GTAV (*Grup de Tecnologies Audio-Visuals*, see [42]*)* from *University of Catalonia* owns an image database containing collected images from Internet: 3325 face image samples of 24x24 pixels and 1931 non-face images of different sizes. In *Appendix I.1.1*, further information can be found and some image samples

In this research project, the faces subset from *GTAV* is only useful in face detection experiments because of its 24x24 pixels size, too small for face recognition purpose. Non-faces subset is used in all face detection experiments, together with GTAV Internet or BioID face database. Moreover, the skin samples to train the skin detector are manually collected from this non-faces subset.

For face detection, as the face in the images are not totally centered, see *(a)* sample image in *Figure 41*, to apply *LBP* operator the images are required to be cropped to fit just the face area and centered. The crop option that best fits these sample images results in 16x16 pixels face images. Although in the literature the recommended face image size for detection is 19x19, to avoid resize artifacts, it is decided to use the 16x16 images for the face detection experiments.

(a) nova1.bmp (24x24) *(b) 16x16_nova1.bmp*

Figure 41. *Original image sample and its 16x16 face extraction result*

Also for face detection experiments, non-faces subset is used. It contains 1931 images of different sizes, of which around 65000 samples of 19x19 pixels size (to be compatible with *BioID* 19x19 face samples) are randomly extracted to be used for face detection experiments as non-faces samples.

For skin detector training stage, several skin images with different skin tones (different races), illumination conditions and camera calibrations are required. They are manually collected from *GTAV Internet* database, as its sample images are colored, resulting in a training set of 85 skin images with a total of 9,163 skin pixel samples.

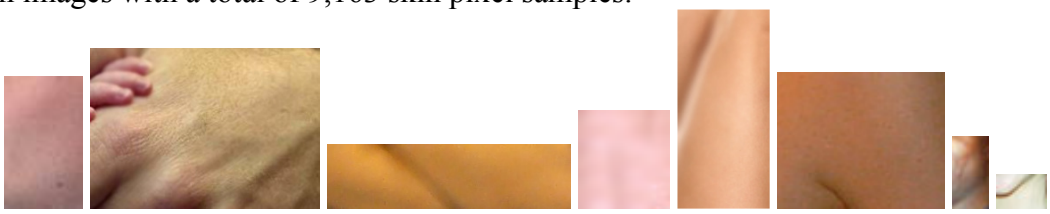

Figure 42. *Skin samples from GTAV Internet database*

6.1.2. BioID Faces Database

Briefly, the *BioID Face Database* is used in both detection and recognition experiments and it contains 1521 images (384x286) having only one face from **23 different persons**, with a large variety of illumination, background and face size. Moreover, each image, labeled ***BioID_xxxx.pgm***, has its corresponding ***BioID_xxxx.pts*** file containing 20 additional feature points, which are very useful for facial analysis and gesture recognition.

In *Appendix* I.1.2, detailed information can be found about the database itself and the procedure followed to adapt these images to our experiments.

An example of the result of this adjustment can be observed in below *Figure 43*, where *(a)* is the original image, *(b)* is the adapted version for face detection and *(c)* for recognition purpose.

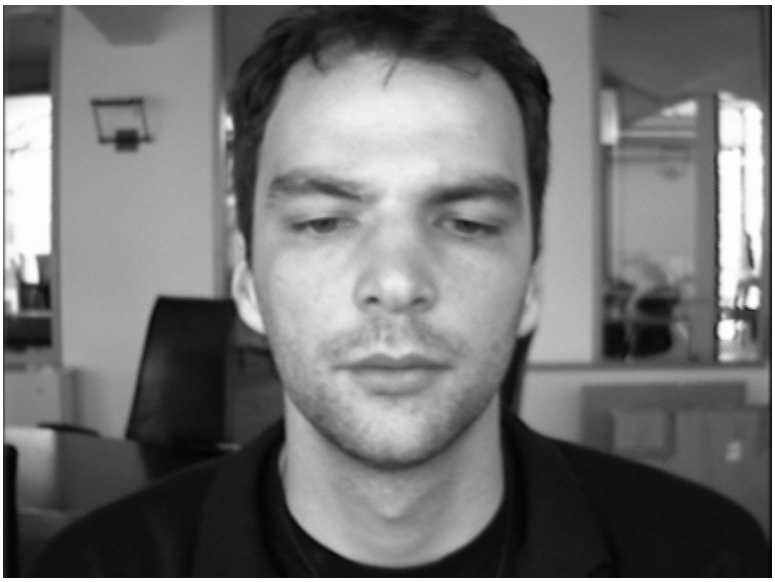

(a) Original image (BioID_0000.bmp)

*(b)Adapted image for face detection (warp_**19x19**_BioID_0000.bmp)*

*(c) Adapted image for face recognition (warp_**130x151**_BioID_0000.bmp)*

Figure 43. *BioID database images adaptation for face detection and recognition purpose*

6.1.3. EPFL Skin Database

For skin detection testing purposes, 300 images from *EPFL* (*Ecole Polytechnique Fédérale de Lausanne*) *skin database* are used. This database contains for each image a mask file in *Portable Bit Map* format (*.pbm*), indicating with ´1´ skin pixels and with ´0´, non skin areas.

(a) Image 973763.bmp

(b) Mask 973763.pbm

Figure 44. *Skin sample from EPFL skin database(973763)*

6.2. Face Detection

In order to build an appearance-based detection scheme, large training sets of images are needed in order to capture the variability of facial appearances.

Training Subset

In the training subset all the available face images have been used and as it can be observed in next *Table 7*, in case of non-faces images, approximately the same number of samples has been taken to be used together with *GTAV* database and about the double to be used together with *BioID* database.

On the other hand, notice that the total number of negative samples will be iteratively increased when using the bootstrap strategy (see section *4.4.1.1*) in the training process.

TRAINING	# Faces			# Non Faces		
Experiment	Database Name	# Samples	Image Size	Database Name	# Samples *	Image Size
1	GTAV	6650 from 6650	16x16	GTAV	6605	16x16
2	Bio ID	2981 from 2981	19x19	GTAV	6605	19x19

Table 7. *Training Subsets for face detection (*before bootsraping)*

Test Subset

Due to the reason that it is very important to have the largest training set available, all face samples are used in the training subset and only a portion is used for test purpose.

The non faces images number is selected so that the sum of faces and non faces is 65536:

TEST	# Faces			# Non Faces		
Experiment	Database Name	# Samples	Image Size	Database Name	# Samples	Image Size
1	GTAV	2000 from 6650	16x16	GTAV	63536	16x16
2	Bio ID	1500 from 2981	16x16	GTAV	64036	16x16

Table 8. *Test Subsets for face detection*

Parameters

The relationship between image size before and after applying LBP operator, block dimension and overlapping is described by the following formulas:

$$\begin{aligned} IMG\_MIN\_WIDTH' &= (NO\_OVERLAPPING \times 3) + OVERLAPPING \\ IMG\_MIN\_HEIGHT' &= (NO\_OVERLAPPING \times 3) + OVERLAPPING \\ NO\_OVERLAPPING &= BLOCK\_DIM - OVERLAPPING \\ IMG\_MIN\_WIDTH &= IMG\_MIN\_WIDTH' + 2r \\ IMG\_MIN\_HEIGHT &= IMG\_MIN\_HEIGHT' + 2r \end{aligned} \tag{53}$$

where r is the LBP operator radius.

And $'$ indicates the image size after applying LBP operator, reduced due to the borders treatment when applying LBP operator of radius r.

6.2.1. Reference Image

In order to visually compare different face detection methods a reference image is selected to perform this task.

Next figures shows reference image that contains 10 faces with size around the minimum size in this research project (16x16 and 19x19) and with some areas, like the knees, with some kind of "face appearance" that can lead to misclassification.

Figure 45. *Reference image equipop.jpg (319x216 pixels)*

6.3. Face Recognition

A part from the Internet face database for face detection purposes, *GTAV* group has another interesting face database for face recognition testing, see [43], with 240x320 pixels images in BMP format. This database includes a total of 44 persons with 27 images per person with different pose views (from 0º to ±90º) and under three different illuminations. But it is decided not to use it because no face features points files are available, requiring a pre-manual marking of the interest point to be able to crop them to the desired size and form.

For that reason, in face recognition experiments the *BioID database* is selected containing:

- An amount of 23 different IDs from men and women.
- For each image the faces points file is available, then it is easy to crop faces to the desired size.
- For each ID, there are samples with different illumination and pose.

Training and Test Subsets

All the available samples are used for both training and testing.

TRAINING/TEST	# Faces		
# IDs	Database Name	# Samples	Image Size
23	Bio ID	3042	130x151

Table 9. *Training and Test Subsets for face detection*

However, for training proposes some aberrant samples has been not taken into account, like the following affected by the image adaptation pre-process (see *Appendix I.1.2*).

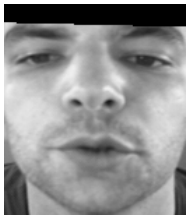

Figure 46. *BioID Database aberrant sample after image adaptation process*

Therefore, in next *Table 10*, it can be observed that in some cases the number of samples used for each individual for training is lower than for testing, where also the aberrant samples has been taken into account.

	Training Samples (Mean Value Model)	**Test Samples**
ID1	188	216
ID2	120	120
ID3	194	194
ID4	80	80
ID5	198	198
ID6	4	4
ID7	113	118
ID8	152	156
ID9	168	176
ID10	176	176
ID11	120	122
ID12	133	142
ID13	212	212
ID14	297	298
ID15	184	188
ID16	100	100
ID17	102	102
ID18	70	70
ID19	80	80
ID20	12	12
ID21	92	92
ID22	102	102
ID23	50	50

Table 10. *Training and Test Subsets for face recognition*

And the following figure shows the image representation selected for each ID subset:

Figure 47. *BioID Database 23 different identities*

Chapter 7

Experimental Results

In this chapter, empirical results of previous sections theory, both face detection and recognition, are exposed. First section is dedicated to *Skin Segmentation* as a previous step to face detection testing.

In order to better understand this chapter, next *Figure 48* is intended to give an overview of the experimental section flow. As it can be observed, there are three main blocks: *Skin Detection*, *Face Detection* and *Face Recognition*.

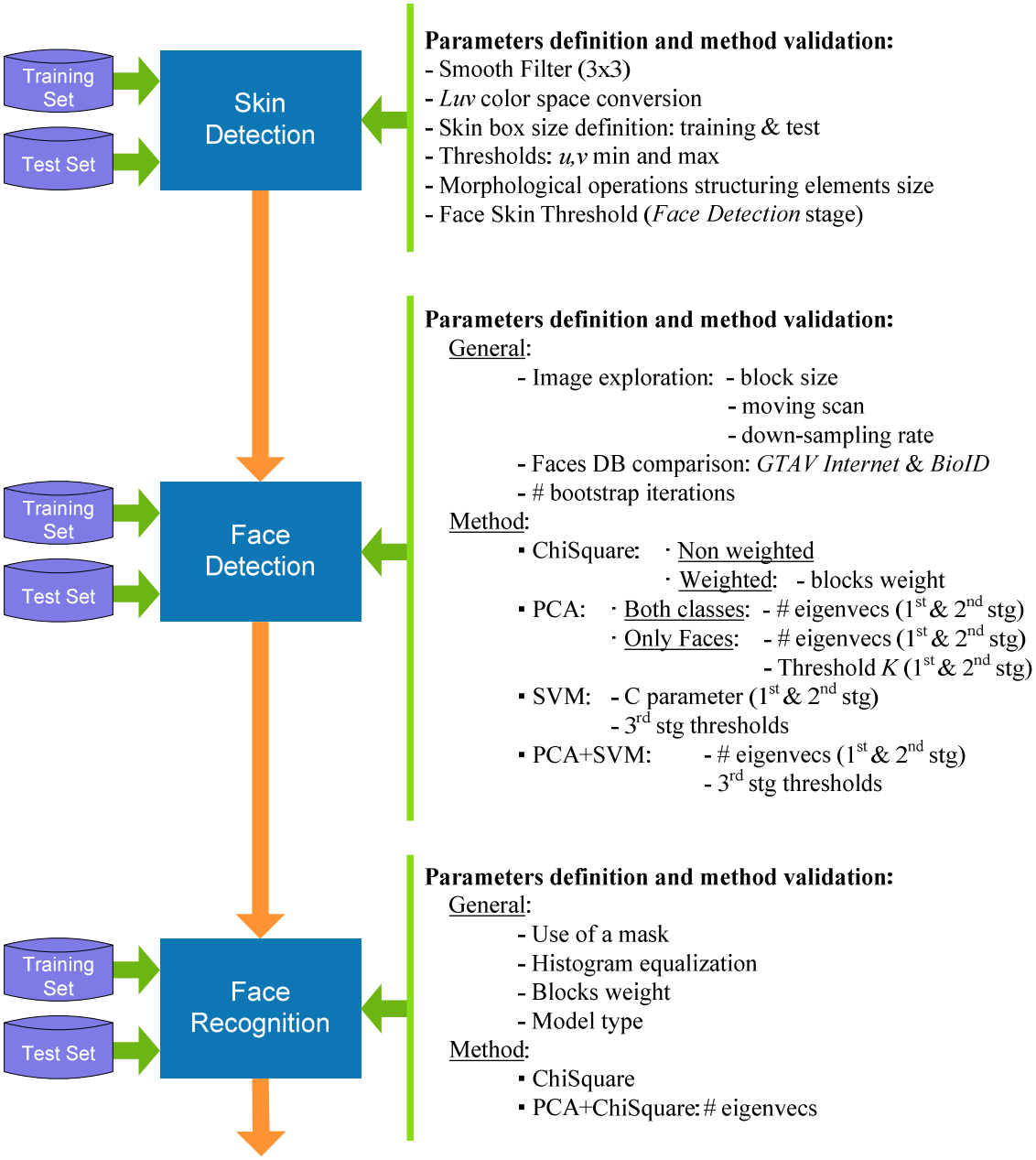

Figure 48. *Experimental Results Overview*

Each block, can be seen as an independent system with two basic stages: training and test. Thus, images set for each stage is required. As they will directly influence in the final performance of the system, the appropriate selection of the images databases takes an important role. Therefore in some cases, such as the face detection experiments, two different databases will be used to compare results. In previous *Chapter 6*, image databases used for each experiment are introduced.

In *Figure 48*, on the right side of each block, most important parameters of each block are listed. In case of having such a large number of unknown variables, a coarse to fine adjustment is recommended, where some initial values are proposed based in the system knowledge, then the system is trained and tested with the different options and afterwards the best option is taken and fine adjusted.

Furthermore, for simplicity in the experiments, some variables are treated independently although they may have an influence in later stages.

7.1. Skin Detection Experiments

This section is intended to describe skin detection experimental results following *4.4.2.1 Skin Segmentation* theory chapter.

The training stage consists of manually select skin areas in collected images, in this case, from *GTAV Internet database*. The main idea is to have several skin images with different skin tones, illumination conditions and camera calibrations. Then extract chromaticity information, *u* and *v* mean values (see equation (35)), in order to be able to define skin decision thresholds.

Using skin training database (see section *6.1.3*), the *u* and *v* mean values is computed for each training block of size defined by equation (36). The result is shown in following *Figure 49,* where the *u* and *v* mean values for each training block from 85 skin training data images (9,163 points) are represented together with 363 non skin data images (36,300 points). In yellow the defined skin region.

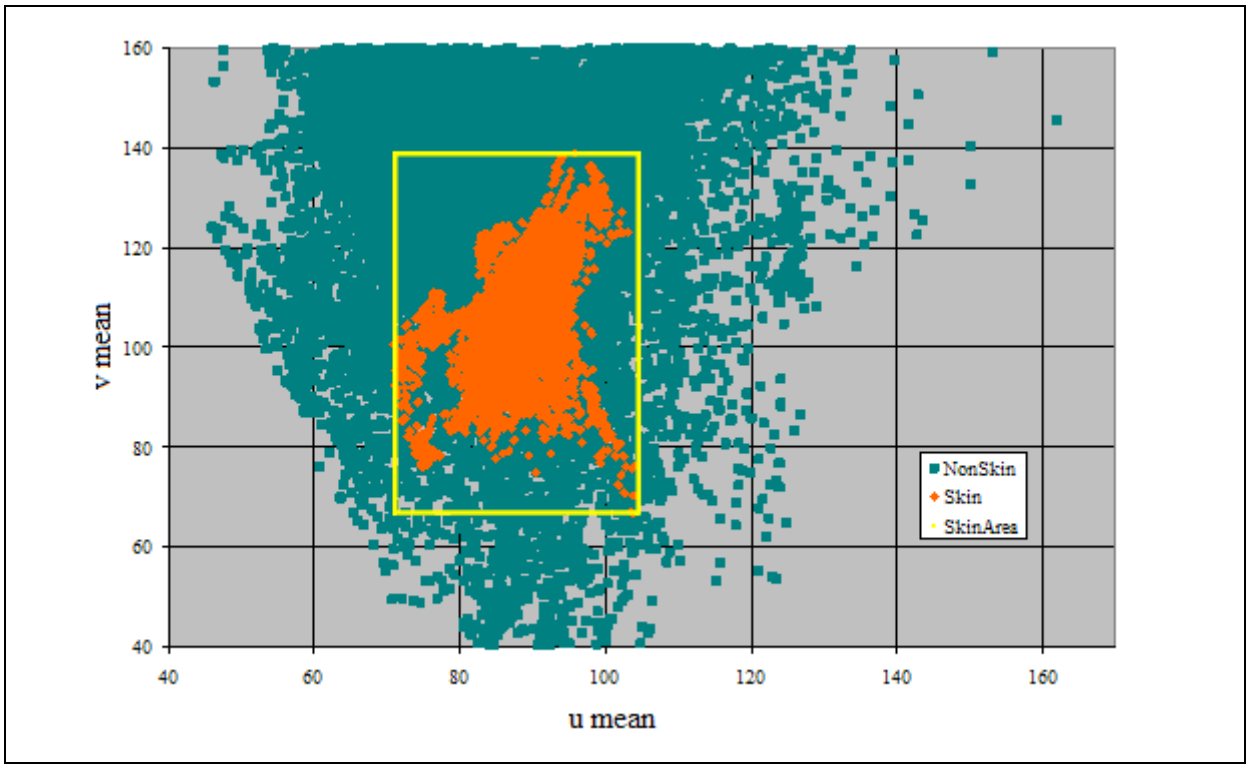

Figure 49. *Skin area definition: u and v mean values plot*

As explained in section *4.4.2.1 Skin Segmentation,* for simplicity, a rectangle is used as a skin region definition. The resulting border limits used as skin thresholds are the following:

$$u\text{ Thresholds} = \begin{cases} u\min = 71 \\ u\max = 104 \end{cases}$$
$$v\text{ Thresholds} = \begin{cases} v\min = 67 \\ v\max = 140 \end{cases} \qquad (54)$$

For the test stage, equation (37) defines the *skin detection box size*. In this research, two minimum face sizes are used depending on the face database: 16x16 and 19x19. For that reason, the resulting ***skin detection box size*** for both cases is **4x4 pixels**.

Once the *u* and *v* chromaticity coordinates mean value of each *skin detection box* is calculated, the above thresholds are applied in order to decide if the box is labeled as skin or not.

In order to validate, the skin detection method 300 images from *EPFL skin database* are used in the test stage resulting in the following results:

	True Positive	**False Positive**
pre-mask	98.68 %	72.67 %
skin mask	**98.45 %**	**72.91 %**

Table 11. *Skin detection results using EPFL skin database*

Above *Table 11* shows the detection ratios in case of using the ***pre-mask*** and the final ***skin mask*** of the:

- *True Positives*: skin pixels correctly detected as skin.
- *False Positives*: non-skin pixels wrongly detected as skin.

As already exposed in section *4.4.2.1*, note that ***pre-mask*** is the result of applying skin model thresholds and ***skin mask*** is the final mask resulting of applying morphological operations to the pre-mask.

In order to be able to correctly interpret these results, it has to be taken into account that the pre-mask post processing with morphological operations is intended to:

- Detect face skin rather than skin: therefore, skin regions smaller than the minimum face size are removed.
- Uniform mask: without holes due to eyes and mouth areas because in face detection process, each new block under analysis will be classified as skin if 95% of the pixels are marked as skin. Therefore, pixels are evaluated taking into account their neighborhood and also dilation is used to achieve uniform mask.

Moreover, any object with "skin" color is detected as skin.

In following *Figure 50*, all these factors can be observed. For instance, notice that:

- The difference between the *pre-mask (c)* and the final *mask (d)* is that the areas smaller than a face resolution have been removed.
- The difference between *original mask (b)* and our process masks *(c)(d)* is that the first one labels each single pixel individually and in *(c)(d)* uniform mask are achieved.
- In *pre-mask (c)*, it can be observed that also non skin areas with skin color are labeled as skin. In that particular case, after morphological operations, in *(d)* it is removed because the size is smaller than face resolution.

(a) Original *(b) pbm_Mask* *(c) skinPreMask* *(d) skinMask* *(e) Result*

Figure 50. *Skin sample from EPFL skin database (2209950): masks comparison*

Now, *Table 11* results can be interpreted and understand why they are very good for this particular face detection application:

- *False positives* are very high because our process is:
  - detecting not only skin but also non-skin objects with skin color.
  - using uniform masks. In final *skin mask*, false detection ratio is higher than in *pre-mask* because dilation is applied.
- *True positives* is not 100% because our process is:
  - removing skin areas smaller than face resolution, therefore the detection ratio is lower in final *skin mask* than in *pre-mask*.
  - using a different skin criterion in some difficult cases such as the one shown in next *Figure 51*.

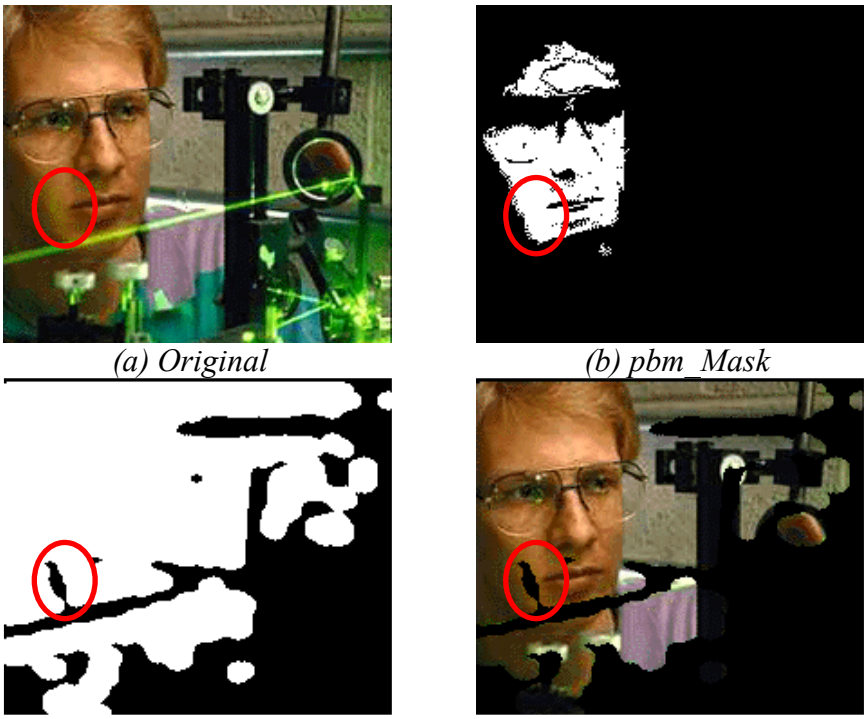

(a) Original *(b) pbm_Mask*

(c) skinMask *(d) Result*

Figure 51. *Skin sample from EPFL skin database (886043): different skin criterion*

The following samples are the result of performing the skin segmentation procedure using 2 moving scan pixels and 1.2 down-sampling (see section *4.1*). The original reference image is shown together with different down-sampling steps masks.

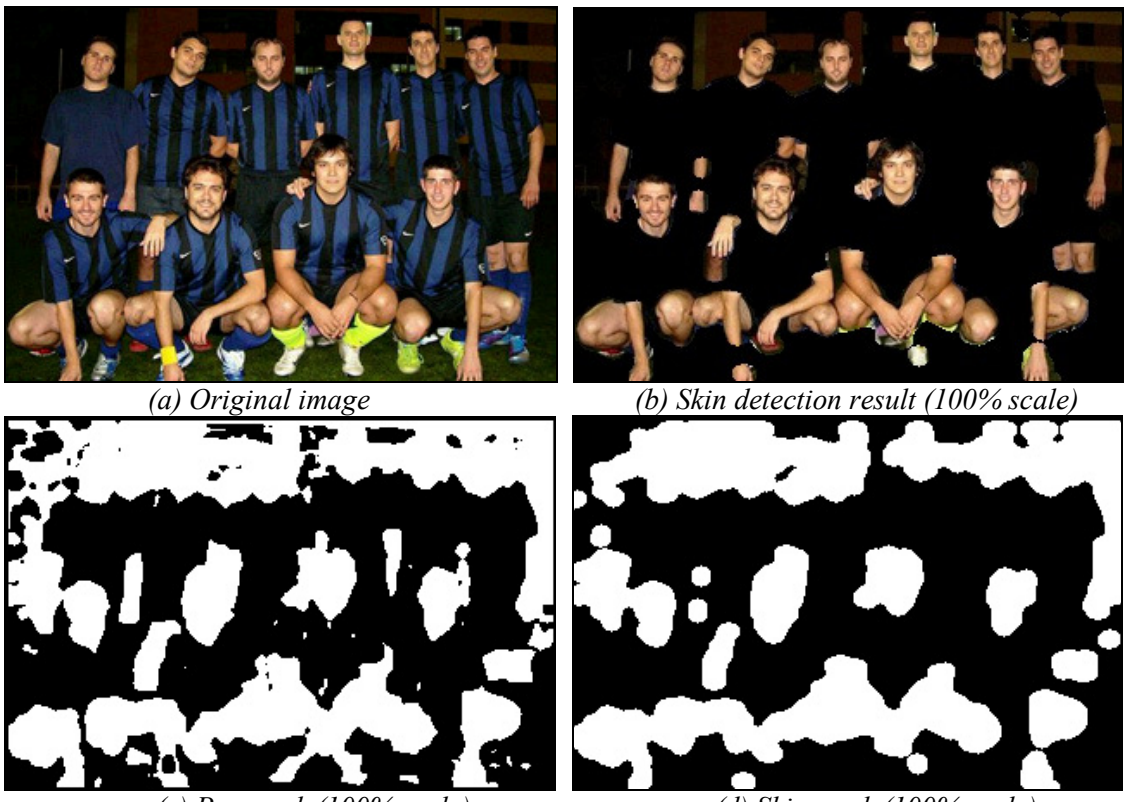

(a) Original image *(b) Skin detection result (100% scale)*

(c) Pre-mask (100% scale) *(d) Skin mask (100% scale)*

(e) Pre-mask (69.44% scale)

(f) Skin mask (69.44% scale)

(g) Pre-mask (33.49% scale)

(h) Skin mask (33.49% scale)

Figure 52. *Skin segmentation example 1 (case 16x16): equipop.jpg*

(a) Faces composite original image (100% scale)

(a) Pre-mask (23.26% scale)

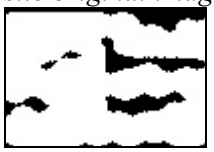

(b) Skin mask (23.26% scale)

(c) Skin result (23.26% scale)

Figure 53. *Skin segmentation example 2 (case 16x16): faces_composite_1.jpg*

As seen in theory chapter *4.4.2.1*, applying morphological operations improves significantly the resulting mask by eliminating:

- Dark and small elements like the eyes and mouth in a face. This effect can be observed in *Figure 53*.
- Skin regions smaller than the minimum face size. That can be clearly observed in above *Figure 52,* where small skin regions like arms, legs or hands smaller than 16x16 are removed.

Spending this time in skin segmentation will save a lot of time when exploring an image for face detection. The time improvement is difficult to quantify, because it obviously depends on the image type and background. The method will be very useful in case of having one person in a field with a green background and blue sky, but not in case of having an image with plenty of people or a color background similar to skin color like brown or orange.

7.2. Face Detection Experiments

Before implementing the face detection method proposed in the literature, *Support Vector Machine*, a first approach to LBP potential is done by means of simpler classification methods.

In order to build an appearance-base detection scheme, large training sets of face images are needed to capture the facial appearance variability. Moreover, it is no easy to find the best non-faces set that best describe all non-faces texture possibilities. Therefore, a first random set is collected from different images and then a bootstrap strategy of different iteration is applied.

As explained before, this bootstrap strategy consists of training the system, classifying the non-faces training set and reintroducing several times non-faces that are wrongly classified in the training set until a trade-off between faces and non-faces correct detection ratios is reached.

For each experiment the same number of test image (see *Table 12*) is used.

	TEST images
faces	2000
non faces	63536
total	65536

Table 12. *Number of test images used in every experiment*

Table 13 contains the different parameters used for each face database in face detection experiments and taking into account (53) equations:

		Faces set	
	Parameters[pixels]	***GTAV***	***BioID***
Before LBP	Minimum Image Width	16	19
	Minimum Image Height	16	19
After LBP	Minimum Image Width	14=(4x3)+2	17=(4x3)+5
	Minimum Image Height	14	17
	Blocks Dimension	6=4+2	9=4+5
	Overlapping factor	2	5

Table 13. *Face detection parameters for both face databases*

Image size difference before and after applying LBP is due to the borders treatment when applying LBP operator of radius 1:

- $LBP_{(4,1)}$ in 1st stage.
- $LBP_{(8,1)}$ in 2nd stage.

7.2.1. Chi Square Classification

As it will be later seen in face recognition experiments, very satisfactory results can be achieved by using this simple dissimilarly metric, called *Chi Square* (see section *4.3.1*). Because of this, it was decided to use it also for evaluating LBP face detection capability.

7.2.1.1. Non Weighted

Using *non weighted Chi Square* scheme, two experiments are performed with different face databases. These tests give an idea of the quality of each face database.

For instance, *GTAV Internet* face database contains approximately twice the number of face images that contains *BioID* face database. Consequently, it can be supposed that *GTAV Internet* will describe better the face appearance variability. On the other hand, *GTAV Internet* set does not have the recommended size of 19x19 (see [5]) for LBP face detection method, but *BioID* has it. That means, that maybe *BioID* can offer better classification results. Therefore, a part from evaluating LBP face detection potential, the aim of the following experiments is also to find an answer to these questions.

Figure 54 presents the classification result using mean value models and *Chi Square* dissimilarly metric. For each bootstrap iteration of the training process, first plot displays faces (in orange) and non-faces (in blue) detection ratio for 16x16 *GTAV Internet* database and second for 19x19 *BioID* database. Detailed information about the plotted values can be found in *Table 32* (16x16) and *Table 33* (19x19) in *Appendix III.1.2*.

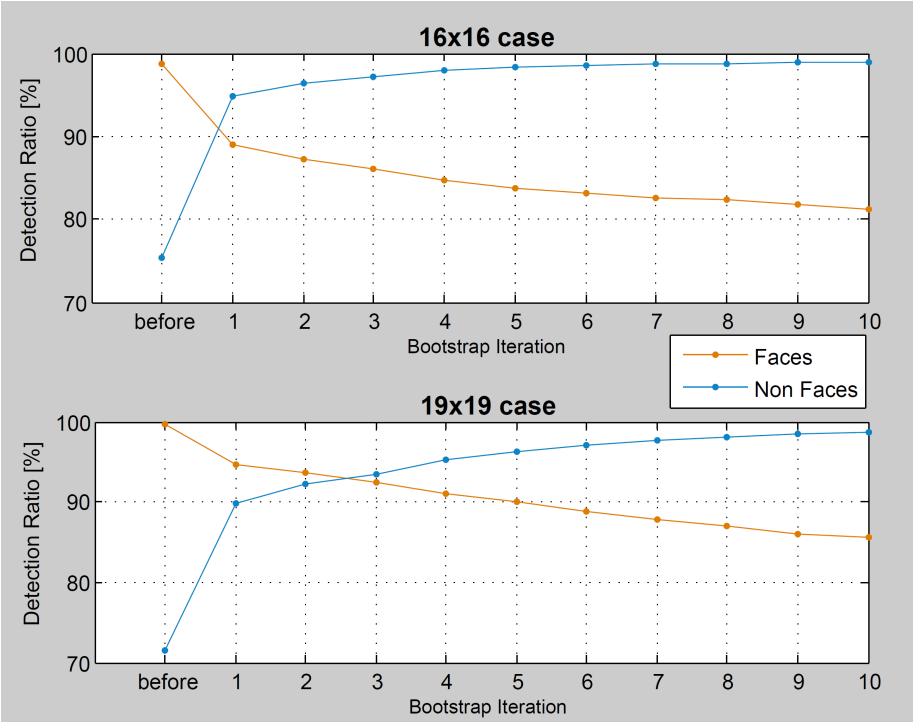

Figure 54. *Bootstrap to improve Mean Models & Chi Square classification ratio (16x16 & 19x19)*

At each bootstrap iteration, face detection rate is decreasing but non-faces detection is increasing. This is an unavoidable compromise in order to be able to correctly classify such a huge class as it is non-faces one.

As already exposed in section *4.4.1.1*, sometimes it is not possible to converge to a point of no false detections and a commitment between detection ratio drop and false alarm ratio improvement is required. Therefore, the best selection should be the intersection between both curves. For instance, taking the first bootstrap iteration for 16x16 case and the second or third iteration for 19x19 case.

Notice that in 19x19 case, although convergence needs more iterations than in 16x16 case, the reached point achieves better results in terms of face correct classification rate.

As a first conclusion, *mean value models* with C*hi Square* is an easy classification method that provides satisfactory classification rates and it is useful to observe *LBP* qualities as a face descriptor.

On the other hand, *BioID* seems to have better qualities as a face dataset. But from a realistic point of view, *GTAV Internet* faces set contains a wider range of different faces than *BioID* faces set which samples correspond to only 23 different people. Because of this, as the test samples are more similar to the training ones in *BioID* better results can be achieved.

Therefore, let us compare both training results classifying a reference image that has nothing to do with both face databases. In both cases, skin segmentation is used in order to improve face detector scheme, see *Figure 52*. Each face candidate is marked with a yellow box and after overlapping detections removal (see section *4.4.2.2*) only one box (in red) is kept per face.

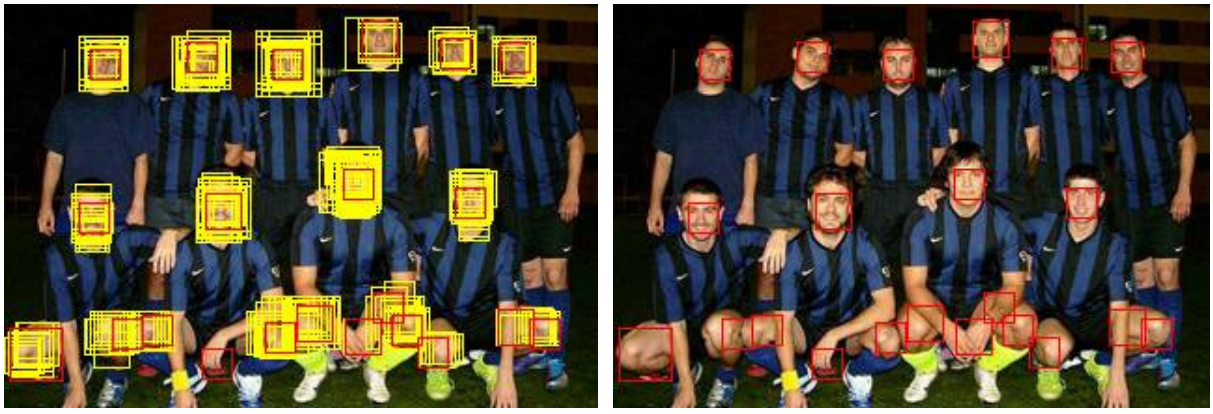

Figure 55. *Chi Square - ref img classification using GTAV Internet training set (16x16)*

The result using *GTAV Internet* as training samples can detect the 10 faces but non faces misclassification is very high. As faces set contains 2000 totally different faces from 2000 different people, face appearance variations is very high and a mean model of the LBP enhanced histogram is not enough to separate faces from non faces, because regions with non flat texture are misclassified as faces.

Figure 56 shows the results of classifying the reference image with *BioID* faces as training set.

Figure 56. *Chi Square - ref img classification using BioID training set (19x19)*

Compared to previous result, *BioID* training samples provides better results when classifying non faces, although only 6 from 10 faces are correctly detected. Nevertheless, notice that misclassified faces have a size in the limit or below of detection resolution, 19x19. Moreover, non faces classification appears in some regions with texture similar to a face.

As a conclusion, *BioID* faces set and size 19x19 offer better general detection ratios. However, this classification method, Chi-Square with mean value models, is not good enough to discern between faces and non-faces. LBP enhanced histograms mean value models are not able to correctly represent whole faces and non faces samples sets.

7.2.1.2. Weighted

One option to improve previous results is to use a different weight for each block of the 2nd classification stage as proposed for face recognition.

The following table shows the result of using different weights when classifying test data. The mean models used for each face database is the one resulting from its last bootstrap iteration. Notice that left columns, in green, display the 3x3 block weight.

		16x16 **GTAV Internet**		*19x19* **BioID**	
		% Faces	% Non Faces	% Faces	% Non Faces
(1)	1 1 1 1 1 1 1 1 1	78.30%	99.41%	78.55%	99.61%
(2)	1 1 1 1 **2** 1 1 1 1	78.45%	99.29%	77.90%	99.63%
(3)	1 1 1 1 1 1 **0** 1 **0**	78.50%	99.12%	75.55%	99.22%
(4)	1 1 1 1 **2** 1 **0** 1 **0**	78.45%	98.83%	74.45%	99.29%
(5)	1 **2** 1 1 **2** 1 1 1 1	78.90%	99.37%	78.15%	99.60%
(6)	1 **2** 1 1 **2** 1 **0** 1 **0**	78.70%	99.00%	74.85%	99.27%

Table 14. *Weighted blocks results in 2nd classification stage for both face databases*

As it can be observed in previous table, for *GTAV Internet* faces set using different blocks weight a better faces classification is achieved, but non faces decreases in all cases.

On the other hand, for *BioID* better results are obtained by giving more weight to the central block (2).

In next figures, it can be observed the classification improvement for the reference image for both face databases.

For 16x16 faces case, the face detection ratio is kept while decreasing non faces misclassification:

Figure 57. *Chi Square Weighted (2) - ref img classification using GTAV training set (16x16)*

On the other hand, for 19x19 faces case, faces and non-faces detection ratio increase. Notice that now 7 from 10 faces have been correctly detected.

Figure 58. *Chi Square Weighted (2) - ref image classification using BioID training set (19x19)*

It can be concluded that *Chi Square* method is improved when using block weights in LBP second fine stage. However, although *Chi Square* is an interesting approach to discover LBP potential but it is not good enough for a valid face detection scheme.

7.2.2. Principle Component Analysis

As explained in previous chapter (see section *4.3.2*), in a first approach, one PCA orthonormal basis for both faces and non faces is calculated in order to minimize data dimensionality. And then, in a second approach, another experiment is proposed using only faces class.

7.2.2.1. Face/Non Face Models & Relative Difference Normalized

In this chapter, the target is to find out the optimal number of eigenvalues to reduce data dimensionality without much data loss and keeping an adequate detection ratio.

The training and test data used for these experiments are the already introduced in *Table 7* and *Table 8*. Following *Figure 59* show the *normalized eigenvalues*[5] plots for both databases and for the 1st and 2nd stage:

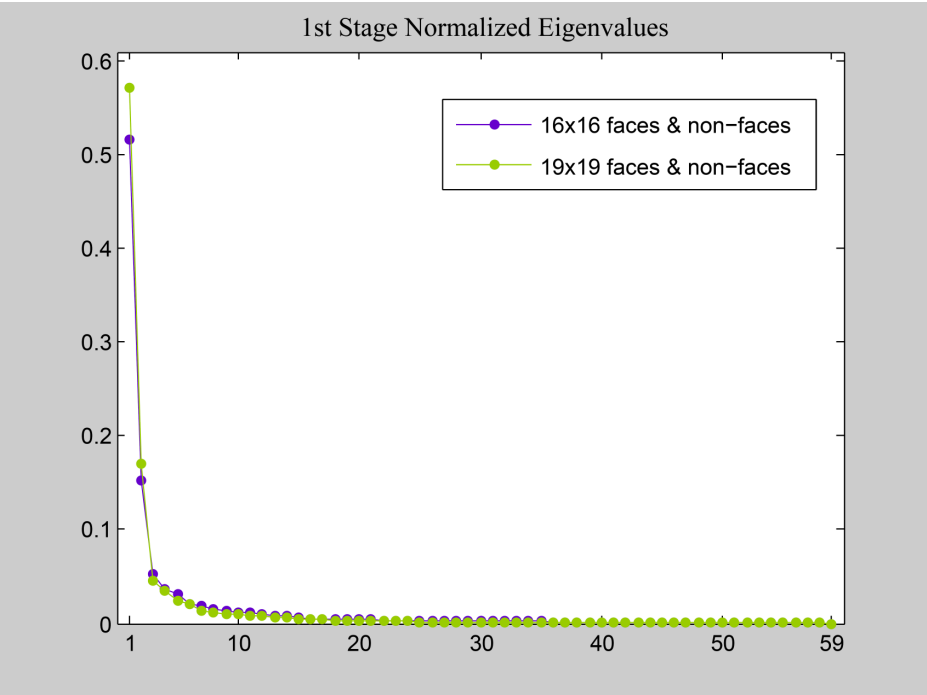

Figure 59. *Face detection PCA - Normalized eigenvalues plot: 1st stage*

The eigenvalues for both face databases are similar, although it can be observed that the *BioID* two first eigenvalues have a higher value than the first two *GTAV Internet* eigenvalues. That means that by keeping only two eigenvalues, a better reconstruction can be achieved with *BioID* face database. Moreover, in both cases, only with this first eigenvalue more than 50% of the information is kept.

[5] Normalized Eigenvalues: $\bar{\lambda} = \frac{\lambda}{\sum_i \lambda_i} \Rightarrow \sum_i \bar{\lambda}_i = 1$

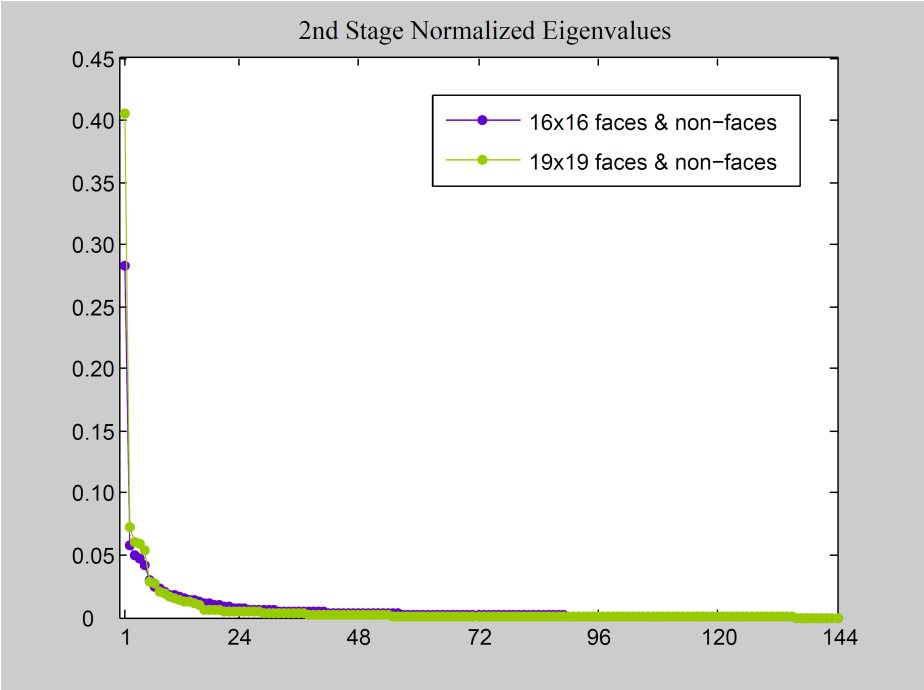

Figure 60. *Face detection PCA - Normalized eigenvalues plot: 2nd stage*

In second stage, it can also be observed that the *BioID* first eigenvalues have a higher value than the first two *GTAV Internet* eigenvalues. But in this case, only the last nine eigenvalues can be considered null.

As explained in previous chapters, these two face databases have different features:

- **16x16 faces**: each face from a different person (more face variety), but faces size is smaller as recommended in the literature (see [5]).
- **19x19 faces**: faces from only 23 different people, but with a large variety of illumination, background and face size (allows to have desired size of 19x19). The number of available samples (2981) is about the half of the 16x16 face database (6650).

Since test faces are included in face training set, it is normal to always obtain better results with 19x19 images *BioID* face database, because for each face exists more samples information than in 16x16 face database where each face is unique. Then with the same amount of eigenvalues a better face detection ratio is obtained with 19x19 face database, although this can indicate a worst generalization to other databases.

In order to better see the above eigenvalues, in *Appendix III.1.3* a table can be found showing the normalized eigenvalues for 1st and 2nd stages for both databases, 16x16 and 19x19 faces.

Different simulations have been done combining the number of eigenvalues (*%Info*) and the two proposed dissimilarity methods in order to find the best parameters to obtain the best detection ratio.

In the following table, some combinations of eigenvalues are proposed to evaluate the method based on the % of information for both face databases. Notice that the % of information is kept the same for both stages.

16x16			19x19		
% Info	Number of Eigenvalues		% Info	Number of Eigenvalues	
	1st Stage	2nd Stage		1st Stage	2nd Stage
51%	1	6	58%	1	4
75%	4	23	79%	3	12
90%	14	56	90%	9	28
95%	25	79	95%	18	48
100%	58	135	100%	58	135
100%	59	144	100%	59	144

Table 15. *Face detection PCA: number of eigenvalues selection based on %Info for both face DB*

Using above combinations of number of eigenvalues, the systems are trained and both test data classified. Next table shows the result of these experiments:

16x16					19x19						
~% Info	Eigenvalues		Detection Ratio		~% Info	Eigenvalues		Detection Ratio		Ratios Sum	Eigenvalues reduction	
	1st Stage	2nd Stage	Faces	Non faces		1st Stage	2nd Stage	Faces	Non faces		1st Stage	2nd Stage
100%	59	144	0.9940	0.6377	100%	59	144	0.9860	0.6701	3.2878	0%	0%
100%	58	135	0.9940	0.6377	100%	58	135	0.9860	0.6701	3.2878	2%	6%
95%	25	79	0.9940	0.6368	95%	18	48	0.9860	0.6693	3.2861	58%	45%
90%	**14**	**56**	**0.9940**	**0.6353**	**90%**	**9**	**28**	**0.9855**	**0.6672**	**3.2820**	**76%**	**61%**
75%	4	23	0.9935	0.6294	79%	3	12	0.9850	0.6628	3.2707	93%	84%
51%	1	6	0.9835	0.5690	58%	1	4	0.9880	0.5445	3.0850	98%	96%

Figure 61. *Face detection PCA: mean detection ratio for different % of information*

The column *Ratios Sum* is the sum of the 4 detection ratios (faces and non faces for both databases). This value is calculated to determinate the best global detection ratio.

The row in yellow is the proposed option for the face detection system under study. A good compromise between eigenvalues reduction and global detection ratio is the followed criterion.

The following experiments are based in the above selection and *Figure 62* presents the classification result using *PCA & Relative Difference Normalized* as dissimilarly metric. For each bootstrap iteration of the training process, first plot displays faces (in orange) and non-faces (in blue) detection ratio for 16x16 *GTAV Internet* database and second for 19x19 *BioID* database. Detailed information about the plotted values can be found in *Table 35* (16x16) and *Table 36* (19x19) in *Appendix III.1.3*.

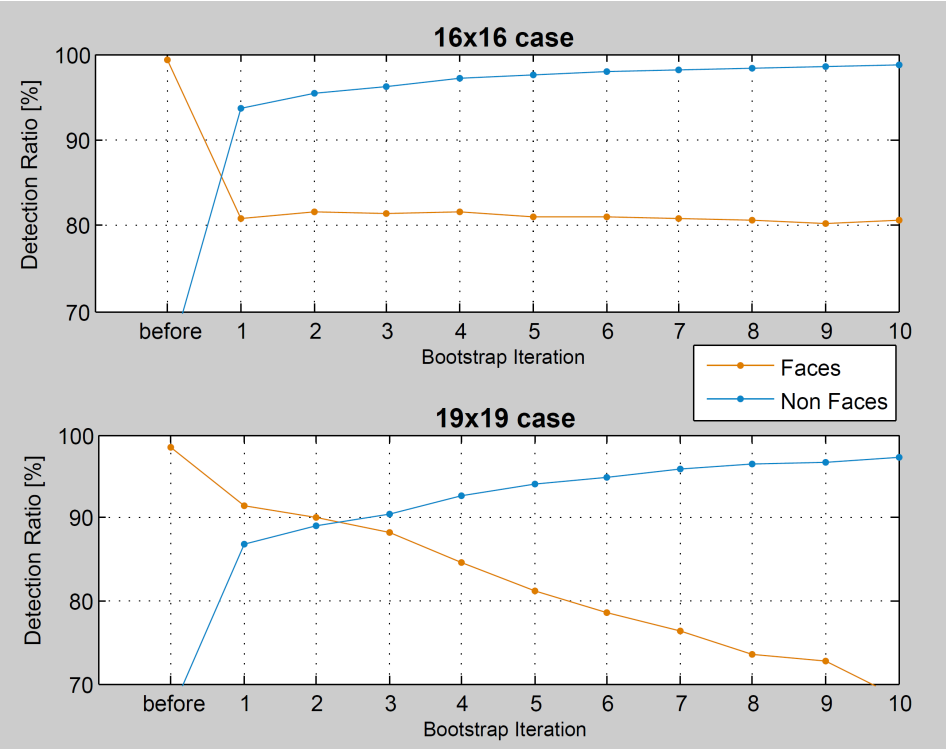

Figure 62. *Bootstrap to improve PCA & RelDiffNorm classification ratio (16x16 & 19x19)*

At each bootstrap iteration, face detection rate is decreasing but non-faces detection is increasing, an unavoidable compromise in order to be able to correctly classify such a huge class as non faces set.

As already exposed previous section, best selection should be the intersection between both curves. For instance, taking the first bootstrap iteration for 16x16 case and the second or third iteration for 19x19 case.

Notice that in 19x19 case, although convergence needs more iterations than in 16x16 case, the reached point achieves better results in terms of face correct classification rate. But on the other hand, it is also interesting to observe that when the number of bootstrap iterations increases, faces detection ratio drops more drastically in case of 19x19 faces size. From that, it can be deduced that 16x16 face database is capable of providing more stable results in terms of generalization, as face detection ratio is less affected by the non-faces classes training set.

As a first conclusion, this classification method provides also satisfactory classification rates and it is useful to observe *LBP* qualities as a face descriptor.

It can also be extracted that *GTAV Internet* faces seems to have better qualities as a face dataset and it achieves better generalization results due to the fact that contains a wider range of different faces than *BioID* faces.

As in previous chapter, the reference image (*equipop.jpg*, see *Figure 52*) is used to compare both results. In both cases, skin detector is used in order to improve face detection scheme.

Each face candidate is marked with a yellow box and no boxes post processing is applied to keep only one box per face. The result is given by simply applying a boxes mask.

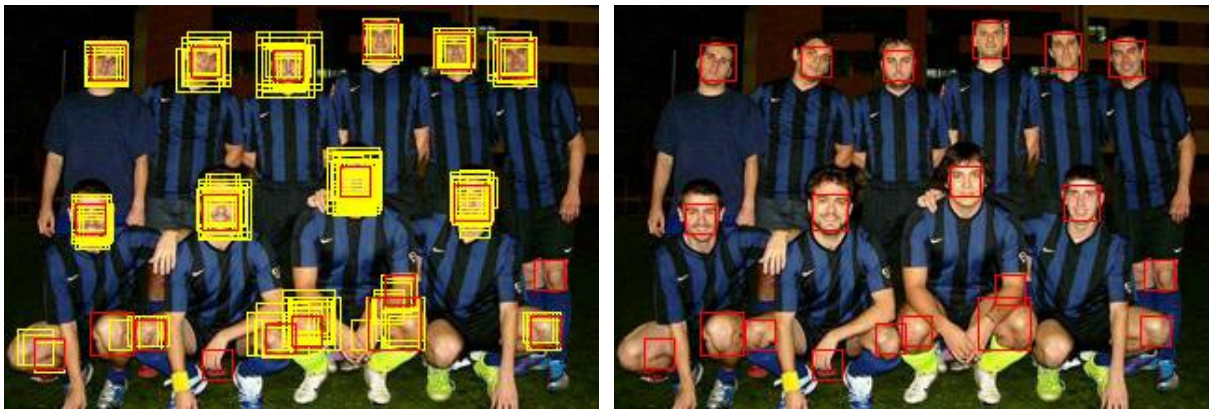

Figure 63. *PCA & RelDiffNorm - ref img classification using GTAV Internet training set*

The result using *GTAV Internet* as training samples can detect the 10 faces but non faces misclassification is very high. As faces set contains 2000 totally different faces from 2000 different people, face appearance variations is very high and a mean model of the LBP enhanced histogram is not enough to separate faces from non faces, because regions with non flat texture are misclassified as faces.

Next *Figure 64* shows the results of classifying the reference image with *BioID* faces set as training samples.

Figure 64. *PCA & RelDiffNorm - ref img classification using BioID training set*

Compared to previous result, *BioID* training samples provides better results when classifying non faces, although only 3 from 10 faces are correctly detected. In this case, the price to correctly detect non faces is too high for faces set.

As a conclusion, it is difficult to decide the best face database option and bootstrapping does not offer the desired final converging results. The effort to reduce input vectors does not lead into a better classification ratio. Therefore, it can be concluded that LBP enhanced histograms mean value models together with PCA and relative difference normalized are not able to correctly represent whole faces and non faces samples sets.

7.2.2.2. Only Faces & Threshold

As explained in previous chapters, one of the most important problems is the complexity of representing non faces class:

- Non faces samples can go from total flat textures to extremely granulated ones. Because of this, it is really difficult to represent such a wide class with a unique enough representative model.
- Some textures can have a similar LBP feature vector to faces one, that means that faces samples are included in non faces LBP space.

Then, it can be reasonable that only taking into account faces model and an appropriate threshold faces can be correctly classified.

Each input vector is projected in the orthonormal matrix for faces class, and then back-projected. Finally the resulting reconstructed vector is compared to the original one. If the distance is less than a give threshold then it will be classified as a face.

See previous section *4.3.2.2* for more detailed information.

Using only the face training samples for both databases the eigenvalues and thresholds are extracted.

Training Faces		
Database Name	# Samples	Image Size
GTAV Internet	6650	16x16
Bio ID	2981	19x19

Table 16. *PCA only faces: Number of samples for each face detection training set.*

The following figures show the normalized eigenvalues plots for both databases and for the 1st and 2nd stage:

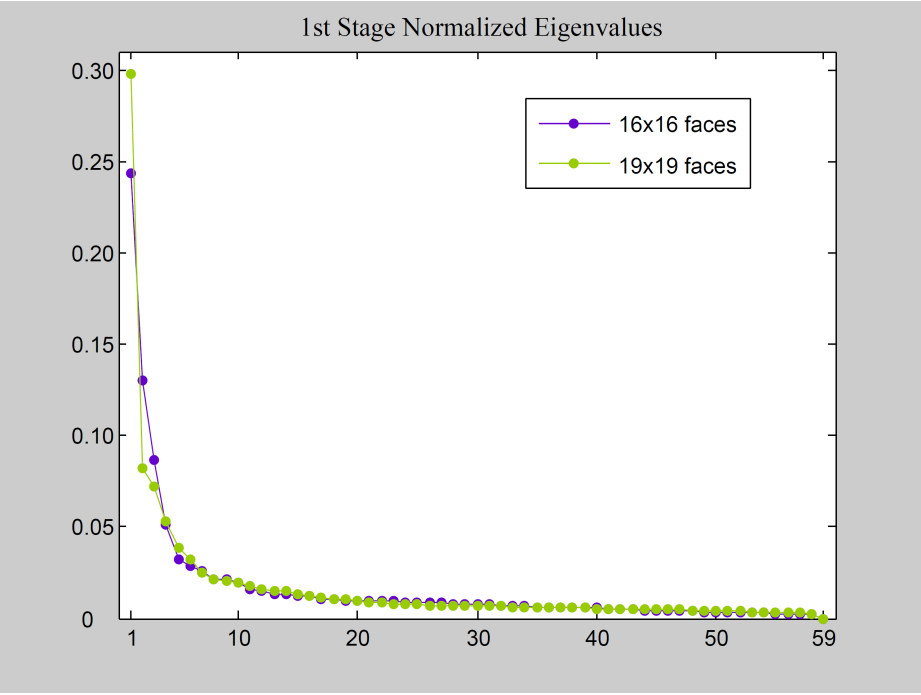

Figure 65. *Face detection PCA only faces - Normalized eigenvalues plot: 1st stage*

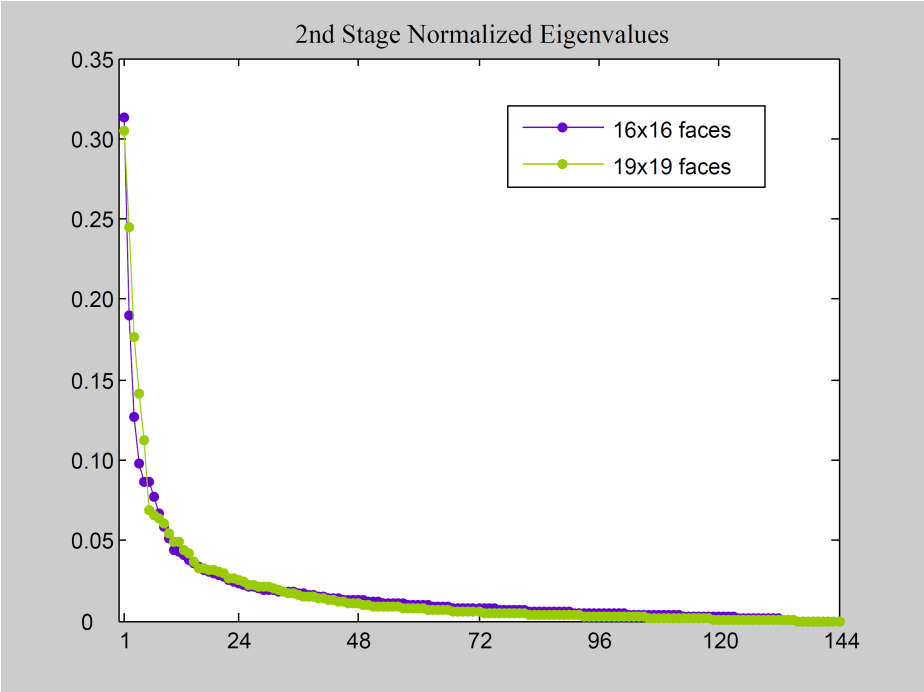

Figure 66. *Face detection PCA only faces - Normalized eigenvalues plot: 2nd stage*

The eigenvalues for both face databases are similar, only in the first stage it can be observed that the *BioID* first eigenvalues has a higher value than the first *GTAV Internet* eigenvalues. That means that by keeping only one eigenvalue, a better reconstruction can be achieved with *BioID* face database.

For both databases, in first stage the last eigenvalue and in second stage the last nine eigenvalues are zero.

The behavior of these eigenvalues is similar to the case of having both negative and positive samples, as seen in previous chapter.

The next step consists of deciding:

- An appropriate number of eigenvalues to keep for each stage. The idea is to have enough eigenvalues to have an acceptable loss rate between original and reconstructed image.
- K_{1stStg} and K_{2ndStg} values to adjust the decision threshold for each stage. Once or twice the deviation should be a proper threshold, but in order to observe the evolution for different K, values between 1 and 6 are evaluated. For simplicity, integer values have been used, although for fine adjustment decimals could be used.

In order to better see the above eigenvalues, in *Appendix III.1.3* a table can be found showing the normalized eigenvalues for 1st and 2nd stages for both databases, 16x16 and 19x19 faces.

Comparing this table with the one from previous chapter, see *Appendix III.1.3,* it can be observed that in the other case the information was more concentrated in first eigenvalues. Just the first eigenvalue has the double information when taking into account faces and non-faces dataset. That can be due to the fact that number of samples is much higher when taking also into account non-faces samples.

Another interesting point is that in this case, the relation between % information and number of eigenvalues between both face databases is more similar just taking into account faces samples. In the following table some combination of eigenvalues are proposed to evaluate the method:

16x16			19x19		
% Info	Number of Eigenvalues		% Info	Number of Eigenvalues	
	1st Stage	2nd Stage		1st Stage	2nd Stage
25%	1	3	29%	1	3
46%	3	10	45%	3	7
54%	5	15	54%	5	12
70%	13	31	70%	13	23
90%	34	72	90%	36	57
100%	59	144	100%	59	144

Table 17. *PCA only faces: number of eigenvalues selection based on % of Info*

Different simulations have been performed combining the number of eigenvalues (*%Info*) and *K* values in order to compare both databases and investigate the possibilities of this method. And finally select the best parameters to obtain the best detection ratio.

			Detection ratio [%]											
			19x19						16x16					
1st stg eigenvals			1	3	5	13	36	59	1	3	5	13	34	59
2nd stg eigenvals			3	7	12	23	57	144	3	10	15	31	72	144
K_{1st}	6	Faces	100%	100%	100%	100%	100%	99.9%	100%	100%	100%	100%	100%	100%
		Non Faces	51.7%	54.9%	40.2%	38.2%	40.5%	32.2%	23.7%	30.3%	32.5%	28.6%	24.6%	9.4%
	5	Faces	100%	100%	100%	100%	100%	99.8%	100%	100%	100%	100%	100%	99.7%
		Non Faces	57.4%	60.6%	46.9%	44.9%	47.5%	39.0%	30.4%	36.0%	37.7%	33.0%	30.1%	12.1%
	4	Faces	100%	99.7%	100%	100%	100%	99.4%	99.8%	99.5%	99.9%	99.9%	99.8%	98.3%
		Non Faces	63.8%	67.0%	54.8%	52.8%	56.0%	46.9%	37.6%	42.7%	44.2%	39.0%	36.8%	18.9%
	3	Faces	98.6%	99.2%	99.4%	99.2%	99.5%	98.3%	99.0%	99.0%	99.3%	99.2%	99.1%	97.2%
		Non Faces	70.6%	73.9%	63.7%	62.0%	65.7%	57.2%	45.7%	50.9%	51.9%	46.5%	42.5%	28.3%
	2	Faces	96.3%	97.7%	97.4%	96.3%	97.0%	95.9%	95.8%	96.2%	95.9%	96.5%	96.5%	96.1%
		Non Faces	78.2%	81.1%	73.5%	72.3%	74.3%	68.1%	55.4%	60.6%	61.4%	55.9%	50.5%	38.7%
	1	Faces	88.4%	90.4%	86.5%	84.6%	83.8%	88.2%	84.0%	85.5%	84.1%	83.6%	85.3%	88.8%
		Non Faces	85.4%	87.6%	84.3%	83.1%	83.1%	79.3%	66.6%	71.5%	72.1%	67.5%	61.5%	54.8%
K_{2nd}	6	Faces	100%	100%	100%	100%	100%	100%	100%	100%	100%	100%	100%	100%
		Non Faces	47.3%	52.0%	48.4%	50.4%	36.4%	11.7%	27.5%	29.5%	29.0%	31.4%	19.8%	0.6%
	5	Faces	100%	100%	100%	100%	100%	100%	100%	100%	100%	100%	100%	100%
		Non Faces	56.8%	62.2%	59.2%	61.4%	49.7%	21.8%	38.7%	40.3%	39.6%	40.6%	31.3%	2.1%
	4	Faces	100%	100%	100%	100%	100%	99.9%	99.9%	100%	100%	100%	100%	99.9%
		Non Faces	67.4%	73.1%	71.3%	73.9%	64.9%	35.8%	54.3%	57.5%	55.6%	54.9%	47.3%	7.0%
	3	Faces	99.6%	99.7%	99.8%	99.7%	99.7%	99.4%	99.5%	99.7%	99.8%	99.9%	99.6%	98.9%
		Non Faces	78.3%	83.6%	82.9%	85.3%	79.6%	52.8%	74.3%	77.6%	74.8%	72.3%	66.1%	20.1%
	2	Faces	97.8%	97.9%	97.9%	97.8%	97.6%	97.0%	96.7%	97.3%	97.6%	97.3%	97.3%	95.0%
		Non Faces	88.4%	92.0%	91.9%	93.9%	91.0%	68.9%	91.7%	92.8%	90.4%	87.8%	82.9%	46.5%
	1	Faces	88.4%	86.4%	86.2%	84.3%	85.5%	87.4%	84.6%	85.1%	84.8%	84.5%	84.5%	85.9%
		Non Faces	95.9%	97.3%	97.3%	98.3%	97.5%	84.2%	98.9%	99.0%	97.9%	96.2%	93.0%	78.7%

Table 18. *PCA only faces: detection ratio for different K_{1st} and K_{2nd}, eigenvalues*

At first sight, it is not obvious the best parameters combination, but it is noticeable that:

- The lower the *K* values the best compromise between faces and non faces detection ration.
- As seen in previous experiments, face detection ratio must be penalized in order to achieve a better non faces detection ratio.
- In first stage, better non faces detection ratio is achieved with 19x19 face database.
- An inflection point exists for the number of eigenvalues to be selected in both cases. Taking into account more eigenvalues does not represent any detection ratio improvement.

In order to decide the best % of information (number of eigenvalues) to obtain the best detection ratio for all cases (faces and non faces, and for both face databases) the mean detection ratio is calculated:

- In each cell: faces and non faces mean detection ratio.
- In horizontal: mean detection ratio for different K_{1st} and K_{2nd} values.
- In vertical: mean detection ratio for different number of eigenvalues.

Mean detection ratio [%]														
Eigenvalues		19x19						16x16						
1st Stage		1	3	5	13	36	59	1	3	5	13	34	59	
2nd Stage		3	7	12	23	57	144	3	10	15	31	72	144	
K_{1st}	6	75.86	77.47	70.09	69.12	70.26	66.06	61.84	65.06	66.25	64.28	62.32	54.72	**66.94**
	5	78.72	80.28	73.44	72.43	73.73	69.37	65.16	67.86	68.83	66.52	65.01	55.90	**69.77**
	4	81.89	83.33	77.39	76.39	77.98	73.10	68.68	71.10	72.04	69.46	68.28	58.58	**73.18**
	3	84.62	86.55	81.57	80.55	82.61	77.70	72.34	74.96	75.62	72.81	70.79	62.77	**76.91**
	2	87.24	89.40	85.406	84.26	85.64	82.01	75.59	78.40	78.65	76.19	73.51	67.38	**80.31**
	1	86.90	89.00	85.407	83.86	83.47	83.72	75.26	78.52	78.08	75.55	73.38	71.81	**80.41**
K_{2nd}	6	73.64	76.00	74.19	75.18	68.22	55.84	63.77	64.75	64.48	65.71	59.88	50.31	**66.00**
	5	78.40	81.10	79.62	80.72	74.84	60.88	69.30	70.17	69.82	70.30	65.63	51.04	**70.99**
	4	83.70	86.55	85.66	86.94	82.41	67.87	77.12	78.74	77.79	77.41	73.67	53.45	**77.61**
	3	88.96	91.66	91.33	92.52	89.67	76.10	86.92	88.64	87.28	86.10	82.86	59.46	**85.13**
	2	93.12	94.93	94.90	95.81	94.32	82.93	94.18	95.01	93.99	92.54	90.08	70.74	**91.04**
	1	92.13	91.82	91.77	91.32	91.45	85.82	91.73	92.01	91.32	90.37	88.71	82.31	**90.06**
		83.77	**85.67**	**82.57**	**82.43**	**81.22**	**73.45**	**75.16**	**77.10**	**77.01**	**75.60**	**72.84**	**61.54**	

Figure 67. *PCA only faces: mean detection ratio for different # eigenvalues and K values*

Then it can be concluded that the best choice for both databases to achieve the optimum detection ratio for both faces and non faces is:

- $K_{1stStg}=1$ and $K_{2ndStg}=2$
- About 45-46% information, that means:
  - 3 eigenvalues for the 1st stage
  - 7-10 eigenvalues for the 2nd stage.

Next step is to classify both test databases with the selected parameters. As the detection ratios are slightly different for near K_{1stStg} and K_{2ndStg} values, two more combinations are used to check the resulting detection ratio.

		19x19		16x16		
		Eigenvalues		Eigenvalues		
		1st Stg.	2nd Stg.	1st Stg.	2nd Stg.	
		3	7	3	10	
		Detection Ratio [%]		Detection Ratio [%]		Mean Detection Ratio [%]
K_{1st}	K_{2nd}	Faces	Non Faces	Faces	Non Faces	
1	1	79.40	97.73	74.20	99.37	**87.67**
1	2	88.80	94.46	84.00	94.97	**90.56**
2	1	85.15	97.53	82.60	99.31	**91.15**

Figure 68. *Mean detection ratio of faces and non faces for 45-46% of information and different K values.*

In this case the best option is to select $K_{1stStg}=2$ and $K_{2ndStg}=1$. Moreover, using $K_{1stStg} > K_{2ndStg}$ allows to be less restrictive in 1st coarse stage and more restrictive in the final 2nd fine stage.

Finally, in order to compare results with the other exposed methods, let us compare training results classifying the reference image that has nothing to do with both face databases. In both cases, skin detector is used in order to improve face detection scheme.

Each face candidate is marked with a yellow box and no boxes post processing is applied to keep only one box per face. The result is given by simply applying a boxes mask.

Figure 69. *PCA Only Faces - ref image classification using GTAV Internet training set (16x16)*

Figure 70. *PCA Only Faces - ref image classification using BioID training set (19x19)*

As a conclusion, it can be extracted that this method is not an optimal one, but it is very interesting that just taking into account faces samples it is possible to implement a face detector. In future works, *K* value could be adjusted with decimals for fine adjustment.

In these experiments, it was also noticeable that lower generalization error is achieved by means of training the face detector using 16x16 faces database, instead of using 19x19 faces database.

7.2.3. Support Vector Machine

This classification method is supposed to achieve the best results for LBP enhanced histograms. In order to evaluate it, SVM classifier is equally configured for both 1st and 2nd stages following *University of Oulu* parameters recommendation (see [6] and equation (31) of section *4.3.3.1*). However, different C coefficients have been test so as to verify if it is also a good solution for our images database.

Detailed information about the SVM parameters can be also found in *Table 45* in *Appendix V. OpenCV Functions Reference*.

The following table shows classification ratios using different C values, before using bootstrap strategy.

16x16					
C		1st Stage coarse		2nd Stage fine - Final	
1st Stage Coarse	2nd Stage Fine	**faces ok (%)**	**non faces ok (%)**	**faces ok (%)**	**non faces ok (%)**
177	576	96.55%	90.44%	96.55%	99.65%
118	432	96.40%	90.13%	96.40%	99.64%
59	144	96.25%	89.40%	96.25%	99.63%
30	72	96.15%	88.75%	96.15%	99.62%
15	36	95.95%	88.20%	95.95%	99.60%
7	18	96.10%	87.35%	96.05%	99.57%
4	9	96.15%	85.80%	96.15%	99.51%
5	**5**	96.20%	86.86%	95.95%	99.52%
3	3	96.35%	85.80%	95.90%	99.46%

Table 19. *SVM classification ratio for different C values (case 16x16 faces DB)*

Due to the reason that the obtained results are similar, it is decided to use the recommended value by *A.Hadid*'s research team (*C=5*).

Next step is to improve non faces detection by applying a bootstrap strategy. Next *Figure 71* shows the evolution of each bootstrap iteration. *Table 38* and *Table 39* of *Appendix III.1.4* contain detailed information of the obtained results.

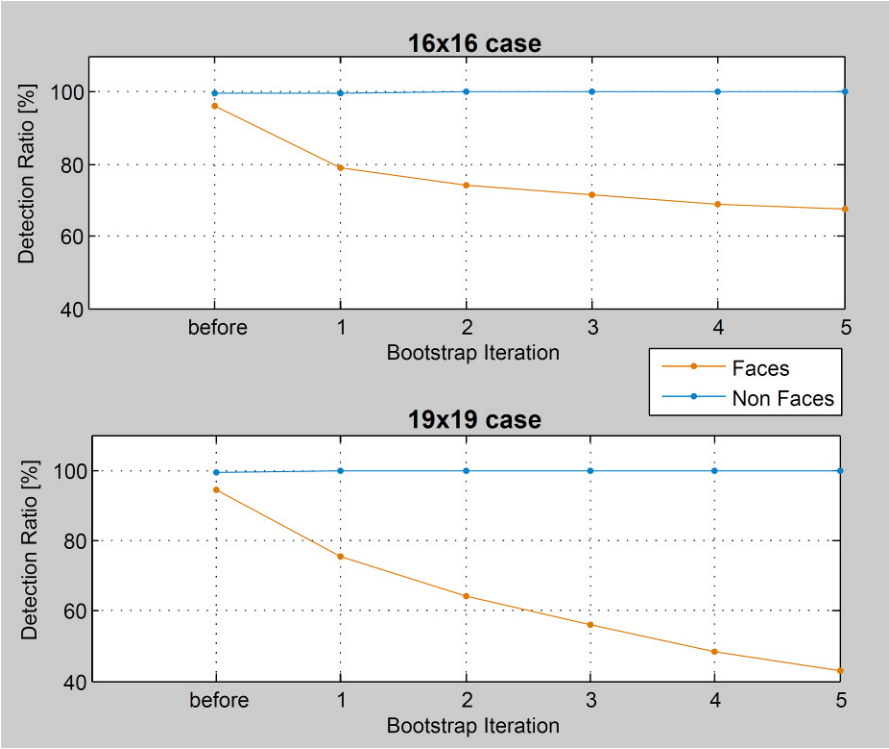

Figure 71. *Bootstrap to improve SVM classification ratio (16x16 & 19x19 faces)*

From above graphs, it can be extracted that best classification results are achieved before applying bootstrap strategy, because faces detection ratio is highly penalized when trying to improve non faces detection ratio. But on the other hand, compared to previous experiments, in that case it is possible to nearly reach 100% of correct detections in non faces case. As already mentioned, non faces dataset contains a wide range of possible textures that make difficult the use of a *mean model* as a reference to compare with new input samples. Therefore, SVM method is capable of defining a better threshold regions between both faces and non-faces classes, achieving a better classifier.

Using reference image to compare this method with previous ones, following *Figure 72* shows the result of applying SVM with *C=5*.

Figure 72. *SVM - reference image classification using GTAV training set (16x16)*

For that case, all faces are still correctly detected and only 3 non faces are misclassified: two knees and one throat.

Then, the same procedure is applied to 19x19 face database in order to compare the robustness of the method in front of the faces database. Following *Figure 73* shows the result of classifying the reference image:

Figure 73. *SVM - reference image classification using BioID training set (19x19)*

For 19x19 case, all faces non faces are correctly classified but only 3 faces are correctly classified from 10. As already exposed, *BioID* face database contains less faces samples than *GTAV Internet* face database and moreover, the faces are for only 23 different people. Because of this, very good results are achieved when classifying training and test data, but not when classifying the reference image. Because of this, it can be concluded that *GTAV Internet* provides a lower generalization error.

7.2.3.1. Additional 3rd stage: SVM score thresholds

In this research work, as a contribution to the two stages face detection scheme introduced by *University of Oulu* researchers, a third stage is proposed to improve final detection results by setting empirical thresholds to avoid non faces misclassification.

For next experiments, only *GTAV Internet* database (16x16 face images) will be used, as it has been generally providing best face detection results.

In order to decide 3rd stage thresholds, some *GTAV Internet* faces samples are classified for the purpose of collecting *SVM* scores for the 1st and 2nd stages. Next *Table 20* shows statistical information of the obtained scores.

	Scores		
	1stStg	*2ndStg*	*1stStg+2ndStg*
Average	-0.6053	-3.8947	-4.5000
StdDev	0.4375	1.2742	1.4669
Min	-2.5243	-9.4057	-11.2732
Max	-0.0007	-0.7344	-1.5225

Table 20. *SVM scores from 3281 faces*

Resulting from above table, the following values are settled as thresholds in a ***third*** stage to decide the final faceness of the image:

$$Threshold_{1stStg + 2ndStg} = -1.5$$
$$Threshold_{2ndStg} = -0.5$$

The flowchart to be followed is shown in next figure:

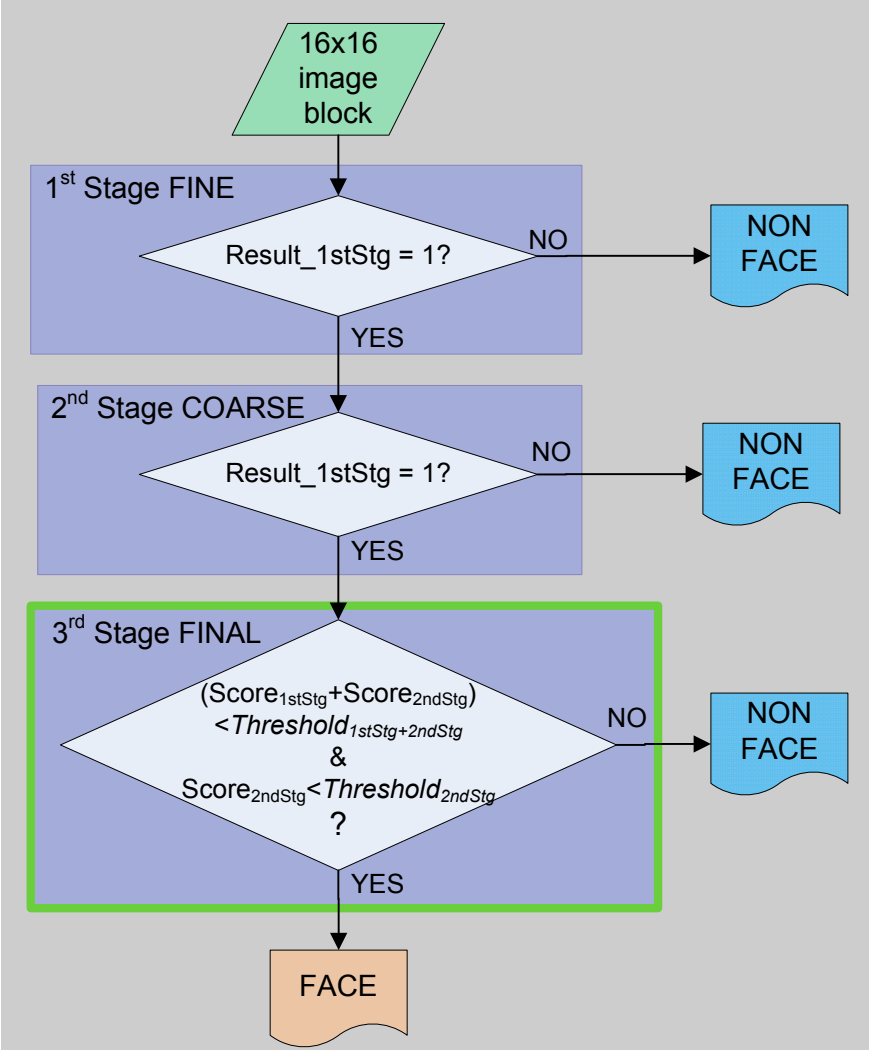

Figure 74. *SVM faces classification flowchart with addition 3rd stage*

The reason why this 3rd stage improves face classification results is because it is capable of avoiding non-faces misclassifications which results in an aberrant score far from the mean value one.

The improvement achieved with this method can be observed in the following sample images, in yellow intermediate face detections and in red final decision after overlapping boxes removal:

Figure 75. *SVM with 3rd Stage classification (16x16): equipop.jpg*

Comparing *Figure 72* with above *Figure 75,* it can be observed how this extra stage is capable of removing false face detections: two knees, with round form and face like appearance, while keeping face detection ratio.

Not only good results are achieved for the reference image, but also for the following sample images:

Figure 76. *SVM with 3rd Stage classification (16x16): boda.jpg*

In above *Figure 76,* no false detections appear, but one face is misclassified due to the fact that the system in not trained on purpose to detect rotated faces. Notice that at least the other rotated face is correctly detected. Therefore, the system could still improved by introducing rotated samples to the face training set.

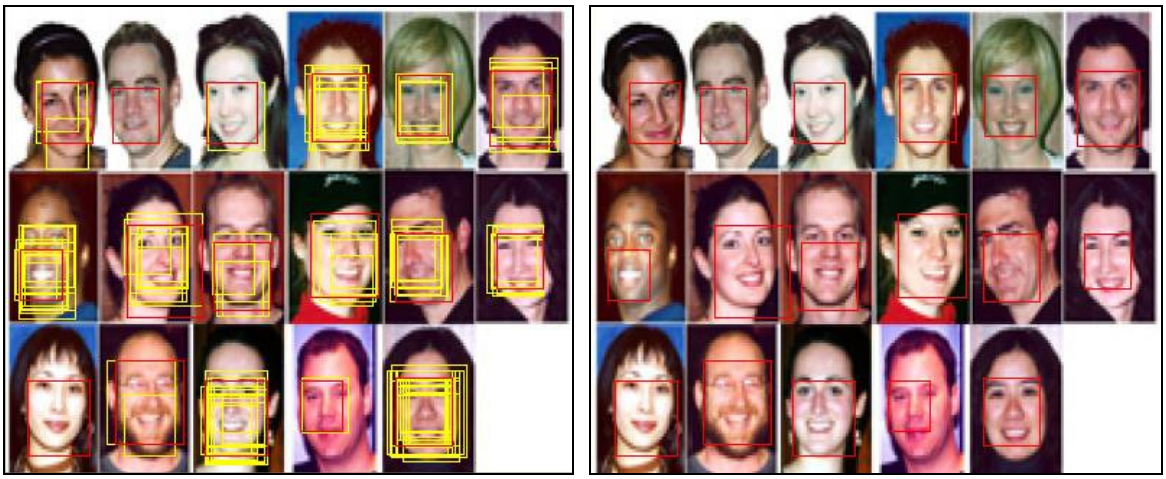

Figure 77. *SVM with 3rd Stage classification (16x16): faces_composite_1.jpg*

In above *Figure 77*, all faces are correctly detected but in some cases as in 1st column, 2nd row and 3rd row faces, the overlapping boxes removal method is not selecting the best box. In those cases, it could be better to use *Overlapping Detection Merge* (see section *4.4.2.2*).

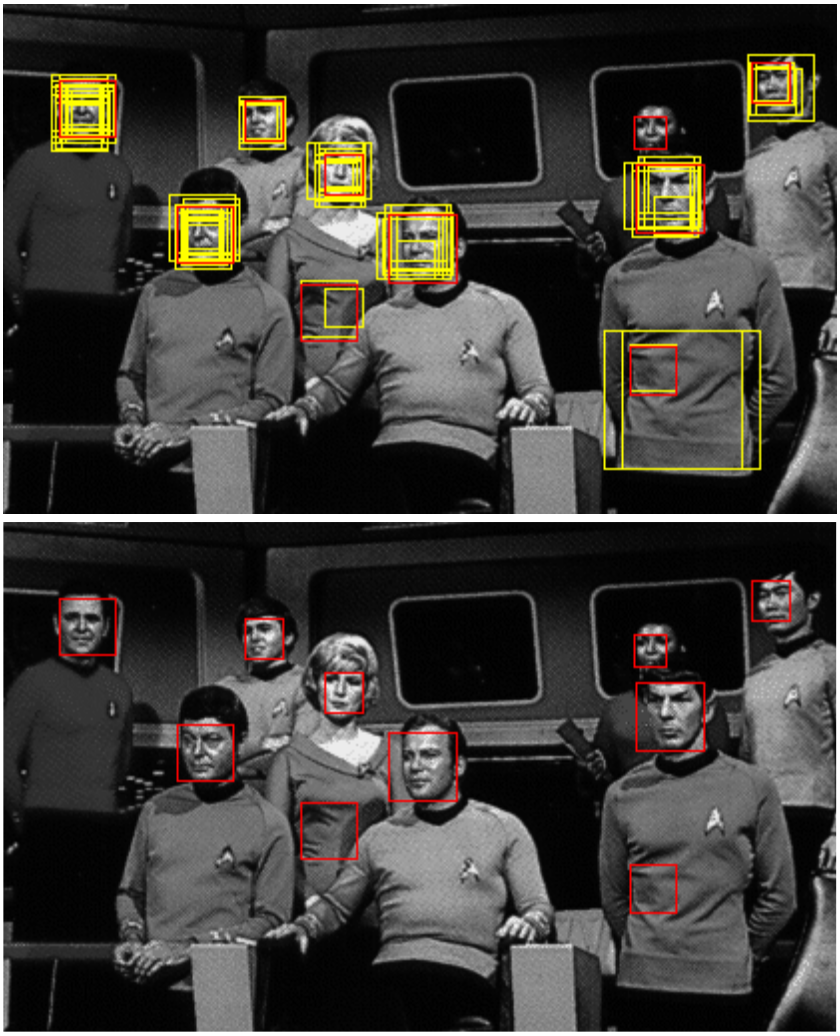

Figure 78. *SVM with 3rd Stage classification (16x16): CMU test-original1.bmp*

In above *Figure 78*, the eight faces are correctly detected although there are two misclassifications that could be avoided using the skin detector in case of having a colored image. However, notice that the misclassified non-faces have face appearance.

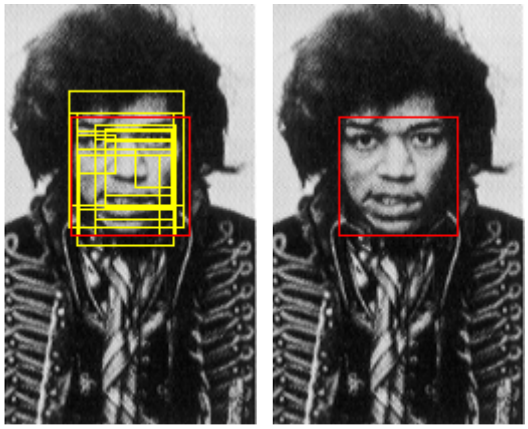

Figure 79. *SVM with 3rd Stage classification (16x16): CMU test- hendrix2.bmp*

In above *Figure 79* case, the overlapping boxes removal method is selecting the best box and no misclassifications are detected.

7.2.3.2. PCA before applying SVM

This section is intended to improve SVM classification potential by applying a PCA pre processing to the input samples in order to reduce data dimensionality and eliminate redundant information.

Only *GTAV Internet* 16x16 face database is used in the experiment because it has already been demonstrated that provides the best generalization results.

Taking advantage from previous section *7.2.2*, dedicated to PCA. The experiments are focused to the following number of eigenvalues (extracted from *Table 15*):

16x16		
% Info	Number of Eigenvalues	
	1st Stage	2nd Stage
90%	14	56
95%	25	79

Table 21. *Face detection PCA (16x16 case): best number of eigenvalues selection*

Next figures show the bootstrap strategy evolution, where it can be observed that face detection ratio drops drastically compared to previous approaches. See *Table 40* and *Table 41* in *Appendix III.1.5* for detailed information.

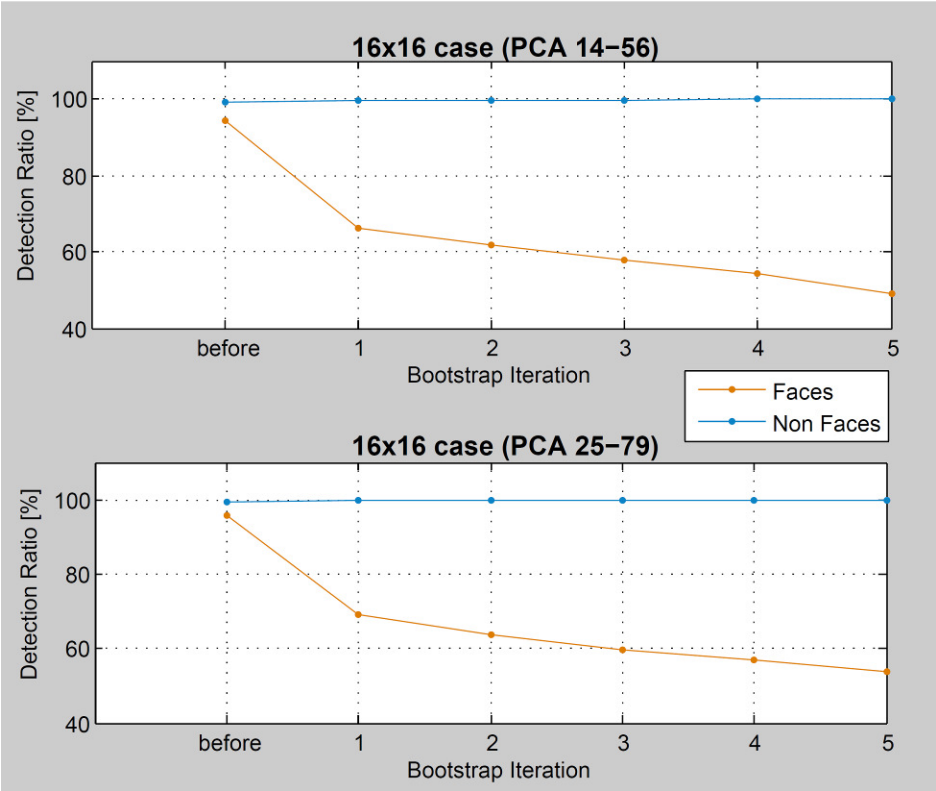

Figure 80. *Bootstrap to improve PCA(14-56 & 25-79) + SVM classification ratio (case 16x16 faces)*

As in SVM approach without PCA improvement, best detection ratios are achieved before applying bootstrap strategy, but also best non faces detection ratios are obtained compared to non SVM methods.

Additional stage (see *Figure 74*) is also used to improve final classification result. Therefore, 3rd stage thresholds need to be readjusted to new classifier conditions:

$$Threshold_{1stStg + 2ndStg} = -1.5$$
$$Threshold_{2ndStg} = -0.19$$

Next *Figure 81* and *Figure 82* shows classifying reference image for the two different numbers of eigenvalues selected:

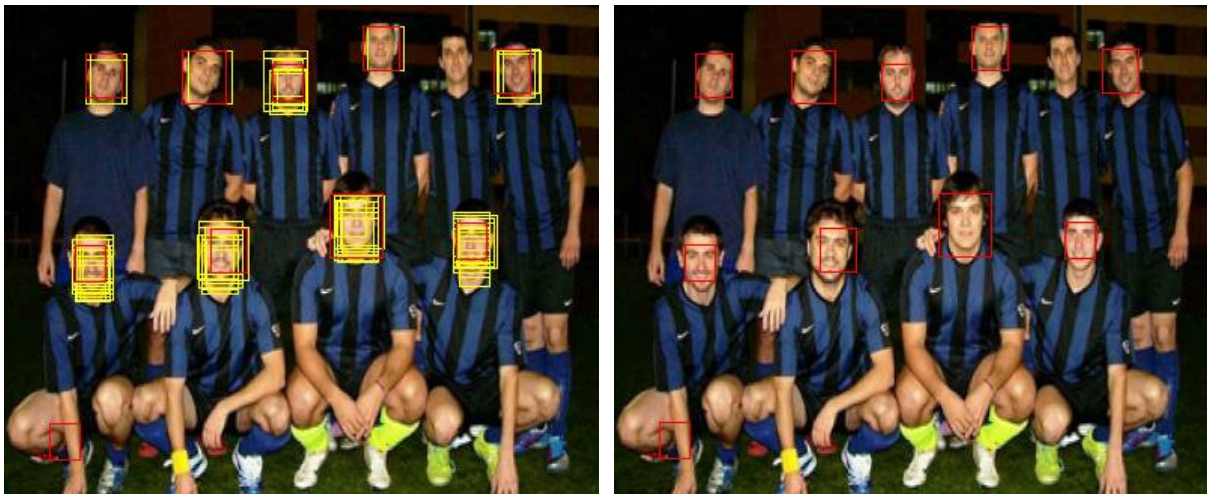

Figure 81. *PCA(14_56)+SVM faces classification: equipop.jpg*

Figure 82. *PCA(25_79)+SVM faces classification: equipop.jpg (Moving step = 1)*

As a conclusion of these last experiments, a reduction of the input data dimensionality provides also satisfactory results although a clearly improvement is not achieved.

7.3. Face Recognition Experiments

This section describes face recognition experimental results following *chapter 5* proposed approaches.

As already explained, face recognition method based in LBP approach consists of extracting a 2891 features vector consisting of ((7x7 blocks) x 59-bin/block) for each input face sample of a given individual in order to create a mean features vector model for each person in the database. Once a new person is to be identified, the LBP features vector is calculated and compared to the stored ID models.

First of all, the original work ([1][3][4]) of simply using *Chi Square* as dissimilarly metric in the identification task will be under study and then it will be improved by means of *Principal Component* extraction in order to remove redundant information and enhance identification ratio.

The *BioID* database will be used for face recognition experiments and the number of samples used in training and test stages is shown in *Table 10. Training and Test Subsets for face*

7.3.1. Chi Square Dissimilarly Metric

In face recognition experiments using *Chi Square* as dissimilarly metric, some pre and post processing methods will be used in order to verify its impact on identification ratio, such as:

- Use of a mask: to avoid non face parts in the face image with no useful information for the identification task (see *Figure 83*).
- Histogram equalization: in order to perform a contrast adjustment to normalize face images to be compared.
- Blocks weight: to emphasize face elements containing relevant information in face recognition task such as the eyes or mouth. After testing different features weights, *Figure 84* shows the two block weight best options.
- Model type: use of only 1 representative image of the individual for the features vector model or mean value of individual's face samples for the model.

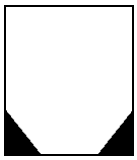

Figure 83. *Face mask used in face recognition testing*

The combination of above approaches leads to 10 different experiments that, for simplicity, will be named from ***Test1*** to ***Test10***.

The results will be presented in three steps, each one fixing the kind of block weights used and combining the use of histogram equalization and mask.

	Histogram equalization versus ***Mask*** using ***no Block Weight***				***Histogram equalization*** versus ***Mask*** using ***Block Weight (1)***			***Histogram equalization*** versus ***Mask*** using ***Block Weight (2)***		
	Test 1	**Test 2**	**Test 3**	**Test 4**	**Test 5**	**Test 6**	**Test 7**	**Test 8**	**Test 9**	**Test 10**
Equalized Histogram	x	x	✓	✓	x	✓	✓	x	✓	✓
Mask	x	✓	x	✓	x	x	✓	x	x	✓
Blocks Weight	x	x	x	x	✓(1)	✓(1)	✓(1)	✓(2)	✓(2)	✓(2)

Table 22. *Face recognition experiments overview*

And to be concluded, a results table (*Table 26*) will help to overview the obtained results and to select the best options.

❖ ***Histogram equalization*** versus ***Mask*** using ***no Block Weight***

Next table shows first experiments combining the use of a mask and histogram equalization for the case of mean value model and 1 image model (see section *5.3.2.1*). The last row

presents the mean ID recognition ratio in %, calculated by weighting each ID ratio by its number of samples, due to the fact that the number of samples for each ID is different (see *Table 10*) and each sample requires the same importance. The complete table with the individual results can be consulted in *Appendix IV.1.1*.

	Test 1		Test 2		Test 3		Test 4	
Equalized Histogram	x		x		✓		✓	
Mask	x		✓		x		✓	
Blocks Weight	x		x		x		x	
Type Model	**1 Img**	**Mean**	**1 Img**	**Mean**	**1 Img**	**Mean**	**1 Img**	**Mean**
ID Recognition Rate	**57.48%**	**97.87%**	**55.75%**	**97.27%**	**57.95%**	**97.74%**	**55.78%**	**97.31%**
	77.67%		76.51%		**77.84%**		76.54%	

Table 23. *ID recognition rate (%). Histogram equalization versus Mask*

The use of mean value model considerably increases the face recognition ratio compared to the case of using 1 image as mean model. Nevertheless, it can be noticed that in some cases 1 image is enough to correctly identify the other faces in the database, in case of low face variations in group set.

Comparing above values, best results are achieved for mean value model case when using neither histogram equalization nor mask, and for 1 image model case when using only histogram equalization. However, taking into account both case models results, the highest score is achieved in case of using only histogram equalization.

❖ ***Histogram equalization*** versus ***Mask*** using ***Block Weight (1)***

Next step consists of using block weights to highlight face relevant information such as the eyes and the mouth and avoid irrelevant or very variable information.

In order to find out best weighting blocks, each individual block of the 7x7 blocks should be used alone in the recognition task to find out its significance and to decide its weight. For simplicity and taking into account theory section *5.3.1 Face Regions Analysis, University* of *Oulu* experience (see [1]) and after some preliminary testing the following weighting map are selected as best candidates:

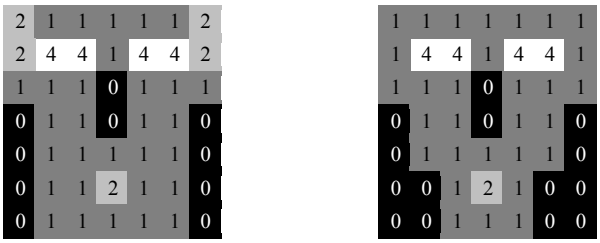

features weight (1) — 98.44%

features weight (2) — 97.27%

Figure 84. *Features weight comparison and its corresponding recognition rate*

Observing above feature masks, most importance is given to eye area and mouth, removing areas with irrelevant information such as the background on bottom sides. Another interesting point to notice is that best results are achieved by removing nose septum area, the least important face feature (see section *5.3.1*).

The following tables combine the use of above features weight (1) with the use of mask and histogram equalization.

	Test 5		Test 6		Test 7	
Equalized Histogram	x		✓		✓	
Mask	x		x		✓	
Blocks Weight	✓(1)		✓(1)		✓(1)	
Type Model	**1 Img**	**Mean**	**1 Img**	**Mean**	**1 Img**	**Mean**
ID Recognition Rate	**62.76%**	**98.60%**	**63.00%**	**98.74%**	**62.20%**	**98.44%**
	80.68%		**80.87%**		80.32%	

Table 24. *ID recognition rate (%). Histogram equalization versus Mask using Block Weight (1)*

In this case, the best option also considers the use of *histogram equalization* as a pre processing step of face samples. Additionally, the identification ratio is increased by using the *Block Weight (1)*.

❖ ***Histogram equalization*** versus ***Mask*** using ***Block Weight (2)***

The same procedure is followed with *Block Weight (2)*.

	Test 8		Test 9		Test 10	
Equalized Histogram	x		✓		✓	
Mask	x		x		✓	
Blocks Weight	✓(2)		✓(2)		✓(2)	
Type Model	**1 Img**	**Mean**	**1 Img**	**Mean**	**1 Img**	**Mean**
ID Recognition Rate	**61.60%**	**97.34%**	**62.00%**	**97.27%**	**62.00%**	**97.27%**
	79.47%		**79.63%**		79.63%	

Table 25. *ID recognition rate (%). Histogram equalization versus Mask using Block Weight (2)*

In this case, the best results are achieved by using *histogram equalization* and using a *mask* so as not the same results are obtained.

Summary

Next table and plots are intended to collect all above results to better visualize the best results. It shows the ID recognition rate (%) for each different test and for both model type, using only 1 representative image of each individual.

	Test 1	**Test 2**	**Test 3**	**Test 4**	**Test 5**	**Test 6**	**Test 7**	**Test 8**	**Test 9**	**Test 10**
Equalized Histogram	x	x	✓	✓	x	✓	✓	x	✓	✓
Mask	x	✓	x	✓	x	x	✓	x	x	✓
Blocks Weight	x	x	x	x	✓(1)	✓(1)	✓(1)	✓(2)	✓(2)	✓(2)
Mean Model	97.87%	97.27%	97.74%	97.31%	98.60%	98.74%	98.44%	97.34%	97.27%	97.27%
1 Img Model	57.48%	55.75%	57.95%	55.78%	62.76%	63.00%	62.20%	61.60%	62.00%	62.00%
	77.68%	**76.51%**	**77.84%**	**76.55%**	**80.68%**	**80.87%**	**80.32%**	**79.47%**	**79.64%**	**79.64%**

Table 26. *ID recognition rate (%) for each experiment and for both model types*

Summarizing, the best results are obtained for ***Test 6*** with a **98.74%** of correct identification ratio:

- No mask.
- Histogram equalization.
- Blocks weight (1).
- Mean model type.

As already exposed, no mask is needed if blocks weight is used because the same target is achieved by given a low value to the bottom side of the image, where normally image background, cloths or hair are to be found.

Moreover histogram equalization (see section *5.1*) is improving face recognition task by counteracting light conditions that affect face appearance by enhancing contrast and at the same time, edges and face details.

Obviously mean model type is the best option, because it is difficult to find out the best image of the ID dataset that can represent the whole dataset. Although from this research experiments in 1 image model case, it can be extracted that our representative ID face selection can describe around 60% of its ID set.

Concluding, it has been demonstrated that by using LBP enhanced histogram and a simply dissimilarly metric very satisfactory results are achieved.

7.3.2. Principal Component Analysis

Following section is intended to improve above results using *Principal Component Analysis* in order to remove redundant information and enhance identification ratio. Experiments will focus on ***Test 6*** (no mask, histogram equalization, block weight (1) and mean model type) but also in ***Test 3*** (no mask, histogram equalization, no block weight and mean model type) due to the fact that ***PCA*** itself will weight the most important blocks in the face image. Therefore, theory suggests that best results can be achieved with ***Test 3*** case.

Following the already explained procedure (see section *5.3.2.2*), the covariance matrix $\boldsymbol{C}$ is computed in order to calculate eigenvectors matrix $\boldsymbol{V}$, together with its corresponding eigenvalues. Different strategies can be followed, but in this case, it is decided to have a unique $\boldsymbol{V}$ matrix calculated using all available data, 2947 face samples, for following reasons:

- A representative transformation matrix for each ID is discarded because: the number of available samples for each ID is different (see *Table 10*), in some cases only 4 samples are available and it is undesirable to manage 23 different eigenvectors matrixes.
- In our concrete case, the number of available samples, 2947, is in the range of the number of elements in the enhanced features vector. Then, the eigenvectors length will be the minimum value between the number of input samples and the input samples length, namely 2891 eigenvectors.

$$\#eigenvectors = \min(\#input\ samples,\ input\ samples\ length) \tag{55}$$

Following table shows the number of eigenvectors selected for the experiments based in eigenvalues information. First column is the number of eigenvectors selected, second column is the last eigenvalue, third column is the last normalized eigenvalue, fourth column is the accumulative information of the number of eigenvectors selected, fifth column is the percentage of eigenvectors selected and the last column is the eigenvectors reduction achieved.

#	Eigenvalue	Norm Eigenvalue	% Accumulative Info	% Eigenvectors
1	0.10162122	0.08160000	8.16%	0.03%
62	0.00304733	0.00244690	75.20%	2.14%
88	0.00183365	0.00147240	80.09%	3.04%
233	0.00043843	0.00035200	90.01%	8.06%
484	0.00014275	0.00011460	95.00%	16.74%
723	0.00007679	0.00006170	97.00%	25.01%
1446	0.00001906	0.00001530	99.37%	50.02%
2024	0.00000535	0.00000430	99.88%	70.01%
2830	0.00000001	0.00000000	100.00%	97.89%
2842	0.00000000	0.00000000	100.00%	98.31%
2891	0.00000000	0.00000000	100.00%	100.00%

Table 27. *PCA for face recognition: eigenvalues information*

Analyzing the obtained eigenvalues, keeping only 25% (~750) of the eigenvectors, about 97.5% of the original vectors information still remains. Moreover, just by keeping 2842 of 2891 eigenvectors (1.69% reduction), no information is lost due to the fact that last 49 eigenvalues have nearly zero value.

While implementing PCA approach applied to face recognition, it was noticed that due to reconstruction error, in some cases, negative or aberrant values appeared when back-projecting feature vectors samples. As a consequence, corrections on *Chi Square* formulation are submitted to avoid the effect of these undesired values and in order to improve identification ratios. Therefore, in the experimental results, these 3 cases are used:

- **Norm (Model + Feature)**:

$$\chi^2_w(S,M) = \sum_{i,j} w_j \frac{(S_{i,j} - M_{i,j})^2}{\left|S_{i,j} + M_{i,j}\right|} \tag{56}$$

- **Norm (Model)**:

$$\chi^2_{\text{w modelNorm}} = \sum_{i,j} w_j \frac{(S_{i,j} - M_{i,j})^2}{\left|M_{i,j}\right|} \tag{57}$$

- **No Norm**:

$$\chi^2_{\text{w noNorm}} = \sum_{i,j} w_j (S_{i,j} - M_{i,j})^2 \tag{58}$$

After above considerations, following figure shows the results of experimenting with ***Test3*** and ***Test6***, for mean models, keeping different number of eigenvectors and with three *Chi Square* formulations:

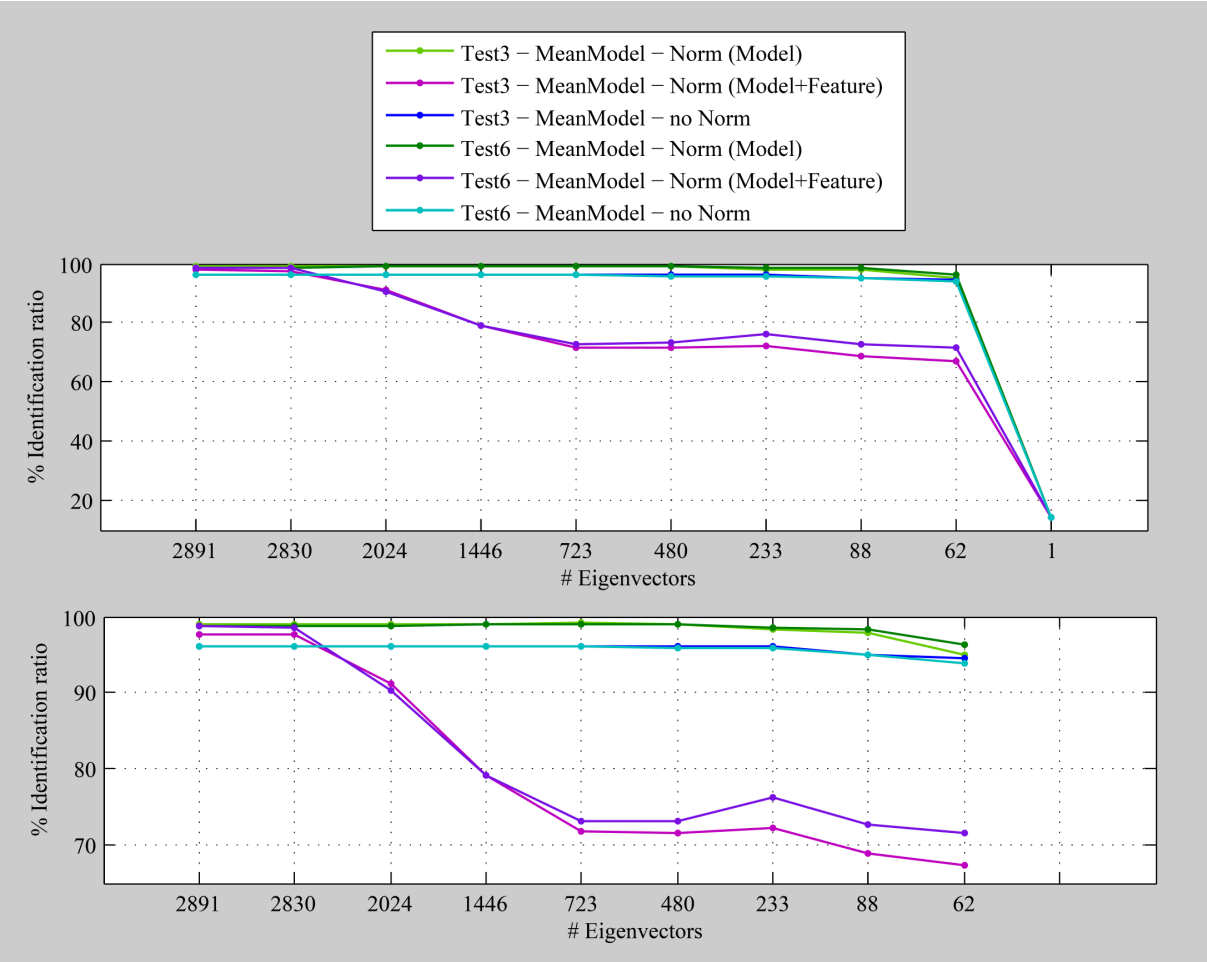

Figure 85. *Face Identification Ratios for different number of eigenvalues*

Here, the effect of the reconstruction error can be clearly observed when the input feature sample ***S*** is kept in the denominator of the *Chi Square* formulation. In case of obtaining aberrant or negative values after back projecting, keeping ***S*** in the denominator can provide undesired and unrealistic low results if ***S*** is very high or high results if ***S*** is very low. Therefore, most interesting results are obtained when keeping only the model ***M*** in the denominator that a priori is not providing aberrant values in the reconstruction process.

Focusing in the case of using *Chi Square* only normalized by the model value, next figure is a zoom of above figures. In this representation, it is important to note that it is possible to improve face identification system up to 99.14% by keeping only around 723 eigenvectors in ***Test 3*** case. Therefore, the use of block weight can already be left aside.

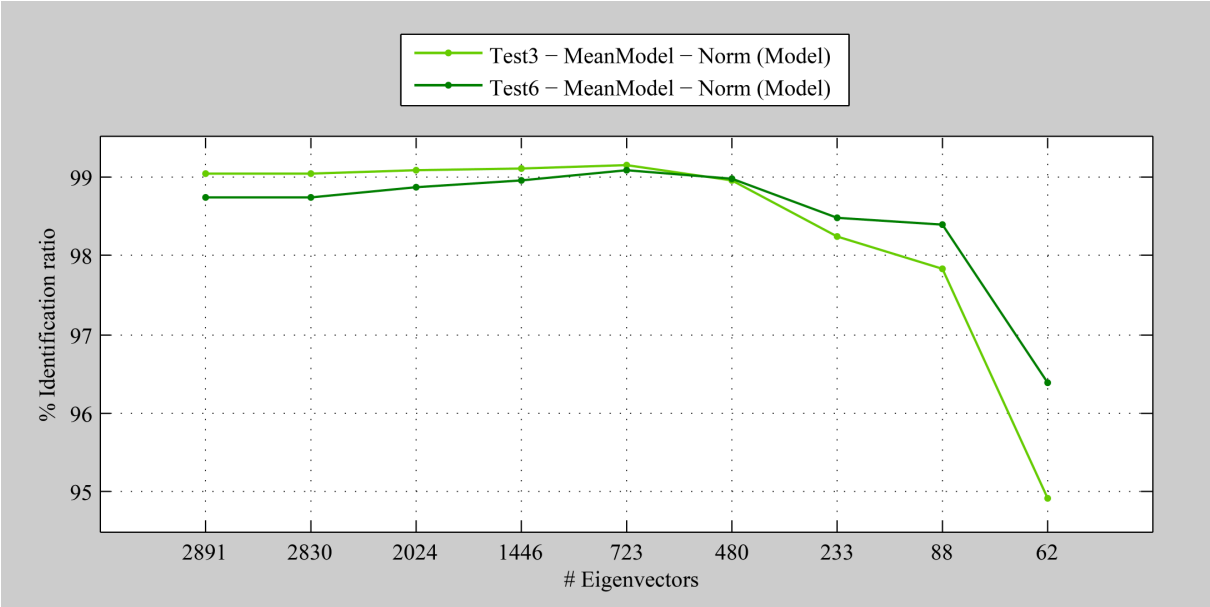

Figure 86. *Norm (Model) Face Identification Ratios*

Before, taking 723 as the value that maximizes the identification ratio, an exploration of the nearby values is performed to find out if another maximum exists.

Next table shows already used values, in gray, and the new ones under investigation, in black.

#	Eigenvalue	Norm Eigenvalue	% Accumulative Info	% Eigenvectors
1	0.10162122	0.08160000	8.16%	0.03%
62	0.00304733	0.00244690	75.20%	2.14%
88	0.00183365	0.00147240	80.09%	3.04%
233	0.00043843	0.00035200	90.01%	8.06%
484	0.00014275	0.00011460	95.00%	16.74%
585	0.00010640	0.00008540	96.00%	20.24%
649	0.00009127	0.00007330	96.51%	22.45%
703	0.00008022	0.00006440	96.88%	24.32%
704	0.00007994	0.00006420	96.89%	24.35%
705	0.00007970	0.00006400	96.89%	24.39%
708	0.00007909	0.00006350	96.91%	24.49%
713	0.00007836	0.00006290	96.94%	24.66%
718	0.00007757	0.00006230	96.97%	24.84%
723	0.00007679	0.00006170	97.00%	25.01%
728	0.00007610	0.00006110	97.04%	25.18%
733	0.00007521	0.00006040	97.07%	25.35%
921	0.00005099	0.00004090	98.00%	31.86%
1446	0.00001906	0.00001530	99.37%	50.02%
2024	0.00000535	0.00000430	99.88%	70.01%
2830	0.00000001	0.00000000	100.00%	97.89%
2842	0.00000000	0.00000000	100.00%	98.31%
2891	0.00000000	0.00000000	100.00%	100.00%

Table 28. *PCA for face recognition: eigenvalues information in the nearby of eigenvalue 723*

Using above number of eigenvectors, the identification ratios are recalculated and next figure shows the results for ***Test3*** case.

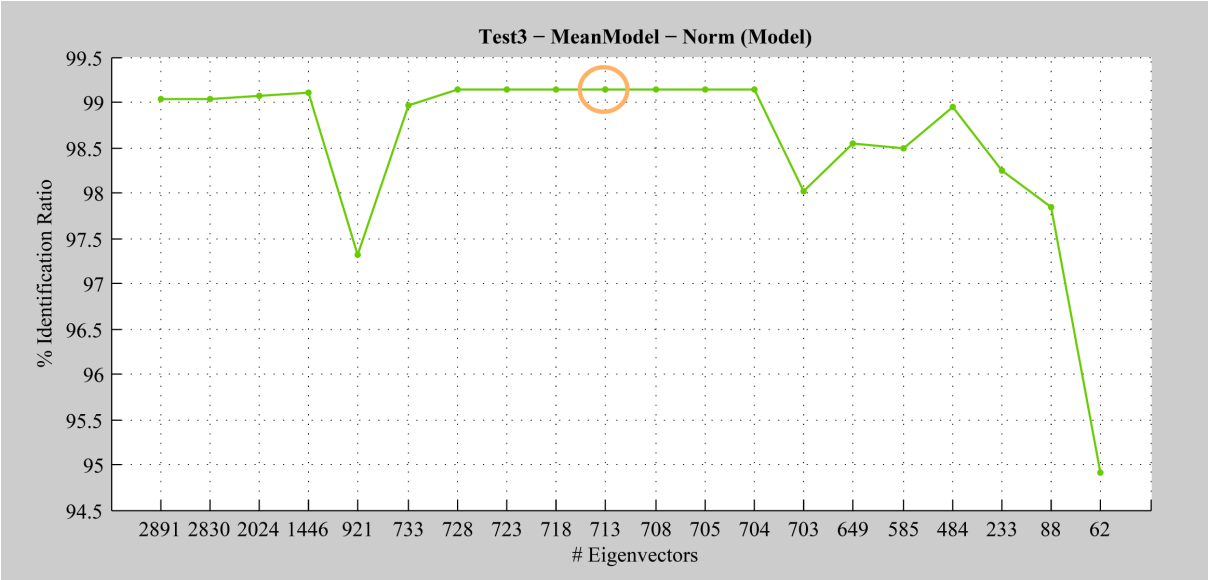

Figure 87. *Test3 – MeanModel - Norm (Model): Face Identification Ratios*

As it can be observed, a maximum identification rate exists between the 703 and 733 number of eigenvectors. Therefore, 713 is taken as the mean value of this area and selected as the best option for face identification task with a 99.14% of identification ratio.

Summing up, the best combination of factors is to use:

- Pre processing: histogram equalization, no mask and no blocks weight.
- Mean model.
- PCA with 713 eigenvectors.
- Chi Square statistic only normalized by the model value.

Concluding it is worth to computationally invest in PCA projecting and back projecting process, because the main target of this procedure is to avoid irrelevant information and therefore enhancing face recognition results.

In this research, the *Chi Square* comparison is not performed in the projected space to be able to apply blocks weight and follow the same procedure as the case without PCA. But after observing that the use of mask or blocks weight is not necessary, as the PCA itself is able of detecting and weighting the most important bins of the enhanced feature vector, for future work it could also be interesting to make the comparison in the PCA projected space.

Chapter 8

Development Tools

This chapter gives an overview of this research used tools, its motivation and a brief reference manual of the implemented application ***FaceProcessingTool***.

8.1. Programming Environment

Microsoft Visual Studio 2005 platform, together with ***Microsoft Visual C++ 2005*** environment, is the preferred option as it provides a powerful and flexible development environment for Windows-based application. Moreover, it enables the possibility of taking advantage of *OpenCV* Library.

***OpenCV* Library 1.0**, *Intel® Open Source Computer Vision* Library is a collection of *C* functions and a few *C++* classes that implement many popular Image Processing and Computer Vision algorithms.

Besides, ***MATLAB 7.0*** is also used as a numerical computing environment useful in this research for matrix manipulation and data plotting.

8.2. Face Processing Tool

An application with a user-friendly graphical user interface (GUI) is developed implementing face detection and recognition algorithms with the aim of helping in the training and testing stages.

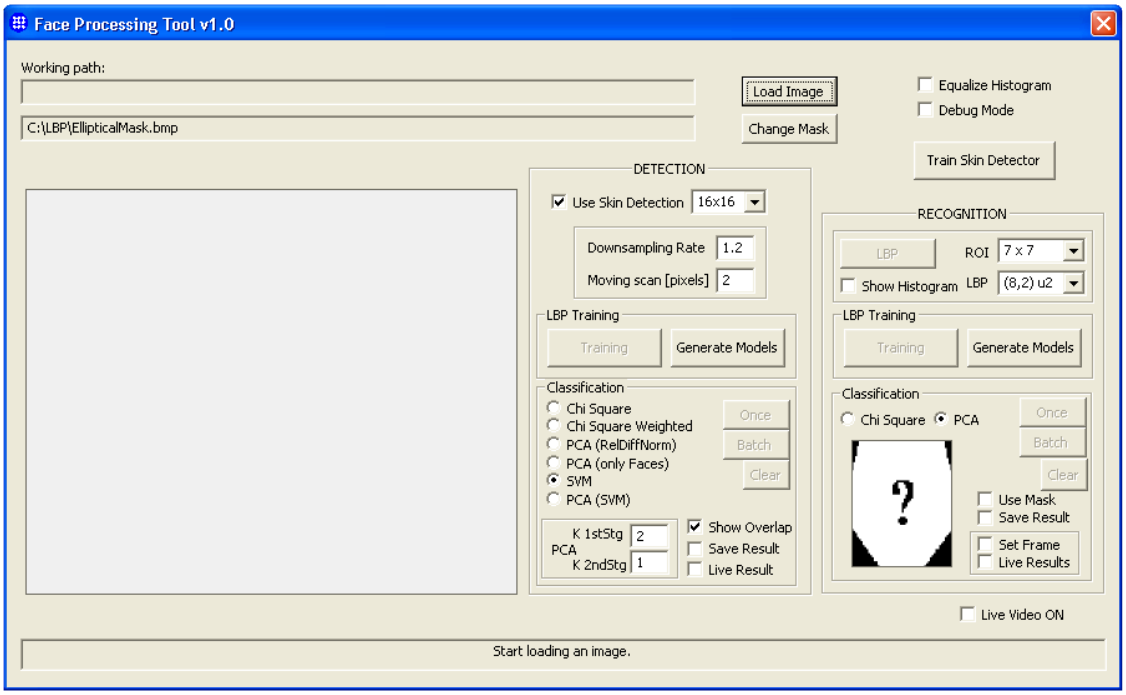

Figure 88. *Face Processing Tool application main dialog*

The GUI contains clearly differentiated sections: input image selection (top-side), picture-box (left-side), face detection (center-region) and face recognition (right-side).

On top-right, the following check-boxes can be used to enable ***histogram equalization*** and ***debug mode*** activation in order to save and view process intermediate images for both face detection and recognition cases.

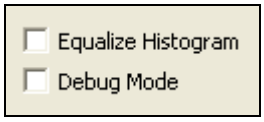

Figure 89. *Common Face Processing GUI section*

8.2.1. Face Detection

Face detection GUI part is divided in three main regions as it can be observed in next figure:

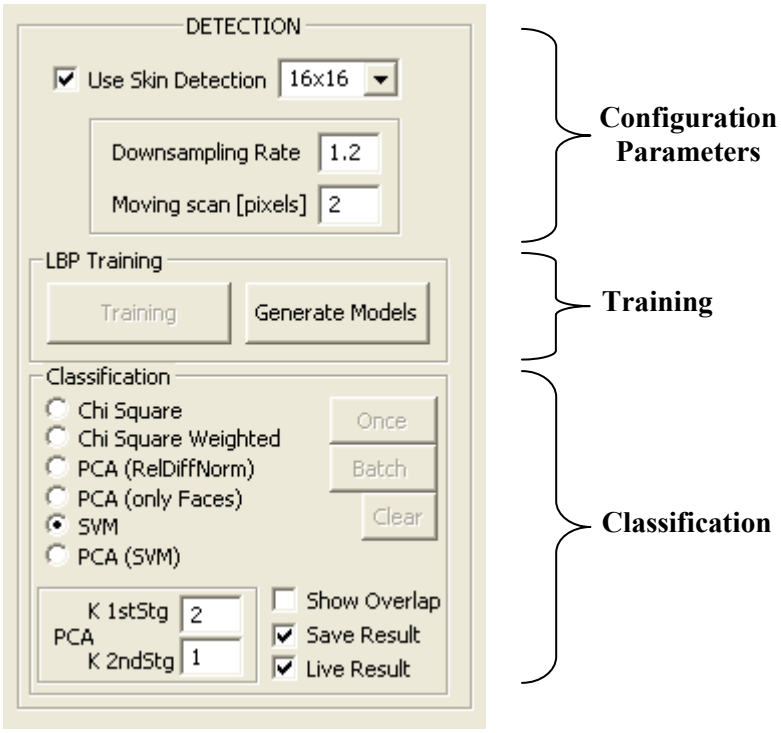

Figure 90. *Face Detection GUI section*

- **Configuration Parameters** (top section): to configure face detection system by selecting the desired *downsampling rate*, *moving scan*, minimum image block size (*16x16* or *19x19*) and the *use of skin detection* method.
- **Training** (central section): divided in *Training* for LBP extraction and *Generate Models* to open *Face Detection Model Generation* dialog (*Figure 94*).
- **Classification** (bottom section): for testing stage, where the desired classification method can be selected by means of a radio-button, the *K* default values for *PCA (only Faces)* method can be modified, check-box options define how to get the results, two buttons are available to start the classification only *once* or in *batch* mode and a *clear* button for removing resulting face boxes.

8.2.1.1. Skin Segmentation Training

Moreover, as a part of the face detection section, on the top-right corner of the main dialog (see *Figure 88*) a *Train Skin Detector* button can be found for skin segmentation training.

Figure 91. *Skin Detection Training Button*

By clicking the above button, the following dialog appears to choose the skin samples path and to perform the calculation of the *Luv* values (see section *4.4.2.1*).

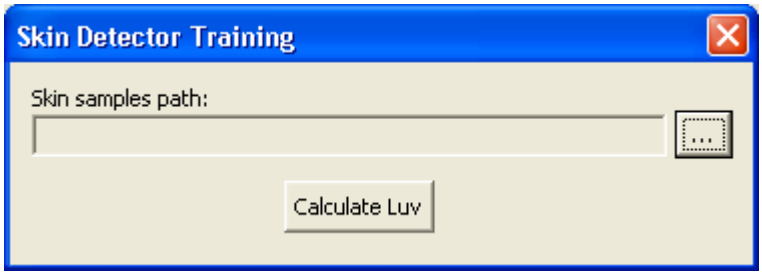

Figure 92. *Skin Detection Training dialog*

As a result, a *skin_uv.txt* file is obtained containing the *uv* mean and standard deviation values for each processed block of size *(imgWidth/10)*x*(imgHeight /10)* of each image available. These results are then used to define the thresholds for skin segmentation procedure.

8.2.1.2. Training

Face detection training phase is split in two stages: LBP extraction (***Training*** Button) and faces and non-faces models generation (***Generate Models*** Button). The purpose of this division is to have a first stage common to the different classification methods that extracts the enhanced feature vector of each training sample and saves it in a training file (*LBP_ForFaceDetection_Training_NxN.txt*) that will be later used to generate the models for the different detection algorithms.

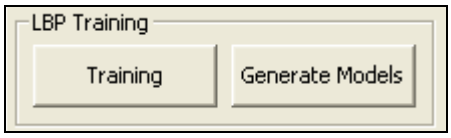

Figure 93. *Face Detection LBP training GUI section*

Once the LBP vectors are obtained, clicking the *Training* button, for face (positive) samples and non-faces (negative) samples, the *Generate Models* button will open the following dialog:

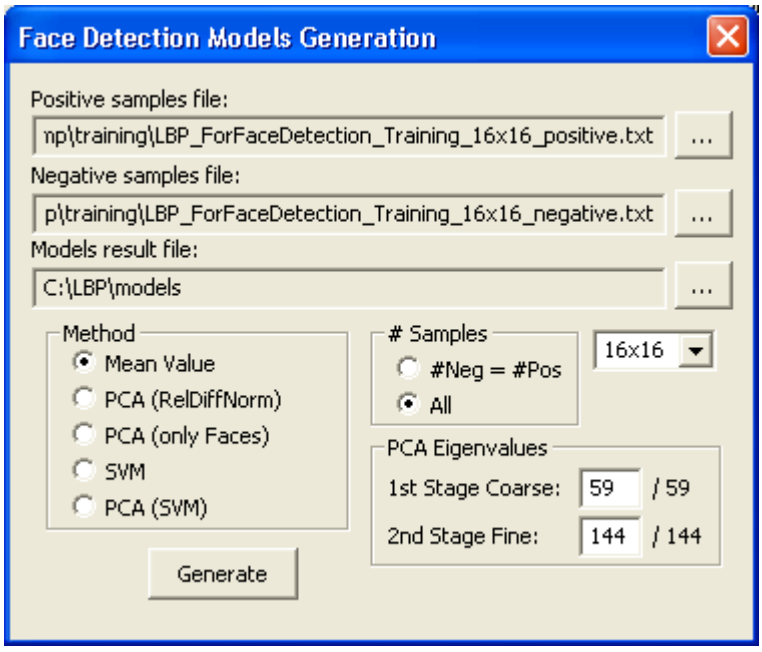

Figure 94. *Face Detection Model Generation dialog*

In order to generate the training models using above dialog:

- The **paths** for the positive and negative sample files have to be indicated.
- Then, the desired method can be changed by means of the ***Method*** radio-buttons.
- If the number of input positive and negative samples is different, the ***# Samples*** radio-buttons enables to get all of them or to select a number of negative samples (normally bigger) equal to the number of positive samples.
- The combo-box enables to switch from ***16x16*** to ***19x19*** pixels face images, for experiments using both available databases (*GTAV Internet* and *BioID*).
- In case of selecting PCA methods, ***PCA Eigenvalues*** section allows to change the number of desired eigenvectors for 1st coarse and for 2nd fine stages.

The final training files will be saved in **C:\LBP** folder:

Face detection method	Result files
Mean value	models_NxN.txt
PCA (RelDiffNorm)	PCA_models_NxN.txt PCA_eigenvalues_NxN.txt PCA_eigenvectors_NxN.txt
PCA (only faces)	PCA_OnlyFaces_eigenvalues_ NxN.txt PCA_OnlyFaces_eigenvectors_NxN.txt PCA_OnlyFaces_MeanStdDev_NxN.txt
SVM	model_SVM_1stStageCoarse_NxN.xml model_SVM_2ndStageFine_NxN.xml
PCA (SVM)	PCA_SVM_eigenvalues_NxN.txt PCA_SVM_eigenvectors_NxN.txt PCA_SVM_models_1stStageCoarse_NxN.xml PCA_SVM_models_2ndStageFine_NxN.xml

Table 29. *Face Detection training stage result files*

8.2.1.3. Test

Once the training files are obtained, the test section is ready for use. But first of all, the desired configuration parameters have to be selected in the following section to determinate the input image exploration method:

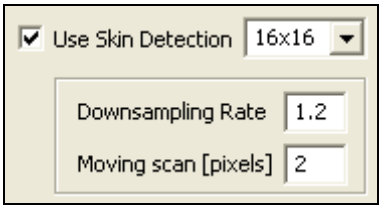

Figure 95. *Face Detection configuration parameters*

- Skin segmentation preprocessing.
- Minimum image block size selection: 16x16 or 19x19.
- Downsampling rate setting.
- Moving scan selection.

Then, the face detection method under study can be chosen in the following section, together with the type of classification (*Once* or *Batch*) and the way of showing the results:

- ***Show Overlap***: displays intermediate face boxes before face overlapping removal.
- ***Live Result***: displays face detection boxes result in the picture box during the classification process. If it is unchecked, then the results are shown at the end of the process in an image window pop-up.
- ***Save Result***: saves results in *LBP_ForFaceDetection_Class_MethodName_NxN.txt* output file.

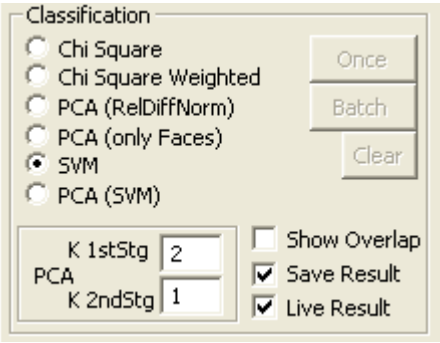

Figure 96. *Face Detection classification options*

Face boxes display options are not available in batch mode, where the results are just stored in an output file.

On the lower-left corner, the *K* default values for *PCA (only Faces)* method for 1st and 2nd stages can be modified if required.

Finally, the *Clear* button removes resulting face boxes after face detection process.

Moreover, the face detection can be performed on:

- **Static images:** which firstly have to be loaded and then displayed in the picture box. The result face boxes can be also shown in the picture box if the *Live Result* check-box is checked.
- **Live video:** that can be activated by means of *Figure 97* check-box. Then, a *Live Video* window is popped up showing the live captured video (see *Figure 98 (a)*). For live face detection, press *Once* button in detection area (see *Figure 96*) and two more extra windows will be displayed (see *Figure 98 (b)* and *(c)*). *Live Video* window *(a)* will show captured video with live face detections marked with green boxes and the two smaller windows will show the intermediate overlapped results, *(b)*, and the skin segmented image if the option is selected, *(c)*, respectively.

Figure 97. *Live Video mode check-box*

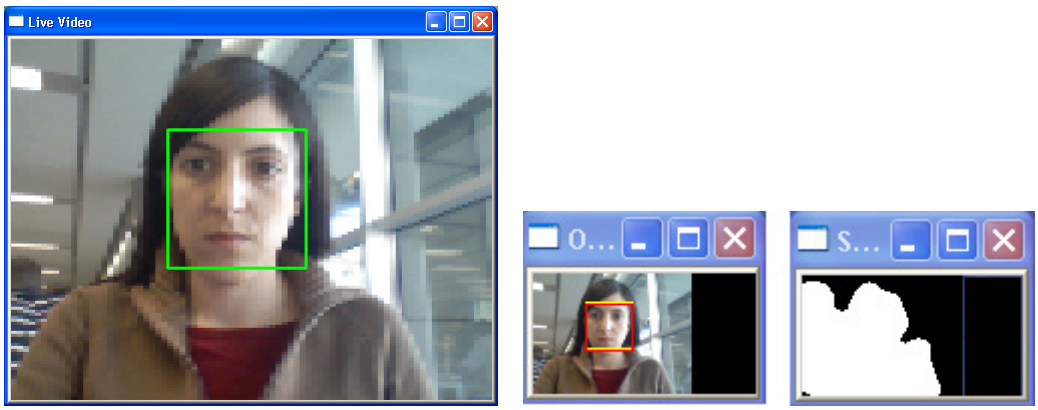

(a) Face detection result *(b) Overlapping* *(c) Skin Mask*

Figure 98. *Face detection live video result image windows*

8.2.2. Face Recognition

Face recognition GUI part is also divided in three main regions as observed in next figure:

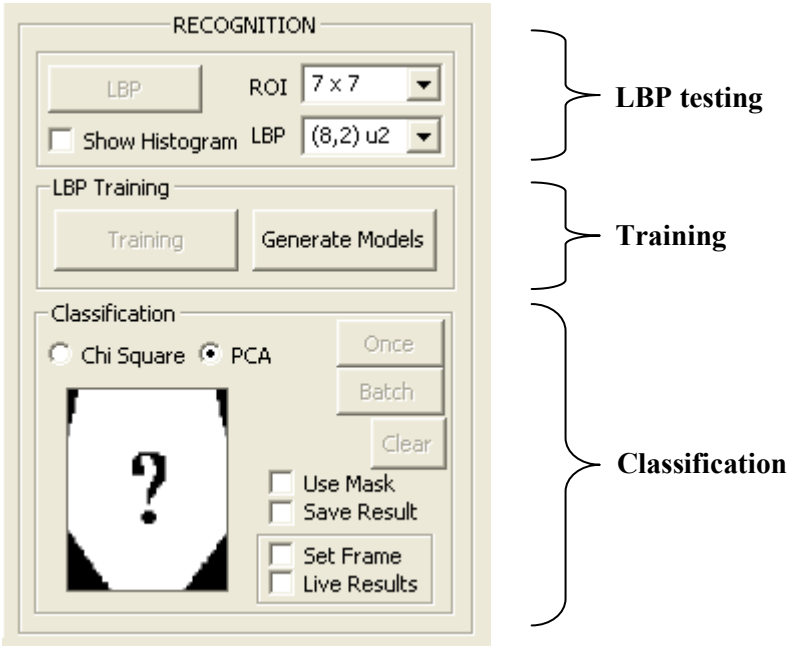

Figure 99. *Face Recognition GUI section*

- **LBP testing** (top section): for LBP firstly evaluation purposes, this section allows to extract *Local Binary Patterns* and calculate the labels histogram by pressing *LBP* button after selecting the following configuration parameters:
  - *ROI* combo-box: input image blocks division (*7x7*, *5x5*, *3x3* and *1x1*).
  - *LBP* combo-box: sampling point and radius (*(8,2)u2*, *(8,1)u2* and *(4,1)*).
  - *Show Histogram* check-box: to plot in an extra window the resulting histogram.
- **Training** (central section): divided in *Training* for LBP extraction and *Generate Models* to open *Face Recognition Model Generation* dialog (*Figure 101*).
- **Classification** (bottom section): for testing stage, containing radio-buttons for recognition method selection, check-boxes to select the use of a mask, the results storage and to enable live face recognition, two buttons to start the recognition process only *Once* or in *Batch* mode and a *Clear* button for removing the identified ID face from picture box.

8.2.2.1. Training

Face recognition training phase is also split in two stages: LBP extraction (***Training*** Button) and ID models generation (***Generate Models*** Button). The purpose of this division is to have a first stage common to the different classification methods that extracts the enhanced feature vector of each training sample and saves it in a training file (*LBP_ForFaceRecognition_Training.txt*) that will be later used to generate the models for the different recognition algorithms.

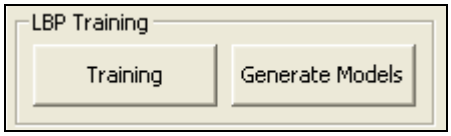

Figure 100. *Face Recognition LBP training GUI section*

Once the LBP vectors are obtained, clicking the *Training* button, for each individual, the *Generate Models* button will open the following dialog:

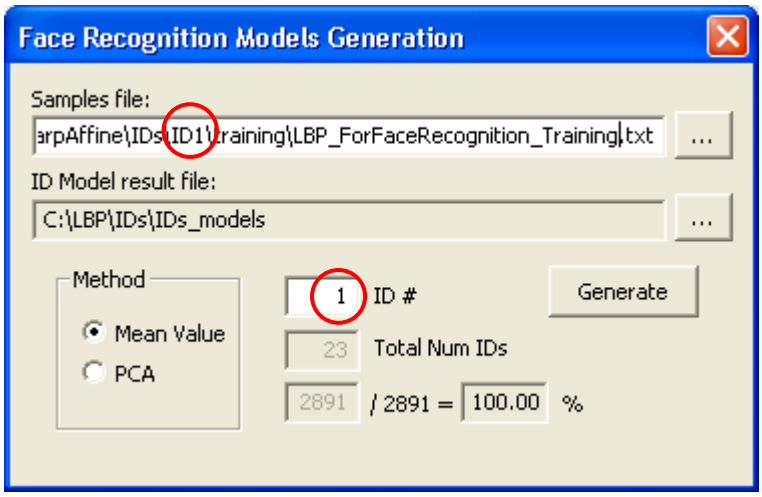

Figure 101. *Face Recognition Model Generation dialog (Mean Value)*

By default, *Mean Value* method is selected and, as it can be observed in above image, to obtain the mean model for each individual, the ID training file has to be selected, then the corresponding *ID #* has to be indicated and, by clicking the *Generate* button, an ID mean model file (see *Table 30*) will be outputted. This procedure has to be repeated for all available IDs.

In case of selecting PCA method, just by clicking the *Generate* button the output files will be generated taking into account all individual samples. The required number of eigenvectors to consider can be changed in the range from 1 to 2891 enhanced feature vector elements (7x7 blocks x 59-bin).

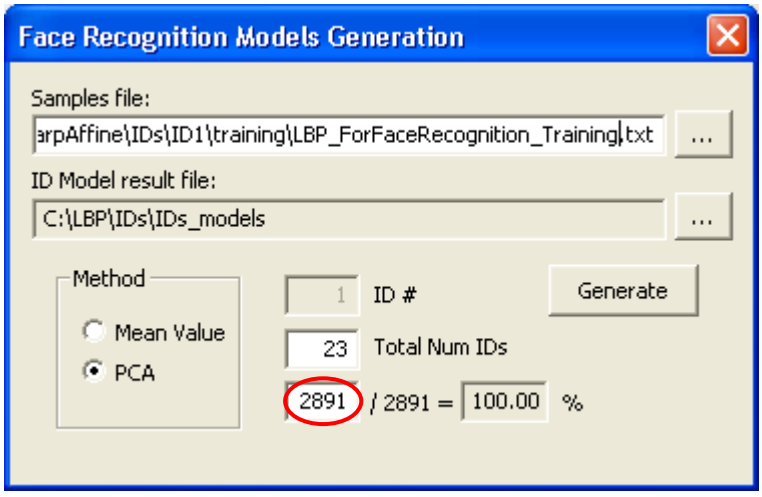

Figure 102. *Face Recognition Model Generation dialog (PCA)*

The final training files will be saved in **C:\LBP\IDs** folder:

Face recognition method	Result files
Mean value	IDX_model.txt
PCA	IDs_models_PCA_projected.txt IDs_models_PCA_eigenvectors.txt IDs_models_PCA_eigenvalues.txt

Table 30. *Face Recognition training stage result files*

8.2.2.2. Test

Once the training files are obtained, the test section is ready for use. But first of all, the desired configuration parameters have to be selected to determinate the required input image preprocessing and if the results have to be stored:

- **Histogram equalization** (see common parameters in *Figure 89*)
- **Mask use** (see *Figure 103*)
- **Save Result** (see *Figure 103*) to indicate that identification results have to be stored in *LBP_ForFacRecognition_Class_MethodName.txt* output file.

Figure 103. *ID picture-box containing identified face*

Then, the face recognition method under study can be chosen in the following section, together with the type of classification (*Once* or *Batch*) and a *Clear* button to remove the identified ID face from picture box (see above *Figure 103*).

Moreover, the face recognition can also be performed on:

- **Static images:** which firstly have to be loaded and then displayed in the ID picture-box. The result ID image is shown in *Figure 103* picture-box.
- **Live video:** that can be activated by means of *Figure 97* check-box. Then, a *Live Video* window is popped up showing the live captured video (see *Figure 104*). For live face recognition, check *Set Frame* option (see *Figure 103*) to display a purple rectangle in the *Live Video* window to place user's face, then when the face is set as shown in *Figure 104* sample, press *Once* button in recognition area (see *Figure 103*) and face recognition ID image result will be shown in ID picture-box. Moreover, an extra window will show the preprocessed image: grayscale converted and resized to face recognition 130x151 size (see *Figure 104*).

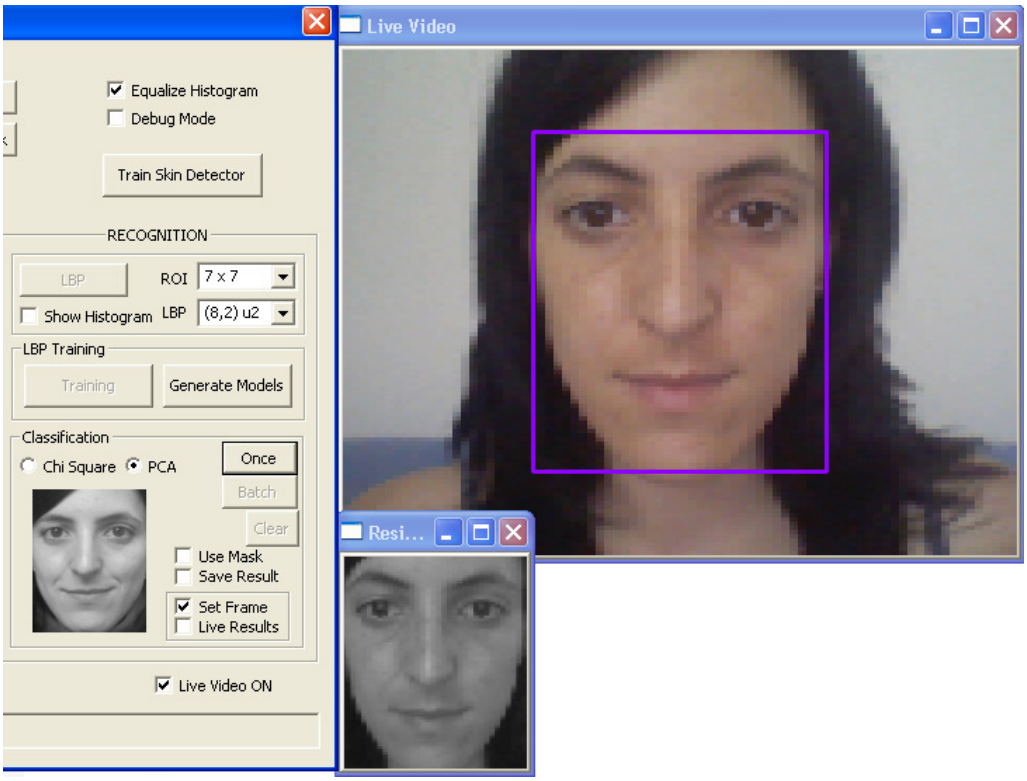

Figure 104. *Face recognition live video result image windows*

Chapter 9

Conclusions

This chapter is intended to give an overview of the complete proposal, the improvements achieved, problems found during the research and moreover to outline future lines of work.

The extensive face analysis area implies a lot of possible or potential applications for researchers. Applications today in the field of surveillance, banking and multimedia equipment are becoming more and more important. For this reason, the face analysis research community has sufficient work in order to completely solve the face detection and recognition challenges, most important of which were discussed in section *2.3*.

It is important to note that each application related to face analysis has different requirements in the analysis process. This is the main reason why almost all algorithms and approaches for face analysis are application dependent and a standardization or generalization is very difficult, at least for the moment.

The panacea for all researchers involved with the face analysis research area is to be able to emulate the human system, which is a heuristic and complicated approach taking into account multiple clues such as textures, color, motion and even audio information. Therefore, and due to the rapid evolution of technology that makes it possible, the recent trend is moving towards multimodal analysis combining multiple approaches to converge towards more accurate and satisfactory results.

Contributions to actual face detection and recognition applications are helpful to enable the face analysis research community to continue building more robust systems by linking different approaches and combining them. Therefore, the aim of this research is to contribute by exploring the *Local Binary Patterns* operator, motivated by the following reasons. On one hand, it can be applied to face detection and recognition, thus its implementation enables the possibility to investigate both research fields, enabling the possibility of building a complete system with both detection and recognition stages, all with a low computation complexity. On the other hand, as presented in the studies [1]-[7] to demonstrate its robustness to pose and illumination changes.

Following the working structure of this research and before reaching the experimental results chapter, image databases selection is a vital component to take into account in order to succeed with such a kind of learning algorithms where input samples are required to train the system. *Chapter 6* introduces the images databases used: faces, non faces and skin. Instead of creating an own database adapted to the requirements of this research, existing databases are used and adapted to the system necessities to save time. In the case of face detection experiments, two different databases have been used to find out which one of them is the best option and moreover to demonstrate how important the training samples for the final system performance are.

The experimental results are first focused in a skin detection algorithm (see section *4.4.2.1*) used as a pre-processing stage to later speed up the face detection task, computationally affected by its scanning algorithm used to explore images (see section *4.1* and *Appendix*

III.1.1). The skin segmentation system implemented (see section *7.1*) not only uses color information but also tries to take into account a system's face resolution by eliminating skin areas smaller than the minimum possible face. The improvement achieved with this method, in terms of efficiency, depends on the type of the input image and the background. The method will be very useful for instances involving one unique person with a green or blue background, but not in cases involving images of a crowded place and with a background of a similar color to skin like brown or orange.

The next step in the experimental section concerns the face detection system, where before implementing the face detection method proposed in the literature (see [5][6]), *Support Vector Machine*, a first approach to explore LBP potential is completed by means of more simple classification methods: Chi Square and PCA (see section *7.2.1* and *7.2.2* respectively). Obviously the detection ratios results obtained are worse when compared to SVM results but are sufficient enough to perceive how a simple texture operator can be used as a face descriptor.

It should be noted that when testing PCA in face detection task (see section *7.2.2.2*), non-negligible values are obtained when using only faces samples for training the system. For future works, it would be interesting to continue exploring the use of only face class since it is not easy to find the best non-faces set that best describes all non-face texture possibilities.

After this first approach to LBP applied to face detection, SVM implementation (see section *7.2.3*) shows the robustness of the system providing very satisfactory results as reveled in the literature [5][6]. This research tries to go one step further and adds one extra stage to the original two-stage system to improve face detection ratio (see section *7.2.3.1*). And in addition, it tries to eliminate redundant information from feature vectors using the PCA method after features extraction (see section *7.2.3.2*). Thereby concluding that a reduction of the input data dimensionality also provides satisfactory results, although a clear improvement is not achieved.

Moreover, also for future improvements, in order to increase face detection and recognition ratios, rotated face samples should also be added to the training databases.

The last section of the experimental results is dedicated to the face recognition method (see section *7.3*). The first part consists in implementing the literature proposal [1][2][4] using Chi Square as a dissimilarly metric in the identification task providing even more encouraging results than in the face detection part. Different experiments are performed to improve the identification ratio by applying different pre-processing methods such as histogram equalization, the use of a face mask and even blocks weights (see *Table 22*).

In the face recognition case, the idea of using PCA to eliminate redundant information takes more importance, since LBP enhanced featured vector for the face recognition task consists of an excessive number of elements, 2891 to be exact (see section *5.2*). Therefore, the PCA method is applied and a more exhaustive search for the optimal number of eigenvectors is performed, resulting in a noticeable improvement of the final identification ratios (see section *7.3.2*).

In future lines of work, the face recognition systems implemented could be improved by solving the problem of having an external individual, not present in training samples that tries to identify itself. In the way in which it is done now, the individual will be identified with the

individual ID with minimum distance, but it should be rejected by the system. Therefore, some kind of maximum distance threshold should be used to avoid this problem.

As already reveled in *Chapter 8*, all the above experiments have been tested using *Microsoft Visual C++* due to the possibility of using *OpenCV* libraries which contain complete and open source image processing and machine learning algorithms. Moreover, another motivation is the possibility of creating a Windows dialog based application with a friendly GUI to test the whole system with static images and video mode. The main intention of the developed *FaceProcessingTool* application is to evaluate experiment results and it could be improved, for example, by speeding face detection algorithm using multi threading, e.g. each down-sampled image processed in a new thread.

For future work, the LBP method is now available in *Matlab* (see [44]) so it is possible to take advantage of powerful image processing toolboxes to evaluate other method combinations.

Appendix

I. Face Databases

I.1.1. GTAV Internet Face Database

One of the databases of the *Grup de Tecnologies Audio-Visuals* of the UPC (see [42]) used in this research consists of:

# Faces		# Non Faces	
Number of samples	Image Size	Number of samples	Image Size
3325	24x24	1931	Different sizes

Table 31. *Test Subsets for face detection*

Images are collected from Internet:

- **Faces set:** faces are extracted from Internet images by manually marking the eye position of each face in the image and then, by automatically collecting each face by means of its eyes position. The resulting 24x24 faces set is a good representation of variability of facial appearance.

Figure 105. *Face image samples from GTAV Internet Face Database (100% scale)*

- **Non faces set:** non faces images are randomly collected from Internet. They have different sizes, resolutions, compression factor and scenarios. Therefore, they form a fine representation of the wide non faces class.

Figure 106. *Non faces image samples from GTAV Internet Face Database (scaled to different sizes)*

I.1.2. The BioID Face Database

http://www.humanscan.de/support/downloads/facedb.php

The BioID Face Database is public database from HumanScan, a biometric software development company focused on multimodal biometric authentication technology.

This faces database has been recorded and published to give all researchers working in the area of face detection the possibility to compare the quality of their face detection algorithms.

Special emphasis has been given to achieve real world conditions. Therefore the test set contains a large variety of illumination, background and face size.

Figure 107. *BioID database image samples (25% scale)*

a) Description of the BioID Face Database

- 1521 gray level images.
- Resolution of 384x286 pixels.
- Each image shows one frontal view of a face.
- 23 different test persons.
- The images are labeled *BioID_xxxx.pgm*.
- The files *BioID_xxxx.eye* contain the eye positions for the corresponding images.
- The files *BioID_xxxx.pts* contain 20 additional feature points, which are very useful for facial analysis and gesture recognition.

b) Image File Format

The images are stored in single files using the ***Portable Gray Map*** (***PGM***) data format. A *PGM* file contains a data header followed by the image data. In this case the header consists of four lines of text:

- 1st line: image data format (ASCII/binary). In this case binary (indicated with ***P5)***.
- 2nd line: image width in text form (384).
- 3rd line: image height in text form (286).
- 4th line: maximum allowed gray value (255).

The header is followed by a data block containing the image data. The data is stored line per line from top to bottom using one byte per pixel.

c) Eye Position File Format

The eye position files are text files containing a single comment line followed by the x and y coordinate of the left eye and the x and y coordinate of the right eye separated by spaces. Note that left eye refers to the person's left eye. Therefore, when captured by a camera, the position of the left eye is on the image's right and vice versa.

```
#LX     LY      RX      RY
231     99      159     98
```

Figure 108. *Eye position file format*

d) FGnet Markup Scheme of the BioID Face Database

The BioID Face Database is being used within the *FGnet* project of the *European Working Group* on face and gesture recognition. PhD students from the department of Imaging Science and Biomedical Engineering at the University of Manchester marked up the images from the BioID Face Database. They selected several additional feature points, which are very useful for facial analysis and gesture recognition.

There are 20 manually placed points with the following markup scheme:

0 = right eye pupil
1 = left eye pupil
2 = right mouth corner
3 = left mouth corner
4 = outer end of right eye brow
5 = inner end of right eye brow
6 = inner end of left eye brow
7 = outer end of left eye brow
8 = right temple
9 = outer corner of right eye
10 = inner corner of right eye
11 = inner corner of left eye
12 = outer corner of left eye
13 = left temple
14 = tip of nose
15 = right nostril
16 = left nostril
17 = centre point on outer edge of upper lip
18 = centre point on outer edge of lower lip
19 = tip of chin

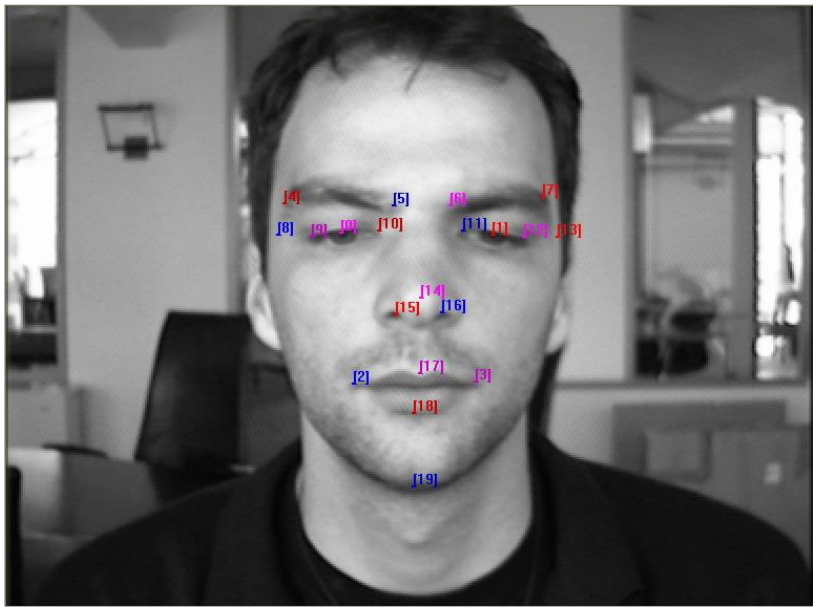


```
version: 1
n_points: 20
{
159.128 108.541
230.854 109.176
164.841 179.633
223.237 178.998
132.469 93.9421
183.883 94.5768
211.177 95.2116
254.974 91.4031
129.295 109.176
144.529 109.811
176.901 107.272
216.89 107.272
246.088 110.445
261.957 109.811
196.578 139.009
184.518 147.261
207.369 145.991
195.943 175.189
193.404 193.597
192.769 229.143
}
```

Figure 109. *Image sample with its corresponding points file*

In order to adequate these images to our experiments a preprocessing step is applied:

PGM to BMP conversion

Due to the fact that our application, *FaceProcessingTool*, only accepts JPG and BMP images, the possibility to implement a *Portable Gray Map* (PGM) image reader was evaluated, but for simplicity, it was decided to batch convert all the images to bmp.

Image crop

19x19 and 130x151 pixels face images are needed for the face detection and face recognition application, respectively. Therefore, a subroutine was developed in order to crop all images by means of the following points extracted from ***BioID_xxxx.pts*** file:

- Right temple (**markup #8**)
- Left temple (**markup #13**)
- Kin (**markup #19**)

```
n_points: 20
{
159.128 108.541
230.854 109.176
164.841 179.633
223.237 178.998
132.469 93.9421
183.883 94.5768
211.177 95.2116
254.974 91.4031
129.295 109.176
144.529 109.811
176.901 107.272
216.89 107.272
246.088 110.445
261.957 109.811
196.578 139.009
184.518 147.261
207.369 145.991
195.943 175.189
193.404 193.597
192.769 229.143
}
```

Figure 110. *The 3 points used in order to crop images and an example file (BioID_0000.pts)*

The image is affine warped by means of matrix affine transform using 3 points. The function *cvGetAffineTransform* from *OpenCV* libraries calculates the matrix of an affine transform as follows:

$$\begin{aligned} &(x'_i, y'_i)^T = map\_matrix \bullet (x_i, y_i, 1)^T \\ &where: \\ &\quad dst[i] = (x'_i, y'_i) \\ &\quad src[i] = (x_i, y_i) \\ &\quad i = 0..2 \end{aligned} \tag{59}$$

where:

- ***src*** is the coordinates vector of the 3 triangle vertices in the source image.
- ***dst*** is the coordinates vector of the 3 corresponding triangle vertices in the destination image.
- ***map_matrix*** is the pointer to the destination 2×3 matrix.

The function *cvWarpAffine* from *OpenCV* transforms source image using the specified matrix:

$$\begin{aligned} &dst(x', y') \leftarrow src(x, y) \\ &(x', y')^T = map\_matrix \bullet (x, y, 1)^T + b \end{aligned} \tag{60}$$

Once the image has been warped the face region is cropped.

Face Detection

In case of face detection database, the following 3 points are used in order to warp face image:

$$\begin{aligned} &src[0].x = cvPtLeftTemple..x - r \quad \Rightarrow \quad dst[0].x = 0 \\ &src[0].y = cvPtLeftTemple.y \quad \Rightarrow \quad dst[0].y = cvPtLeftTemple.y \\ \\ &src[1].x = cvPtRightTemple.x + r \quad \Rightarrow \quad dst[1].x = 2r + Width \\ &src[1].y = cvPtRightTemple.y \quad \Rightarrow \quad dst[1].y = dst[0].y \\ \\ &src[2].x = cvPtKin.x \quad \Rightarrow \quad dst[2].x = \lfloor dst[1].x/2 \rfloor \\ &src[2].y = cvPtKin.y + r \quad \Rightarrow \quad dst[2].y = dst[0].y + \lceil (2r + Height) \cdot (5/7) \rceil \end{aligned} \tag{61}$$

where:

- ***[0]*** *point is face* ***left temple****.*
- ***[1]*** *point is face* ***right temple****.*
- ***[2]*** *point is face* ***kin****.*
- ***Width*** *is face image width, after* $LBP_{(8,1)}$*:* ***17*** *pixels.*
- ***Height*** *is face image height, after* $LBP_{(8,1)}$*:* ***17*** *pixels.*
- ***r*** *is LBP radius:* ***1*** *pixels.*

Then, the face region is extracted from the image:

$$
\begin{aligned}
x_0 &= dst[0].x \\
y_0 &= dst[0].y - \lceil (2r + Height) \cdot (2/7) \rceil \\
Width' &= (Width + 2r) \\
Height' &= (Height + 2r)
\end{aligned}
\tag{62}
$$

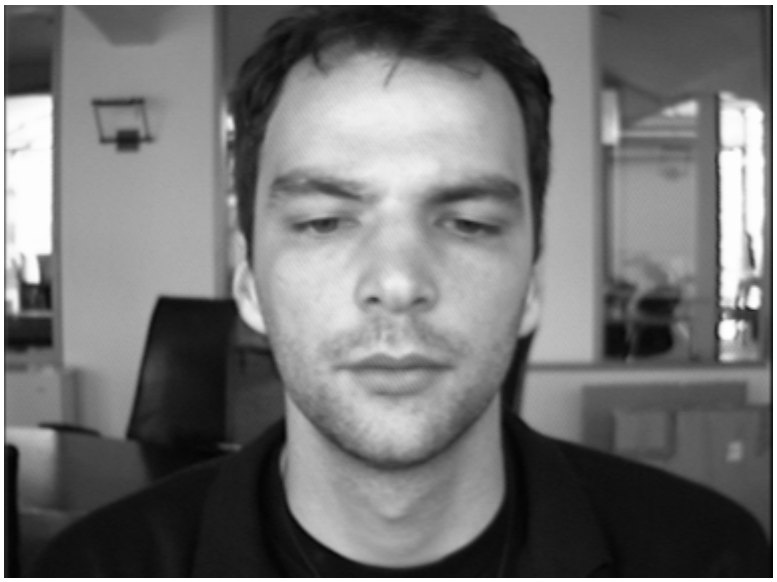

(a) Original image (BioID_0000.bmp)

(b) Warped and cropped result image (warp_19x19_BioID_0000.bmp)

Figure 111. *Face Detection: Image warping and cropping example*

Face Recognition

In case of face recognition database, the following 3 points are used in order to warp face image:

$$
\begin{aligned}
&src[0].x = cvPtLeftTemple..x - r \quad \Rightarrow \quad dst[0].x = 0 \\
&src[0].y = cvPtLeftTemple.y \quad \Rightarrow \quad dst[0].y = cvPtLeftTemple.y \\
&\\
&src[1].x = cvPtRightTemple.x + r \quad \Rightarrow \quad dst[1].x = 2r + (BlockW \cdot nXBlocks) \\
&src[1].y = cvPtRightTemple.y \quad \Rightarrow \quad dst[1].y = dst[0].y \\
&\\
&src[2].x = cvPtKin.x \quad \Rightarrow \quad dst[2].x = dst[1].x/2 \\
&src[2].y = cvPtKin.y + r \quad \Rightarrow \quad dst[2].y = dst[0].y + r + (nYBlocks - 2) \cdot BlockH
\end{aligned}
\tag{63}
$$

where:

- ***[0]*** *point is face* ***left temple****.*
- ***[1]*** *point is face* ***right temple****.*
- ***[2]*** *point is face* ***kin****.*
- ***BlockW*** *is block width:* ***18*** *pixels.*
- ***BlockH*** *is block height:* ***21*** *pixels.*
- ***nXBlocks*** *is the number of x blocks:* ***7*** *blocks.*
- ***nYBlocks*** *is the number of y blocks:* ***7*** *blocks.*
- ***r*** *is LBP radius:* ***2*** *pixels.*

Then, the face region is extracted from the image:

$$\begin{aligned} x_0 &= dst[0].x \\ y_0 &= dst[0].y - (BlockH \cdot 2 + r) \\ Width &= (BlockW \cdot nXBlocks + 2r) \\ Height &= (BlockH \cdot nYBlocks + 2r) \end{aligned} \tag{64}$$

(a) Original image (BioID_0000.bmp) *(b) Warped and cropped result image (warp_130x151_BioID_0000.bmp)*

Figure 112. *Face Recognition: Image warping and cropping example*

I.1.3. The Facial Recognition Technology (FERET) Database

http://www.itl.nist.gov/iad/humanid/feret/feret_master.html

The FERET program (1993-1997) was sponsored by the *Department of Defense's Counterdrug Technology Development Program* through the *Defense Advanced Research Products Agency* (DARPA). Its primary mission was to develop automatic face recognition capabilities that could be employed to assist security, intelligence and law enforcement personnel in the performance of their duties.

The FERET image corpus was assembled to support government monitored testing and evaluation of face recognition algorithms using standardized tests and procedures. The final dataset consists of 14051 eight-bit grayscale images of human heads, 1199 different persons, with views ranging from frontal to left and right profiles.

The images contain variations in lighting, facial expressions, pose angle, etc.

I.1.4. CMU Database

This image dataset is used by the CMU Face Detection Project and is provided for evaluating algorithms for detecting frontal views of human faces. This particular test set was originally assembled as part of work in Neural Network Based Face Detection. It combines images collected at CMU and MIT.

Ground truth in face location is provided in the following format with one line per face (extreme side views are ignored):

filename left-eye right-eye nose left-corner-mouth center-mouth right-corner-mouth

For each feature on a face to be detected, two numbers are given. These numbers are the x and y coordinates (measured from the upper left corner) of the feature in the image.
The images are in Compuserve GIF format and are grayscale. The images are available individually or collectively in a tar file. This file will unpack into four directories:

test: containing the images in Test Set A.
test-low: containing Test Set B.
newtest: containing Test Set C.
rotated: containing the Rotated Test Set.

Test Set B was provided by Kah-Kay Sung and Tomaso Poggio at the AI/CBCL Lab at MIT, and Test Sets A,C and the rotatated test set were collected at CMU (by Henry A. Rowley, Shumeet Baluja, and Takeo Kanade).

*a) From **test** (to 30 reduced)*

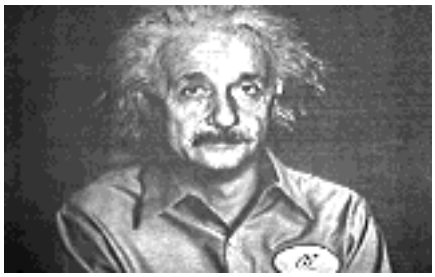

*b) From **test-low** (100)*

*c) From **newtest** (to 50 reduced)*

*d) From **rotated** (to 30 reduced)*

***Figure 113.** CMU database image samples*

II. Skin Chromaticity

A color can be described as a mixture of three other colors or *tristimuli*. The amount of each stimulus defines the color. However, it is frequently useful to separate the color definition into *luminance* (luminous intensity) and *chromaticity* (color information).

Each color representation system has its benefits and disadvantages depending on the application. In case of skin representation, the most widely used are the chromaticity based ones due to its robustness against intensity and illumination.

The evolution of the chrominance based systems is exposed in the following lines:

CIE Standard XYZ (1931)

The standard defines the positive *tristimuli* for all visible light sources, which can be calculated as follows:

$$\begin{bmatrix} X \\ Y \\ Z \end{bmatrix} = \begin{bmatrix} 0.490 & 0.310 & 0.200 \\ 0.177 & 0.813 & 0.011 \\ 0.000 & 0.010 & 0.990 \end{bmatrix} \begin{bmatrix} R \\ G \\ B \end{bmatrix} \tag{65}$$

XYZ are virtual primaries, based on human eye response and *metamerism* effect (two light sources can have the same *apparent color* to an observer).

As a result, the spectrum locus is represented as shown in the following figure (2D projection: X+Y+Z=1):

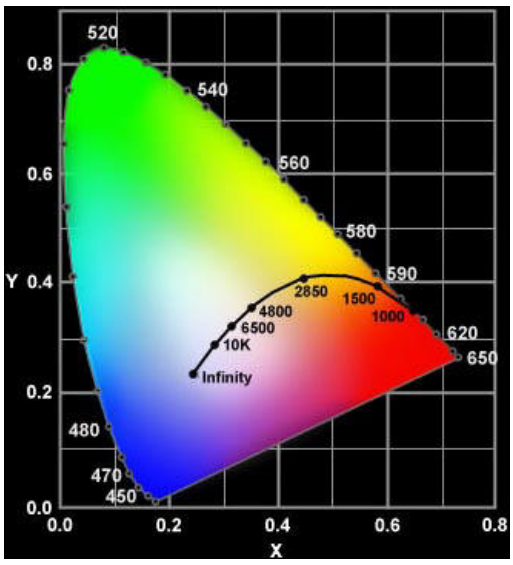

Figure 114. *Spectrum Locus*

The XYZ normalized values can be also calculated as follows:

$$x = \frac{X}{X+Y+Z}, \qquad y = \frac{Y}{X+Y+Z}, \qquad z = \frac{Z}{X+Y+Z} = 1 - x - y \tag{66}$$

Mac Adam's Ellipses

In the spectrum locus, elliptical areas with *equal color* can be represented, as seen next figure.

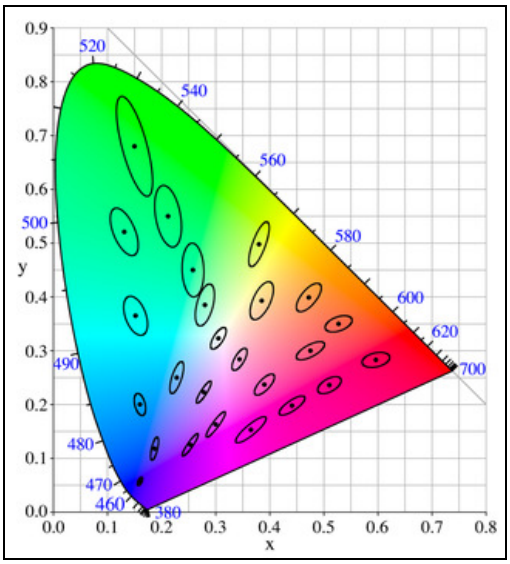

Figure 115. *Mac Adam's Ellipses*

The minimum change in XYZ to appreciate chrominance variations is called JND (*Just Noticeable Difference*).

As it can be observed in the figure, human eye is very sensible to variations in skin color but not in green levels.

CIE UCS: Uniform Chromaticity Scale (1960)

Lately a uniform chromaticity representation is proposed where these ellipses become circles:

$$u = \frac{4X}{X+15Y+3Z} = \frac{4x}{-2x+12y+3}$$
$$v = \frac{6Y}{X+15Y+3Z} = \frac{6y}{-2x+12y+3} \qquad (67)$$

CIE LUV: Perceptual Uniformity (1976)

Some years later, a modification in the v component generates the LUV perceptual uniformity representation:

$$u' = u = \frac{4X}{X+15Y+3Z}$$
$$v' = \frac{3}{2}v = \frac{9Y}{X+15Y+3Z} = \frac{9y}{-2x+12y+3} \qquad (68)$$

III. Face Detection Result

This section contains some detailed information that can help to understand face detection experimental results.

III.1.1. Face Detection Computational Cost Analysis

In such a kind of algorithms, such as face detection, one of the most important limitations is the algorithm speed affected by the scanning method used for input image exploration for face candidates searching (see section *4.1*).

Although two stages algorithm is proposed in order to improve efficiency, when searching in high resolution images, using down-sampling and a moving scan smaller than one block width the detection algorithm can be very slow.

It can be demonstrated that the total number of blocks to be analyzed can be calculated as follows:

$$\#blocks = \sum_{n=0}^{\#iterations-1} \left(\frac{\frac{ImgWidth}{DS^n} - (BlockWidth - MS)}{MS} \right) \times \left(\frac{\frac{ImgHeight}{DS^n} - (BlockHeight - MS)}{MS} \right) \quad (69)$$

The number of iterations in the down-sampling process can be calculated by means of the following expressions:

$$\#iterations = \sum_{n=0}^{\infty} w\left(\left\lfloor \frac{ImgWidth}{DS^n} \right\rfloor \right) \cdot h\left(\left\lfloor \frac{ImgHeight}{DS^n} \right\rfloor \right) \quad (70)$$

where functions *w(x)* and *h(y)* are defined as follows:

$$w(x) = \begin{cases} 1 & if \quad x \geq BlockWidth \\ 0 & if \quad x < BlockWidth \end{cases} \quad (71)$$

$$h(y) = \begin{cases} 1 & if \quad y \geq BlockHeight \\ 0 & if \quad y < BlockHeight \end{cases} \quad (72)$$

and:

- *DS* is the down-sampling rate.
- *MS* is the moving scan pixels.
- *ImgWidth* and *ImgHeight* are the image size.
- *BlockWidth* and *BlockHeight* are the block size.
- *n* is the current iteration.

For example, in the following situation:

- VGA resolution (640x480)
- Down-sampling rate of 1.2
- Moving scan of 2 pixels
- Block size of 19x19 pixels

The number of iterations is calculated as follows:

$$\#iterations = \sum_{n=0}^{\infty} w\left(\left\lfloor \frac{640}{1.2^n} \right\rfloor\right) \cdot h\left(\left\lfloor \frac{480}{1.2^n} \right\rfloor\right) = \sum_{n=0}^{\infty} h\left(\left\lfloor \frac{480}{1.2^n} \right\rfloor\right) = 18\, iterations \tag{73}$$

$$h(y) = \begin{cases} 1 & if \quad y \geq 19 \\ 0 & if \quad y < 19 \end{cases} \tag{74}$$

Then, the total number of blocks is:

$$\#blocks = \sum_{n=0}^{17} \left(\frac{\frac{640}{1.2^n} - (19-2)}{2} \right) \times \left(\frac{\frac{480}{1.2^n} - (19-2)}{2} \right) = \sum_{n=0}^{17} \frac{\left(\frac{640}{1.2^n} - 17\right) \times \left(\frac{480}{1.2^n} - 17\right)}{4} = \tag{75}$$

$$= 223{,}535\, blocks$$

III.1.2. Chi Square Classification

Following section presents the classification result using mean value models and *Chi Square* dissimilarly metric for the cases of weighted and non weighted blocks and for both databases: ***GTAV Internet (16x16)*** and ***BioID (19x19)***.

Non Weighted

GTAV Internet (16x16)

The following table presents the classification result using mean value models and *Chi Square* dissimilarly metric. Each row contains a bootstrap iteration with the following information (from left to right):

- Current bootstrap iteration.
- Number of repetition of the false classified samples reintroduced in the training set.
- The number of non faces training samples incorrectly classified.
- Number of positive and negative training samples.
- Percentage of faces and non faces correctly classified.

GTAV Internet database 16x16 - mean value & chi square non weighted						
Bootstrap			***Training Samples***		***Correct classification***	
#	False classified samples repetition	# False Positive	Positive	Negative	**Faces (%)**	**Non faces (%)**
Before	-	1467	6650	6605	98.70%	75.45%
1	5	213	6650	13940	88.90%	94.81%
2	5	153	6650	15005	87.15%	96.46%
3	5	119	6650	15770	86.00%	97.15%
4	10	82	6650	16960	84.75%	97.89%
5	10	58	6650	17780	83.80%	98.25%
6	10	52	6650	18360	83.15%	98.47%
7	10	49	6650	18880	82.65%	98.67%
8	10	37	6650	19370	82.35%	98.79%
9	15	35	6650	19925	81.85%	98.93%
10	15	31	6650	20450	81.25%	99.00%

Table 32. *Bootstrap strategy to improve Mean Models & Chi Square classification ratio (16x16 faces)*

BioID (19x19)

The following figure presents the results from *BioID* database with 19x19face size.

BioID database 19x19 - mean value & chi square non weighted						
Bootstrap			***Training Samples***		***Correct classification***	
#	False classified samples repetition	# False Positive	Positive	Negative	**Faces (%)**	**Non faces (%)**
Before	-	1437	2981	6605	99.65%	71.47%
1	5	386	2981	13790	94.65%	89.81%
2	5	276	2981	15720	93.70%	92.15%
3	5	224	2981	17100	92.40%	93.50%
4	10	165	2981	19340	91.00%	95.28%
5	10	127	2981	20990	89.95%	96.35%
6	10	113	2981	22260	88.80%	97.09%
7	10	88	2981	23390	87.75%	97.65%
8	10	69	2981	24270	87.05%	98.07%
9	15	58	2981	25305	86.05%	98.42%
10	15	48	2981	26175	85.55%	98.65%

Table 33. *Bootstrap strategy to improve Mean Models & Chi Square classification ratio (19x19 faces)*

III.1.3. Principal Component Analysis

Faces and Non-Faces

In order to better see the eigenvalues information, the following table shows the normalized eigenvalues for 1st and 2nd stages and for both databases, 16x16 and 19x19 faces. The *%Info* column is the accumulated % information if eigenvalues from number 1 to *n* row are kept.

	Norm_eigenvals_1stStageCoarse					**norm_eigenvals_2ndStageFine**			
	16x16		19x19			16x16		19x19	
	Eigenvalue	% Info	Eigenvalue	% Info		Eigenvalue	% Info	Eigenvalue	% Info
1	0.51587569	51.59%	0.57079131	57.08%	1	0.28315487	28.32%	0.40479755	40.48%
2	0.15332067	66.92%	0.17053065	74.13%	2	0.05828740	34.14%	0.07213775	47.69%
3	0.05217609	72.14%	0.04577915	78.71%	3	0.05038590	39.18%	0.06041664	53.74%
4	0.03602537	75.74%	0.03461586	82.17%	4	0.04706113	43.89%	0.05917424	59.65%
5	0.03045715	78.79%	0.02339686	84.51%	5	0.04149003	48.04%	0.05408509	65.06%
6	0.02096952	80.88%	0.01985427	86.50%	6	0.02994824	51.03%	0.02890813	67.95%
7	0.01921549	82.80%	0.01298886	87.80%	7	0.02422030	53.45%	0.02664519	70.62%
8	0.01429545	84.23%	0.01110365	88.91%	8	0.02272362	55.73%	0.02107954	72.72%
9	0.01366349	85.60%	0.00999613	89.91%	9	0.02002354	57.73%	0.01876637	74.60%
10	0.01189272	86.79%	0.00909007	90.81%	10	0.01863823	59.59%	0.01724930	76.33%
11	0.01110972	87.90%	0.00846822	91.66%	11	0.01764229	61.36%	0.01518112	77.84%
12	0.00960095	88.86%	0.00841359	92.50%	12	0.01649092	63.01%	0.01424158	79.27%
13	0.00862218	89.72%	0.00646510	93.15%	13	0.01583933	64.59%	0.01277142	80.55%
14	0.00832235	90.55%	0.00639613	93.79%	14	0.01410298	66.00%	0.01209003	81.75%
15	0.00607505	91.16%	0.00428605	94.22%	15	0.01367489	67.37%	0.01169190	82.92%
16	0.00533436	91.70%	0.00399355	94.62%	16	0.01250842	68.62%	0.01024895	83.95%
17	0.00503598	92.20%	0.00372116	94.99%	17	0.01195735	69.81%	0.00602279	84.55%
18	0.00469275	92.67%	0.00345817	95.33%	18	0.01100291	70.92%	0.00591119	85.14%
19	0.00433177	93.10%	0.00334573	95.67%	19	0.01061569	71.98%	0.00573715	85.72%
20	0.00386887	93.49%	0.00293533	95.96%	20	0.01017296	72.99%	0.00562257	86.28%

21	0.00384998	93.87%	0.00264048	96.23%
22	0.00336312	94.21%	0.00226910	96.45%
23	0.00325174	94.54%	0.00192051	96.65%
24	0.00285728	94.82%	0.00184784	96.83%
25	0.00278820	95.10%	0.00175048	97.01%
26	0.00253596	95.35%	0.00170683	97.18%
27	0.00240194	95.59%	0.00154537	97.33%
28	0.00232774	95.83%	0.00150178	97.48%
29	0.00224248	96.05%	0.00142928	97.62%
30	0.00220935	96.27%	0.00136621	97.76%
31	0.00216400	96.49%	0.00130902	97.89%
32	0.00211282	96.70%	0.00125141	98.02%
33	0.00194541	96.89%	0.00121934	98.14%
34	0.00183274	97.08%	0.00118606	98.26%
35	0.00178422	97.26%	0.00111286	98.37%
36	0.00177571	97.43%	0.00109354	98.48%
37	0.00176087	97.61%	0.00103416	98.58%
38	0.00162683	97.77%	0.00097534	98.68%
39	0.00162284	97.93%	0.00095583	98.77%
40	0.00153230	98.09%	0.00092125	98.87%
41	0.00151964	98.24%	0.00087780	98.95%
42	0.00148929	98.39%	0.00085568	99.04%
43	0.00132962	98.52%	0.00083480	99.12%
44	0.00132068	98.65%	0.00079166	99.20%
45	0.00130722	98.78%	0.00076410	99.28%
46	0.00126383	98.91%	0.00075455	99.35%
47	0.00120971	99.03%	0.00072046	99.43%
48	0.00114648	99.15%	0.00069969	99.50%
49	0.00112464	99.26%	0.00062998	99.56%
50	0.00108433	99.37%	0.00060846	99.62%
51	0.00103090	99.47%	0.00057013	99.68%
52	0.00099991	99.57%	0.00054818	99.73%
53	0.00099471	99.67%	0.00053307	99.79%
54	0.00091429	99.76%	0.00051049	99.84%
55	0.00071232	99.83%	0.00047868	99.88%
56	0.00058314	99.89%	0.00041422	99.93%
57	0.00057849	99.95%	0.00037611	99.96%
58	0.00051969	100.00%	0.00036543	100.00%
59	0.00000000	100.00%	0.00000000	100.00%

21	0.00878285	73.87%	0.00507942	86.79%
22	0.00819471	74.69%	0.00482032	87.27%
23	0.00769814	75.46%	0.00472973	87.74%
24	0.00757896	76.22%	0.00462768	88.20%
25	0.00701158	76.92%	0.00436151	88.64%
26	0.00663225	77.58%	0.00415496	89.06%
27	0.00634174	78.22%	0.00412608	89.47%
28	0.00626315	78.84%	0.00402869	89.87%
29	0.00608913	79.45%	0.00390397	90.26%
30	0.00580846	80.03%	0.00385912	90.65%
31	0.00541565	80.58%	0.00377147	91.02%
32	0.00524517	81.10%	0.00351214	91.38%
33	0.00520855	81.62%	0.00348078	91.72%
34	0.00510704	82.13%	0.00337905	92.06%
35	0.00506198	82.64%	0.00291573	92.35%
36	0.00471481	83.11%	0.00278744	92.63%
37	0.00469698	83.58%	0.00270394	92.90%
38	0.00458505	84.04%	0.00255300	93.16%
39	0.00448266	84.49%	0.00223955	93.38%
40	0.00428407	84.91%	0.00221890	93.60%
41	0.00404259	85.32%	0.00205373	93.81%
42	0.00398414	85.72%	0.00193034	94.00%
43	0.00390931	86.11%	0.00188352	94.19%
44	0.00377014	86.49%	0.00184141	94.37%
45	0.00363486	86.85%	0.00179327	94.55%
46	0.00353552	87.20%	0.00174147	94.73%
47	0.00336184	87.54%	0.00171307	94.90%
48	0.00328433	87.87%	0.00168989	95.07%
49	0.00324154	88.19%	0.00162199	95.23%
50	0.00315878	88.51%	0.00158940	95.39%
51	0.00299024	88.81%	0.00156632	95.55%
52	0.00297613	89.10%	0.00151389	95.70%
53	0.00282973	89.39%	0.00143222	95.84%
54	0.00281541	89.67%	0.00139190	95.98%
55	0.00275922	89.94%	0.00132063	96.11%
56	0.00269353	90.21%	0.00125785	96.24%
57	0.00264634	90.48%	0.00125020	96.36%
58	0.00254321	90.73%	0.00118116	96.48%
59	0.00244297	90.98%	0.00116615	96.60%
60	0.00240195	91.22%	0.00115676	96.71%
61	0.00237404	91.45%	0.00113328	96.83%
62	0.00233838	91.69%	0.00110225	96.94%
63	0.00233179	91.92%	0.00108304	97.04%
64	0.00230396	92.15%	0.00103022	97.15%
65	0.00229540	92.38%	0.00100639	97.25%
66	0.00221018	92.60%	0.00094121	97.34%
67	0.00216622	92.82%	0.00092935	97.44%
68	0.00210121	93.03%	0.00092273	97.53%
69	0.00202553	93.23%	0.00091832	97.62%
70	0.00199898	93.43%	0.00088186	97.71%
71	0.00195723	93.63%	0.00084622	97.79%
72	0.00190545	93.82%	0.00084432	97.88%
73	0.00186714	94.00%	0.00080869	97.96%
74	0.00184162	94.19%	0.00079370	98.04%
75	0.00182702	94.37%	0.00076363	98.11%
76	0.00181639	94.55%	0.00074276	98.19%
77	0.00172557	94.73%	0.00072300	98.26%

78	0.00165868	94.89%	0.00070604	98.33%
79	0.00164190	95.06%	0.00068077	98.40%
80	0.00160754	95.22%	0.00063146	98.46%
81	0.00158134	95.37%	0.00061951	98.52%
82	0.00154523	95.53%	0.00060073	98.58%
83	0.00149310	95.68%	0.00058105	98.64%
84	0.00147240	95.83%	0.00057427	98.70%
85	0.00144812	95.97%	0.00052266	98.75%
86	0.00140841	96.11%	0.00050666	98.80%
87	0.00137859	96.25%	0.00049411	98.85%
88	0.00135566	96.38%	0.00048640	98.90%
89	0.00134574	96.52%	0.00048396	98.95%
90	0.00133008	96.65%	0.00047541	99.00%
91	0.00129663	96.78%	0.00047012	99.04%
92	0.00127984	96.91%	0.00046061	99.09%
93	0.00127104	97.04%	0.00045398	99.13%
94	0.00123614	97.16%	0.00044060	99.18%
95	0.00119924	97.28%	0.00041819	99.22%
96	0.00118590	97.40%	0.00040744	99.26%
97	0.00114838	97.51%	0.00039236	99.30%
98	0.00113702	97.63%	0.00038103	99.34%
99	0.00109612	97.74%	0.00037617	99.38%
100	0.00108231	97.85%	0.00034740	99.41%
101	0.00100609	97.95%	0.00033384	99.44%
102	0.00098101	98.04%	0.00030674	99.47%
103	0.00093275	98.14%	0.00030082	99.51%
104	0.00090496	98.23%	0.00028225	99.53%
105	0.00089488	98.32%	0.00026555	99.56%
106	0.00086437	98.40%	0.00026017	99.59%
107	0.00083505	98.49%	0.00025738	99.61%
108	0.00082588	98.57%	0.00025410	99.64%
109	0.00081080	98.65%	0.00023549	99.66%
110	0.00079569	98.73%	0.00022845	99.68%
111	0.00077668	98.81%	0.00021945	99.71%
112	0.00077126	98.89%	0.00021018	99.73%
113	0.00074330	98.96%	0.00020000	99.75%
114	0.00073141	99.03%	0.00019185	99.77%
115	0.00068140	99.10%	0.00018942	99.78%
116	0.00067462	99.17%	0.00018362	99.80%
117	0.00065082	99.23%	0.00018024	99.82%
118	0.00064491	99.30%	0.00017823	99.84%
119	0.00061407	99.36%	0.00016273	99.85%
120	0.00057858	99.42%	0.00014789	99.87%
121	0.00056771	99.47%	0.00013148	99.88%
122	0.00052382	99.53%	0.00012467	99.90%
123	0.00049012	99.58%	0.00012031	99.91%
124	0.00048330	99.62%	0.00011620	99.92%
125	0.00045867	99.67%	0.00011513	99.93%
126	0.00045417	99.71%	0.00011308	99.94%
127	0.00043720	99.76%	0.00008819	99.95%
128	0.00041351	99.80%	0.00008673	99.96%
129	0.00039382	99.84%	0.00007933	99.97%
130	0.00036495	99.88%	0.00007457	99.97%
131	0.00030746	99.91%	0.00007154	99.98%

132	0.00029116	99.94%	0.00006111	99.99%
133	0.00026594	99.96%	0.00005573	99.99%
134	0.00021677	99.98%	0.00003530	99.997%
135	0.00016163	100.00%	0.00002918	100.00%
136	0.00000000	100.00%	0.00000000	100.00%
137	0.00000000	100.00%	0.00000000	100.00%
138	0.00000000	100.00%	0.00000000	100.00%
139	0.00000000	100.00%	0.00000000	100.00%
140	0.00000000	100.00%	0.00000000	100.00%
141	0.00000000	100.00%	0.00000000	100.00%
142	0.00000000	100.00%	0.00000000	100.00%
143	0.00000000	100.00%	0.00000000	100.00%
144	0.00000000	100.00%	0.00000000	100.00%

Table 34. *Face Detection: PCA eigenvalues for both stages and DBs*

GTAV Internet (16x16)

The following table presents the classification result using *PCA & Relative Difference Normalized* as dissimilarly metric. Each row contains a bootstrap iteration with the following information (from left to right):

- Current bootstrap iteration.
- Number of repetition of the false classified samples reintroduced in the training set.
- The number of non faces training samples incorrectly classified.
- Number of positive and negative training samples.
- Percentage of faces and non faces correctly classified.

GTAV database 16x16 - PCA & RelDiffNorm						
Bootstrap			***Training Samples***		***Correct classification***	
#	False classified samples repetition	# False Positive	Positive	Negative	**Faces (%)**	**Non faces (%)**
Before	-	2216	6650	6605	99.40%	63.53%
1	5	270	6650	15180	80.75%	93.66%
2	5	188	6650	18260	81.60%	95.47%
3	5	159	6650	20655	81.35%	96.26%
4	10	110	6650	24645	81.50%	97.18%
5	10	89	6650	27495	81.10%	97.64%
6	10	67	6650	29805	81.00%	97.94%
7	15	59	6650	32625	80.85%	98.20%
8	15	43	6650	34905	80.55%	98.40%
9	15	39	6650	36885	80.30%	98.51%
10	20	36	6650	39285	80.55%	98.66%

Table 35. *Bootstrap strategy to improve PCA & RelDiffNorm classification ratio (case 16x16 faces)*

BioID (19x19)

The following table presents the results from *BioID* database with 19x19 face size.

BioID database 19x19 - PCA & RelDiffNorm						
Bootstrap			***Training Samples***		***Correct classification***	
#	False classified samples repetition	# False Positive	Positive	Negative	**Faces (%)**	**Non faces (%)**
Before	-	1715	6650	6605	98.55%	66.72%
1	5	616	6650	15180	91.40%	86.82%
2	5	479	6650	18260	90.05%	88.98%
3	5	399	6650	20655	88.15%	90.52%
4	10	285	6650	24645	84.60%	92.75%
5	10	231	6650	27495	81.25%	94.06%
6	10	188	6650	29805	78.65%	94.96%
7	15	152	6650	32625	76.25%	95.85%
8	15	132	6650	34905	73.50%	96.41%
9	15	120	6650	36885	72.75%	96.68%
10	20	98	6650	39285	68.50%	97.28%

Table 36. *Bootstrap strategy to improve PCA & RelDiffNorm classification ratio (case 19x19 faces)*

Only Faces

The following table shows the normalized eigenvalues for 1st and 2nd stages and for both databases, 16x16 and 19x19 faces. The *%Info* column is the accumulated % information if eigenvalues from number 1 to *n* row are kept.

	norm_eigenvals_1stStageCoarse					**norm_eigenvals_2ndStageFine**			
	16x16		19x19			16x16		19x19	
	Eigenvalue	*% Info.*	*Eigenvalue*	*% Info.*		*Eigenvalue*	*% Info.*	*Eigenvalue*	*% Info.*
1	0.24353742	24.35%	0.29741349	29.74%	1	0.12535461	12.54%	0.12179501	12.18%
2	0.13038176	37.39%	0.08162850	37.90%	2	0.07598462	20.13%	0.09811051	21.99%
3	0.08686595	46.08%	0.07197417	45.10%	3	0.05063172	25.20%	0.07055342	29.05%
4	0.05157236	51.24%	0.05300276	50.40%	4	0.03906026	29.10%	0.05674052	34.72%
5	0.03253504	54.49%	0.03872715	54.27%	5	0.03471171	32.57%	0.04486154	39.21%
6	0.02898263	57.39%	0.03175230	57.45%	6	0.03450795	36.03%	0.02742524	41.95%
7	0.02587469	59.97%	0.02456580	59.91%	7	0.03094502	39.12%	0.02637600	44.59%
8	0.02158141	62.13%	0.02148120	62.05%	8	0.02660298	41.78%	0.02553036	47.14%
9	0.02150633	64.28%	0.02015647	64.07%	9	0.02347530	44.13%	0.02426999	49.57%
10	0.01907075	66.19%	0.01940468	66.01%	10	0.02038604	46.17%	0.02161654	51.73%
11	0.01608041	67.80%	0.01761172	67.77%	11	0.01763669	47.93%	0.01984888	53.71%
12	0.01536905	69.34%	0.01609845	69.38%	12	0.01727806	49.66%	0.01961418	55.67%
13	0.01338253	70.67%	0.01493478	70.88%	13	0.01647619	51.31%	0.01750427	57.42%
14	0.01309971	71.98%	0.01486216	72.36%	14	0.01523997	52.83%	0.01657147	59.08%
15	0.01249585	73.23%	0.01295198	73.66%	15	0.01447897	54.28%	0.01476142	60.56%
16	0.01242373	74.48%	0.01196932	74.85%	16	0.01366803	55.64%	0.01292665	61.85%
17	0.01077525	75.55%	0.01119256	75.97%	17	0.01246691	56.89%	0.01288924	63.14%
18	0.01064632	76.62%	0.01083215	77.06%	18	0.01203106	58.09%	0.01261934	64.40%
19	0.00996030	77.61%	0.01016144	78.07%	19	0.01173005	59.27%	0.01258439	65.66%
20	0.00966332	78.58%	0.00942472	79.01%	20	0.01158040	60.42%	0.01202771	66.86%
21	0.00960634	79.54%	0.00881636	79.90%	21	0.01090926	61.52%	0.01198856	68.06%
22	0.00948366	80.49%	0.00871129	80.77%	22	0.01030516	62.55%	0.01074194	69.14%
23	0.00931850	81.42%	0.00815068	81.58%	23	0.00961189	63.51%	0.01060525	70.20%
24	0.00900385	82.32%	0.00803854	82.39%	24	0.00950403	64.46%	0.01001269	71.20%

25	0.00874649	83.20%	0.00766501	83.15%
26	0.00865047	84.06%	0.00723305	83.88%
27	0.00818064	84.88%	0.00712770	84.59%
28	0.00805734	85.69%	0.00706184	85.30%
29	0.00777323	86.46%	0.00685356	85.98%
30	0.00758397	87.22%	0.00684330	86.66%
31	0.00746809	87.97%	0.00650565	87.32%
32	0.00709702	88.68%	0.00638851	87.95%
33	0.00680969	89.36%	0.00612301	88.57%
34	0.00637637	90.00%	0.00600579	89.17%
35	0.00620387	90.62%	0.00594304	89.76%
36	0.00619757	91.24%	0.00590618	90.35%
37	0.00605538	91.84%	0.00575636	90.93%
38	0.00585918	92.43%	0.00556645	91.48%
39	0.00552127	92.98%	0.00551295	92.04%
40	0.00545338	93.53%	0.00538084	92.57%
41	0.00527897	94.05%	0.00525316	93.10%
42	0.00503820	94.56%	0.00508522	93.61%
43	0.00481770	95.04%	0.00494117	94.10%
44	0.00432901	95.47%	0.00488741	94.59%
45	0.00426101	95.90%	0.00484839	95.08%
46	0.00418303	96.32%	0.00476083	95.55%
47	0.00409667	96.73%	0.00467173	96.02%
48	0.00386853	97.11%	0.00443943	96.46%
49	0.00357816	97.47%	0.00440883	96.90%
50	0.00356541	97.83%	0.00432886	97.34%
51	0.00325301	98.15%	0.00412146	97.75%
52	0.00308699	98.46%	0.00387573	98.14%
53	0.00298577	98.76%	0.00353820	98.49%
54	0.00278570	99.04%	0.00348123	98.84%
55	0.00260892	99.30%	0.00321532	99.16%
56	0.00251061	99.55%	0.00304941	99.46%
57	0.00227481	99.78%	0.00275796	99.74%
58	0.00222639	100.00%	0.00259975	100.00%
59	0.00000000	100.00%	0.00000000	100.00%

25	0.00879985	65.34%	0.00965452	72.16%
26	0.00865356	66.20%	0.00906038	73.07%
27	0.00845531	67.05%	0.00879003	73.95%
28	0.00822124	67.87%	0.00869687	74.82%
29	0.00786503	68.66%	0.00864928	75.68%
30	0.00755500	69.41%	0.00846978	76.53%
31	0.00751580	70.16%	0.00804449	77.33%
32	0.00735088	70.90%	0.00747040	78.08%
33	0.00721965	71.62%	0.00717165	78.80%
34	0.00720880	72.34%	0.00694999	79.49%
35	0.00705804	73.05%	0.00682832	80.18%
36	0.00692655	73.74%	0.00647355	80.82%
37	0.00665413	74.41%	0.00621243	81.44%
38	0.00634823	75.04%	0.00612236	82.06%
39	0.00622386	75.66%	0.00591965	82.65%
40	0.00619481	76.28%	0.00573830	83.22%
41	0.00595773	76.88%	0.00565814	83.79%
42	0.00579434	77.46%	0.00526694	84.32%
43	0.00566498	78.02%	0.00506287	84.82%
44	0.00543237	78.57%	0.00471086	85.29%
45	0.00535854	79.10%	0.00463231	85.76%
46	0.00535320	79.64%	0.00453850	86.21%
47	0.00523636	80.16%	0.00426753	86.64%
48	0.00519859	80.68%	0.00420569	87.06%
49	0.00514256	81.20%	0.00395871	87.45%
50	0.00496768	81.69%	0.00395061	87.85%
51	0.00490638	82.18%	0.00371788	88.22%
52	0.00464763	82.65%	0.00363730	88.58%
53	0.00454663	83.10%	0.00355528	88.94%
54	0.00447461	83.55%	0.00348685	89.29%
55	0.00440652	83.99%	0.00342219	89.63%
56	0.00429981	84.42%	0.00335189	89.97%
57	0.00419875	84.84%	0.00323566	90.29%
58	0.00413507	85.25%	0.00320924	90.61%
59	0.00401268	85.66%	0.00318983	90.93%
60	0.00392479	86.05%	0.00299907	91.23%
61	0.00391857	86.44%	0.00297466	91.53%
62	0.00390397	86.83%	0.00279602	91.81%
63	0.00362503	87.19%	0.00277648	92.08%
64	0.00357767	87.55%	0.00269814	92.35%
65	0.00342822	87.89%	0.00256979	92.61%
66	0.00339517	88.23%	0.00253929	92.86%
67	0.00323549	88.56%	0.00247039	93.11%
68	0.00320742	88.88%	0.00244557	93.36%
69	0.00317632	89.20%	0.00239928	93.60%
70	0.00315771	89.51%	0.00231715	93.83%
71	0.00305668	89.82%	0.00222184	94.05%
72	0.00302072	90.12%	0.00217934	94.27%
73	0.00300564	90.42%	0.00194956	94.46%
74	0.00297712	90.72%	0.00192056	94.65%
75	0.00290602	91.01%	0.00190236	94.84%
76	0.00278255	91.29%	0.00184928	95.03%
77	0.00277422	91.56%	0.00184149	95.21%
78	0.00271203	91.83%	0.00177424	95.39%
79	0.00264234	92.10%	0.00176544	95.57%
80	0.00258579	92.36%	0.00167142	95.73%

81	0.00257527	92.62%	0.00167010	95.90%
82	0.00248434	92.86%	0.00162258	96.06%
83	0.00247439	93.11%	0.00154356	96.22%
84	0.00239421	93.35%	0.00147870	96.37%
85	0.00231199	93.58%	0.00145658	96.51%
86	0.00228449	93.81%	0.00139190	96.65%
87	0.00220468	94.03%	0.00135088	96.79%
88	0.00216097	94.25%	0.00134025	96.92%
89	0.00213004	94.46%	0.00132940	97.05%
90	0.00209399	94.67%	0.00131632	97.18%
91	0.00202191	94.87%	0.00127480	97.31%
92	0.00201318	95.07%	0.00125149	97.44%
93	0.00192284	95.26%	0.00120773	97.56%
94	0.00190648	95.46%	0.00114775	97.67%
95	0.00189100	95.64%	0.00111585	97.78%
96	0.00185387	95.83%	0.00111239	97.90%
97	0.00181938	96.01%	0.00110587	98.01%
98	0.00175717	96.19%	0.00104420	98.11%
99	0.00171840	96.36%	0.00103750	98.21%
100	0.00169826	96.53%	0.00099337	98.31%
101	0.00168513	96.70%	0.00095946	98.41%
102	0.00159251	96.86%	0.00095299	98.51%
103	0.00148896	97.01%	0.00095090	98.60%
104	0.00148299	97.15%	0.00093801	98.69%
105	0.00140249	97.29%	0.00083023	98.78%
106	0.00139934	97.43%	0.00082190	98.86%
107	0.00135412	97.57%	0.00072448	98.93%
108	0.00133676	97.70%	0.00072258	99.00%
109	0.00131675	97.84%	0.00066984	99.07%
110	0.00130370	97.97%	0.00065563	99.14%
111	0.00126017	98.09%	0.00055989	99.19%
112	0.00125414	98.22%	0.00054890	99.25%
113	0.00121040	98.34%	0.00051210	99.30%
114	0.00119124	98.46%	0.00046783	99.35%
115	0.00115773	98.57%	0.00046374	99.39%
116	0.00111848	98.68%	0.00045062	99.44%
117	0.00109330	98.79%	0.00044689	99.48%
118	0.00104392	98.90%	0.00044337	99.53%
119	0.00097247	99.00%	0.00040027	99.57%
120	0.00092149	99.09%	0.00038846	99.60%
121	0.00087244	99.18%	0.00038544	99.64%
122	0.00086715	99.26%	0.00037030	99.68%
123	0.00083928	99.35%	0.00035805	99.72%
124	0.00074846	99.42%	0.00034957	99.75%
125	0.00072517	99.49%	0.00034225	99.79%
126	0.00068522	99.56%	0.00032488	99.82%
127	0.00065956	99.63%	0.00028246	99.85%
128	0.00059138	99.69%	0.00027660	99.87%
129	0.00058092	99.74%	0.00024553	99.90%
130	0.00056629	99.80%	0.00021736	99.92%
131	0.00051924	99.85%	0.00019889	99.94%
132	0.00043977	99.90%	0.00018680	99.96%
133	0.00040052	99.94%	0.00017359	99.98%
134	0.00035491	99.97%	0.00013062	99.99%

135	0.00027124	100.00%	0.00011160	100.00%
136	0.00000000	100.00%	0.00000000	100.00%
137	0.00000000	100.00%	0.00000000	100.00%
138	0.00000000	100.00%	0.00000000	100.00%
139	0.00000000	100.00%	0.00000000	100.00%
140	0.00000000	100.00%	0.00000000	100.00%
141	0.00000000	100.00%	0.00000000	100.00%
142	0.00000000	100.00%	0.00000000	100.00%
143	0.00000000	100.00%	0.00000000	100.00%
144	0.00000000	100.00%	0.00000000	100.00%

Table 37. *Face Detection: PCA only faces eigenvalues for both stages and DB*

III.1.4. Support Vector Machine

The following table presents the classification result using *SVM*. Each row contains a bootstrap iteration with the following information (from left to right):

- Current bootstrap iteration.
- Number of repetition of the false classified samples reintroduced in the training set.
- The number of non faces training samples incorrectly classified.
- Number of positive and negative training samples.
- Percentage of faces and non faces correctly classified.

GTAV database 16x16 - SVM									
Bootstrap				***Training Samples***		***Correct classification***			
#	False classified samples repetition	# False Positive		Positive	Negative	1st Stage Classification Ratio		2nd Stage (Final) Classification Ratio	
		1st Stage	2nd Stage			Faces (%)	Non faces (%)	Faces (%)	Non faces (%)
before	-	698	9	6650	6605	96.20%	86.861%	95.95%	99.525%
1	5	151	0	6650	10123	79.20%	95.996%	79.15%	99.863%
2	5	98	0	6650	10878	74.25%	97.316%	74.20%	99.907%
3	5	70	0	6650	11368	71.65%	97.751%	71.60%	99.912%
4	5	54	0	6650	11718	69.05%	98.078%	69.00%	99.926%
5	5	37	0	6650	11988	67.40%	98.237%	67.35%	99.929%

Table 38. *Bootstrap strategy to improve SVM classification ratio (case 16x16 faces)*

BioID database 19x19 - SVM									
Bootstrap				***Training Samples***		***Correct classification***			
#	False classified samples repetition	# False Positive		Positive	Negative	1st Stage Classification Ratio		2nd Stage (Final) Classification Ratio	
		1st Stage	2nd Stage			Faces (%)	Non faces (%)	Faces (%)	Non faces (%)
before	-	357	10	6650	6605	94.40%	89.216%	94.40%	99.493%
1	5	124	0	6650	8390	76.10%	97.672%	75.65%	99.915%
2	5	50	0	6650	9010	64.60%	98.657%	64.20%	99.932%
3	5	28	0	6650	9260	56.55%	98.977%	56.15%	99.937%
4	5	14	0	6650	9400	48.80%	99.216%	48.45%	99.950%
5	5	7	0	6650	9470	43.30%	99.377%	43.00%	99.965%

Table 39. *Bootstrap strategy to improve SVM classification ratio (case 19x19 faces)*

III.1.5. PCA & SVM

The following tables presents the classification result using *PCA & SVM* for the case of using 14 and 56 eigenvalues (1st and 2nd stage) and the case of using 25 and 79 eigenvalues. Each row contains a bootstrap iteration with the following information (from left to right):

- Current bootstrap iteration.
- Number of repetition of the false classified samples reintroduced in the training set.
- The number of non faces training samples incorrectly classified.
- Number of positive and negative training samples.
- Percentage of faces and non faces correctly classified.

GTAV database 16x16 - PCA (14_56) + SVM									
Bootstrap				***Training Samples***		***Correct classification***			
#	False classified samples repetition	# False Positive		Positive	Negative	1st Stage Classification Ratio		2nd Stage (Final) Classification Ratio	
		1st Stage	2nd Stage			Faces (%)	Non faces (%)	Faces (%)	Non faces (%)
before	-	958	5	8171	6605	94.35%	81.333%	94.30%	99.097%
1	5	155	0	8171	11395	66.05%	95.269%	66.00%	99.748%
2	5	100	0	8171	12170	61.80%	96.767%	61.75%	99.824%
3	5	69	0	8171	12670	57.65%	97.491%	57.65%	99.857%
4	5	55	0	8171	13015	54.30%	97.965%	54.30%	99.890%
5	10	34	0	8171	13565	49.00%	98.582%	49.00%	99.924%

Table 40. *Bootstrap strategy to improve PCA(14_56)+SVM classification ratio (case 16x16 faces)*

GTAV database 16x16 - PCA (25_79) + SVM									
Bootstrap				***Training Samples***		***Correct classification***			
#	False classified samples repetition	# False Positive		Positive	Negative	1st Stage Classification Ratio		2nd Stage (Final) Classification Ratio	
		1st Stage	2nd Stage			Faces (%)	Non faces (%)	Faces (%)	Non faces (%)
before	-	893	0	8171	6605	95.65%	83.030%	95.65%	99.301%
1	5	155	0	8171	11070	69.25%	95.710%	69.25%	99.806%
2	5	104	0	8171	11845	63.75%	97.117%	63.75%	99.854%
3	5	61	0	8171	12365	59.55%	97.883%	59.55%	99.899%
4	5	48	0	8171	12670	57.10%	98.154%	57.10%	99.918%
5	10	34	0	8171	13150	53.55%	98.448%	53.55%	99.934%

Table 41. *Bootstrap strategy to improve PCA(25_79)+SVM classification ratio (case 16x16 faces)*

IV. Face Recognition Result

This section contains some detailed information that can help to understand face recognition experimental results.

IV.1.1. Chi Square Dissimilarly Metric

In experimental results chapter, in section *7.3.1*, results table show summarized information, given the global *ID recognition rate* for each experiment. Following tables contains more detailed information for each individual ID.

- ***Histogram equalization*** versus ***Mask*** using ***no Block Weight***

		Test 1		Test 2		Test 3		Test 4	
Equalized Histogram		x		x		✓		✓	
Mask		x		✓		x		✓	
Blocks Weight		x		x		x		x	
Number ID Samples	**Type Model**	**1 Img**	**Mean**	**1 Img**	**Mean**	**1 Img**	**Mean**	**1 Img**	**Mean**
	ID#	**ID Recognition Rate %**							
216	ID1	55.09%	95.37%	54.63%	96.30%	55.09%	95.37%	53.70%	96.30%
120	ID2	70.00%	100.00%	60.83%	100.00%	70.83%	100.00%	60.00%	100.00%
194	ID3	45.36%	98.97%	42.27%	98.97%	47.42%	98.97%	43.30%	98.97%
80	ID4	63.75%	100.00%	62.50%	100.00%	63.75%	100.00%	62.50%	100.00%
198	ID5	40.40%	100.00%	37.88%	100.00%	39.90%	100.00%	37.37%	100.00%
4	ID6	100.00%	100.00%	100.00%	100.00%	100.00%	100.00%	100.00%	100.00%
118	ID7	27.12%	100.00%	27.12%	100.00%	27.12%	100.00%	27.12%	100.00%
156	ID8	71.15%	98.72%	71.79%	91.67%	71.79%	96.15%	71.79%	91.67%
176	ID9	28.98%	84.09%	30.68%	83.52%	29.55%	84.09%	30.68%	82.95%
176	ID10	96.02%	100.00%	92.61%	100.00%	97.73%	100.00%	93.18%	100.00%
122	ID11	49.18%	100.00%	49.18%	100.00%	49.18%	100.00%	49.18%	100.00%
142	ID12	44.37%	98.59%	45.77%	98.59%	44.37%	98.59%	45.07%	98.59%
212	ID13	44.81%	95.28%	41.04%	93.40%	44.34%	95.28%	41.51%	93.87%
298	ID14	76.85%	100.00%	69.13%	100.00%	77.85%	100.00%	71.14%	100.00%
188	ID15	37.23%	100.00%	35.11%	100.00%	37.23%	100.00%	34.57%	100.00%
100	ID16	96.00%	100.00%	99.00%	100.00%	96.00%	100.00%	99.00%	100.00%
102	ID17	58.82%	100.00%	57.84%	100.00%	58.82%	100.00%	57.84%	100.00%
70	ID18	44.29%	85.71%	40.00%	80.00%	42.86%	85.71%	38.57%	81.43%
80	ID19	50.00%	100.00%	50.00%	100.00%	51.25%	100.00%	50.00%	100.00%
12	ID20	50.00%	100.00%	58.33%	100.00%	50.00%	100.00%	58.33%	100.00%
92	ID21	100.00%	100.00%	98.91%	100.00%	100.00%	100.00%	98.91%	100.00%
102	ID22	50.00%	100.00%	54.90%	100.00%	50.98%	100.00%	52.94%	100.00%
50	ID23	94.00%	100.00%	100.00%	100.00%	98.00%	100.00%	100.00%	100.00%
		57.48%	**97.87%**	**55.75%**	**97.27%**	**57.95%**	**97.74%**	**55.78%**	**97.31%**
		77.67%		76.51%		**77.84%**		76.54%	

Table 42. *ID recognition rate (%) for each ID. Histogram equalization versus Mask*

❖ ***Histogram equalization*** versus ***Mask*** using ***Block Weight (1)***

		Test 5		Test 6		Test 7	
Equalized Histogram		x		✓		✓	
Mask		x		x		✓	
Blocks Weight		✓(1)		✓(1)		✓(1)	
Number ID Samples	**Type Model**	**1 Img**	**Mean**	**1 Img**	**Mean**	**1 Img**	**Mean**
	ID#	**ID Recognition Rate %**					
216	ID1	59.72%	97.22%	61.11%	97.22%	62.04%	96.30%
120	ID2	76.67%	100.00%	76.67%	100.00%	76.67%	100.00%
194	ID3	30.93%	100.00%	30.93%	100.00%	29.38%	100.00%
80	ID4	81.25%	100.00%	82.50%	100.00%	82.50%	100.00%
198	ID5	46.46%	100.00%	45.96%	100.00%	47.47%	100.00%
4	ID6	100.00%	100.00%	100.00%	100.00%	100.00%	100.00%
118	ID7	28.81%	100.00%	27.97%	100.00%	25.42%	100.00%
156	ID8	83.33%	96.15%	83.33%	96.15%	83.33%	93.59%
176	ID9	43.18%	89.77%	43.75%	89.77%	42.61%	92.05%
176	ID10	97.16%	100.00%	98.30%	100.00%	98.30%	100.00%
122	ID11	67.21%	100.00%	67.21%	100.00%	68.03%	100.00%
142	ID12	48.59%	98.59%	48.59%	98.59%	47.18%	98.59%
212	ID13	54.72%	97.17%	53.77%	98.11%	50.94%	94.81%
298	ID14	77.18%	100.00%	79.19%	100.00%	76.85%	100.00%
188	ID15	45.74%	98.94%	45.74%	100.00%	45.21%	100.00%
100	ID16	93.00%	100.00%	92.00%	100.00%	89.00%	100.00%
102	ID17	60.78%	100.00%	60.78%	100.00%	60.78%	100.00%
70	ID18	38.57%	97.14%	38.57%	97.14%	37.14%	97.14%
80	ID19	53.75%	100.00%	53.75%	100.00%	53.75%	100.00%
12	ID20	83.33%	100.00%	83.33%	100.00%	83.33%	100.00%
92	ID21	98.91%	100.00%	98.91%	100.00%	98.91%	100.00%
102	ID22	74.51%	100.00%	73.53%	100.00%	71.57%	100.00%
50	ID23	100.00%	100.00%	100.00%	100.00%	100.00%	100.00%
		62.76%	**98.60%**	**63.00%**	**98.74%**	**62.20%**	**98.44%**
		80.68%		**80.87%**		80.32%	

Table 43. *ID recognition rate (%) for each ID. Histogram equalization vs Mask using Block Weight (1)*

❖ ***Histogram equalization*** versus ***Mask*** using ***Block Weight (2)***

		Test 8		Test 9		Test 10	
Equalized Histogram		x		✓		✓	
Mask		x		x		✓	
Blocks Weight		✓(2)		✓(2)		✓(2)	
Number ID Samples	**Type Model**	**1 Img**	**Mean**	**1 Img**	**Mean**	**1 Img**	**Mean**
	ID#	**ID Recognition Rate %**					
216	ID1	57.87%	97.22%	58.33%	97.22%	58.33%	97.22%
120	ID2	75.83%	100.00%	72.50%	100.00%	72.50%	100.00%
194	ID3	28.87%	97.94%	29.90%	97.94%	29.90%	97.94%
80	ID4	70.00%	100.00%	73.75%	100.00%	73.75%	100.00%
198	ID5	43.94%	97.98%	43.43%	97.98%	43.43%	97.98%
4	ID6	100.00%	100.00%	100.00%	100.00%	100.00%	100.00%
118	ID7	29.66%	98.31%	30.51%	98.31%	30.51%	98.31%
156	ID8	84.62%	80.77%	83.97%	80.77%	83.97%	80.77%
176	ID9	47.16%	90.91%	47.16%	88.64%	47.16%	88.64%
176	ID10	97.73%	100.00%	98.86%	100.00%	98.86%	100.00%
122	ID11	74.59%	100.00%	72.13%	100.00%	72.13%	100.00%
142	ID12	51.41%	98.59%	52.11%	98.59%	52.11%	98.59%
212	ID13	53.77%	95.28%	53.77%	95.28%	53.77%	95.28%
298	ID14	72.82%	100.00%	76.17%	100.00%	76.17%	100.00%
188	ID15	41.49%	98.94%	40.96%	98.94%	40.96%	98.94%
100	ID16	73.00%	100.00%	71.00%	100.00%	71.00%	100.00%
102	ID17	60.78%	100.00%	60.78%	100.00%	60.78%	100.00%
70	ID18	35.71%	94.29%	35.71%	97.14%	35.71%	97.14%
80	ID19	53.75%	100.00%	55.00%	100.00%	55.00%	100.00%
12	ID20	75.00%	100.00%	75.00%	100.00%	75.00%	100.00%
92	ID21	98.91%	100.00%	98.91%	100.00%	98.91%	100.00%
102	ID22	84.31%	100.00%	87.25%	100.00%	87.25%	100.00%
50	ID23	100.00%	100.00%	100.00%	100.00%	100.00%	100.00%
		61.60%	**97.34%**	**62.00%**	**97.27%**	**62.00%**	**97.27%**
		79.47%		**79.63%**		79.63%	

Table 44. *ID recognition rate (%) for each ID. Histogram equalization vs Mask using Block Weight (2)*

V. *OpenCV* Functions Reference

***OpenCV* Library 1.0**, *Intel® Open Source Computer Vision* Library (see [32][33]) is a collection of *C* functions and a few *C++* classes that implement many popular Image Processing and Computer Vision algorithms.

Following section describes the most important OpenCV functions used in this research.

Principal Component Analysis

PCA algorithm is already implemented in the ***CxCore*** library of ***OpenCV*** and following functions are the ones needed to perform *Principal Component Analysis*:

- ***cvCalcPCA***: this function performs *Principal Component Analysis* of a given vector set. First, *cvCalcCovarMatrix* is used to compute covariation matrix and its eigenvalues and eigenvectors. The returned values are:
  - Mean (average) vector.
  - Output eigenvalues of covariation matrix.
  - Output eigenvectors of covariation matrix (principal components).

- ***cvProjectPCA***: this function projects input vectors to the specified subspace represented by the orthonormal basis (eigenvectors). First of all, average vector is subtracted from the input vectors. The returned value is:
  - Output matrix of decomposition coefficients.

- ***cvBackProjectPCA***: this function reconstructs the original vectors from the projection coefficients. It is used only in case of using only faces class. The returned value is:
  - The output matrix of reconstructed vectors.

Support Vector Machine

The implementation of *SVM* is available in the ***OpenCV***'s ***Machine Learning Library*** (MLL), a set of classes and functions for statistical classification, regression and clustering of data.

Due to the fact that it is an open source library, some modifications have been made in order to get the score of the classification and not only the result face/non-face.

SVM parameters (*CvSVMParams*) definition:

- **svm_type:** Type of SVM, one of the following:

  CvSVM::C_SVC - *n*-class classification ($n \geq 2$), allows imperfect separation of classes with penalty multiplier C for outliers.
  CvSVM::NU_SVC - *n*-class classification with possible imperfect separation. Parameter *nu* is used instead of *C*. *nu* is in the range 0 to 1 and the larger the value, the smoother the decision boundary.
  CvSVM::ONE_CLASS - one-class SVM. All the training data are from the same class, SVM builds a boundary that separates the class from the rest of the feature space.

CvSVM::EPS_SVR - regression. The distance between feature vectors from the training set and the fitting hyperplane must be less than *p*. For outliers the penalty multiplier *C* is used.
CvSVM::NU_SVR - regression. *nu* is used instead of *p*.

- **kernel_type:** The kernel type, one of the following:

  CvSVM::LINEAR - no mapping is done, linear discrimination (or regression) is done in the original feature space. It is the fastest option:
  $$d(x,y) = x \bullet y == (x,y) \quad (1)$$
  CvSVM::POLY - polynomial kernel:
  $$d(x,y) = (gamma*(x \bullet y)+coef0)^{degree} \quad (2)$$
  CvSVM::RBF - radial-basis-function kernel; a good choice in most cases:
  $$d(x,y) = exp(-gamma*|x-y|^2) \quad (3)$$
  CvSVM::SIGMOID - sigmoid function is used as a kernel:
  $$d(x,y) = tanh(gamma*(x \bullet y)+coef0) \quad (4)$$

- **degree, gamma, coef0:** Parameters of the kernel, used in the formulas above.

- **C, nu, p:** Parameters in the generalized SVM optimization problem.

- **class_weights:** Optional weights, assigned to particular classes. They are multiplied by *C* and thus affect the misclassification penalty for different classes. The larger the weight is, the larger the penalty on misclassification of data from the corresponding class is.

- **term_crit:** Termination procedure for iterative SVM training procedure, which solves a partial case of constrained quadratic optimization problem. It stops either after a certain number of iterations (*term_crit.num_iter*) or when the parameters change too little (no more than *term_crit.epsilon*) from iteration to iteration.

In experimental results (see section *7.2.3*), following SVM parameters are used:

svm_type	CvSVM::C_SVC
kernel_type	CvSVM::POLY
degree	2
gamma	1
coef0	1
C	5
term_crit	only *term_crit.epsilon* with value 0.000000001

Table 45. *SVM parameters using OpenCV Machine Learning Library*

The epsilon termination criterion is empirically found as a trade off between computation time and optimal results.

Skin Segmentation

Skin Segmentation procedure is implemented by means of *OpenCV* library image processing algorithms.

- **Image preprocessing (training / test)**

In image preprocessing step, the original image is smoothed to avoid compression noise and other artifacts. Therefore, a 3x3 simple blur filter from *OpenCV Library* is used, consisting of the sum over a pixel 3×3 neighborhood with subsequent scaling by 1/(3x3).

```
// image PRE processing
cvSmooth( ipl_Orig_RGB_Image, ipl_RGB_Image, CV_BLUR, 3, 3, 0, 0 );
```

- **LUV conversion (training / test)**

A function to perform LUV conversion and another one to split the 3 components are also available in *OpenCV* library:

```
// calculate Luv
cvCvtColor( ipl_RGB_Image, ipl_Luv_Image, CV_RGB2Luv );
// split
cvSplit( ipl_Luv_Image, ipl_L_Image, ipl_u_Image, ipl_v_Image, NULL);
```

The function *cvCvtColor* converts input image from one color space to another. And the parameter CV_RGB2Luv indicates that the transformation selected is from RGB to CIE LUV.

- **Skin model definition (training)**

After color conversion, for each pixel and taking into account a given neighborhood, *u* and *v* components mean value are calculated by mean of the following *OpenCV Library* function:

```
// mean value u & v
cvAvgSdv( ipl_u_Image, &u_mean, &u_std_dev, NULL );
cvAvgSdv( ipl_v_Image, &v_mean, &v_std_dev, NULL );
```

The function *cvAvgSdv* calculates the average value and standard deviation of array elements.

- **Skin segmentation (test)**

Given an image to be segmented and after preprocessing and converting to LUV color space, *u* and *v* components mean values are calculated as in training stage. Then, for each pixel and taking into account a *SkinDetBoxSize* region (see equation (37)), the mean value is calculated using above *cvAvgSdv* function.

Then, skin model thresholds are applied to determinate if the box region is skin or not resulting in a skin mask, where some morphological operations need to be applied to eliminate isolated pixels after each down-sampling step:

1st) ***Closing***: using a 3x5 pixels ellipse structuring element.

```
// Create an elliptic structuring element
nSize=3;
IplConvKernel* structElem1 =
cvCreateStructuringElementEx(nSize+2,                // columns
                             nSize,                  // rows
                             floor((nSize+2)/2.0),   // anchor_x
                             floor(nSize/2.0),       // anchor_y
                             CV_SHAPE_ELLIPSE,       // shape
                             NULL); // CV_SHAPE_CUSTOM values
```

```
// Perform advanced morphological transformations - CLOSING
cvMorphologyEx(   iplSkinMask,      // source
                  iplSkinMask,      // destination
                  NULL,             // temporary image (not required)
                  structElem2,      // structuring element
                  CV_MOP_ CLOSE,    // morphological operation closing
                  1);               // number of iterations
```

2nd) ***Opening***: using a 11 pixels radius circle structuring element.

```
// Create a circular structuring element
nSize=11;
IplConvKernel* structElem2 =
cvCreateStructuringElementEx( nSize,                  // columns
                              nSize,                  // rows
                              floor(nSize/2.0),       // anchor_x
                              floor(nSize/2.0),       // anchor_y
                              CV_SHAPE_ELLIPSE,       // shape
                              NULL); // CV_SHAPE_CUSTOM values

// Perform advanced morphological transformations - OPENING
cvMorphologyEx(   iplSkinMask,      // source
                  iplSkinMask,      // destination
                  NULL,             // temporary image (not required)
                  structElem2,      // structuring element
                  CV_MOP_OPEN,      // morphological operation opening
                  1);               // number of iterations
```

Acronyms & Abbreviations List

ASA	American Standards Association
DB	Database
CIE	International Commission on Illumination (abbreviated French name)
CMU	Carnegie Mellon University
DARPA	Defense Advanced Research Products Agency
EPFL	Ecole Polytechnique Fédérale de Lausanne
FERET	Face Recognition Technology
FGNET	Face and Gesture Recognition Working Group
GIF	Graphics Interchange Format
GTAV	Audio Visual Technologies Group (abbreviated Catalan name)
GUI	Graphical User Interface
HSV	color space (Hue, Saturation, Value)
JPEG	Joint Photographic Experts Group
KLT	Karhunen-Loéve Transform
LBP	Local Binary Patterns
MATLAB	Matrix Laboratory (Mathworks, Inc.)
MIT	Massachusetts Institute of Technology
MLL	Machine Learning Library
OpenCV	Open Source Computer Vision
RelDiffNorm	Relative Difference Normalized
PBM	Portable Bit Map
PCA	Principal Component Analysis
PGM	Portable Gray Map
RGB	color space (Red, Green, Blue)
ROI	Region Of Interest
SVM	Support Vector Machine
UCS	Uniform Chromaticity Scale
UPC	Universitat Politècnica de Catalunya

Bibliography

Publications:

[1] T.Ahonen, A.Hadid & M.Pietikäinen, *Face Description with Local Binary Patterns: Application to Face Recognition.* Draft, 5th June 2006.

[2] A.Hadid, M.Heikkilä, T.Ahonen & M.Pietikäinen. *A Novel Approach to Access Control based on Face Recognition*. Machine Vision Group, InfoTech Oulu and Department of Electrical and Information Engineering. University of Oulu, Finland.

[3] T.Ahonen, M.Pietikäinen, A.Hadid & T.Mäenpaä. *Face Recognition Based on the Appearance of Local Regions*. Machine Vision Group, InfoTech. University of Oulu, Finland. 2004 IEEE.

[4] T.Ahonen, A.Hadid & M.Pietikäinen. *Face Recognition with Local Binary Patterns*. Machine Vision Group, InfoTech. University of Oulu, Finland. T.Pajdla and J.Matas (Eds): ECCV 2004, LNCS 3021, pp.469-481, 2004. Spring-Verlag Berlin Heidelberg 2004.

[5] A.Hadid & M.Pietikäinen. *A Hybrid Approach to Face Detection under Unconstrained Environments*. Machine Vision Group, Dept. of Electrical and Information Engineering. University of Oulu, Finland.

[6] A.Hadid, M.Pietikäinen & T.Ahonen. *A Discriminative Feature Space for Detecting and Recognizing Faces*. Machine Vision Group, InfoTech Oulu and Dept. of Electrical and Information Engineering. University of Oulu, Finland.

[7] T.Ojala, M.Pietikäinen & T.Mäenpaä. *Multiresolution gray-scale and rotation invariant texture classification with Local Binary Patterns*. IEEE Transactions on Pattern Analysis and Machine Intelligence, vol. 24, no. 7, pp. 971-987, July 2002.

[8] G.Heusch, Y.Rodriguez & S.Marcel. *Local Binary Patterns as an Image Preprocessing for Face Authentication*. IDIAP Research Institute, Martigny, Switzerland. Ecole Polytechnique Fédérale de Lausanne (EPFL), Switzerland.

[9] Y.Rodriguez & S.Marcel. *Face Authentication using Adapted Local Binary Pattern Histograms*. IDIAP Research Institute, Martigny, Switzerland.

[10] S.Marcel, Y.Rodriguez & G.Heusch. *On the Recent Use of Local Binary Patterns for Face Authentication*. IDIAP Research Institute, Martigny, Switzerland. International Journal of Image and Video Processing, Special Issue on Facial Image Processing. May 2007.

[11] E.Osuna, R.Freund & F.Girosi. *Training Support Vector Machine: an Application to Face Detection*. In Proc. Computer Vision and Pattern Recognition, pages 130-136, June 1997.

[12] Josep R. Casas, F. Marqués & P.Salembier. *Apunts de l'assignatura: Processament d'Imatge*. Image Processing Group, Signal Theory & Comm. Dept, UPC. Barcelona, Fall 2004.

[13] Lindsay I Smith. *A tutorial on Principal Components Analysis*. February 26, 2002.

[14] K.-K. Sung, *Learning and Example Selection for Object and Pattern Detection*, PhD thesis, MIT AI Lab, Jan. 1996. Available as AI Technical Report 1572.

[15] G.Yang & T.S.Huang. *Human Face Detection in Complex Background*, Pattern Recognition, vol. 27, no. 1, pp. 53-63, 1994.

[16] K.C.Yow & R.Cipolla. *Feature-based human face detection*, Image and Vision Computing, vol. 15, no. 9, pp. 713 – 735, 1997.

[17] A.L.Yuille, P.W.Hallinan & D.S.Cohen. *Feature extraction from faces using deformable templates*, International Journal of Computer Vision vol. 8, no. 2, 99–111, 1992.

[18] P.Juell & R.Marsh. *A hierarchical neural network for human face detection*, Pattern Recog. 29, 1996, 781–787.

[19] E.Viennet & F.Fogelman Soulié. *Connectionist methods for human face processing*, *in Face Recognition: From Theory to Application,* Springer-Verlag, Berlin/New York, 1998.

[20] M.Schulze, K.Scheffler, & K.W.Omlin. *Recognizing Facial Actions with Support Vector Machines*, In Proc. PRASA, pp. 93-96, 2002.

[21] L.R.Rabiner. *A tutorial on Hidden Markov Models and Selected Applications in Speech Recognition*, Proceedings IEEE, vol. 77, no. 2, Feb 1989.

[22] M.A.Turk & A.P.Pentland. *Face recognition using eigenfaces*, Proceedings of the IEEE Computer Society Conf. on Computer Vision and Pattern Recognition, pp. 586-591, Maui, Hawaii 1991.

[23] B.Zarit, B.J.Super & F.Quek. *Comparison of five color models in skin pixel classification*, ICCV'99 Int'l Workshop on Recognition, Analysis and Tracking of Faces and Gestures in Real-Time Systems, pp. 58–63, Corfu, Greece, September 1999.

[24] P.Viola & M.Jones. *Rapid Object Detection using a Boosted Cascade of Simple Features,* Computer Vision and Pattern Recognition, 2001.

[25] C.H.Lee, J.S.Kim & K.H.Park. *Automatic human face location in a complex background*, Pattern Recognition Letters, 29, 1877–1889, 1996.

[26] R.J.Qian, M.I.Sezan & K.E.Matthews. *A Robust Real-Time Face Tracking Algorithm*, ICIP (1) 1998: 131-135.

[27] M.Lades, J.C.Vorbruggen, J.Buhmann, J.Lange, C.von der Malsburg, R.P.Wurtz & W.Konen. *Distortion Invariant Object Recognition in the Dynamic Link Architecture* IEEE Transactions on Computers archive Volume 42 , Issue 3 Pages: 300 – 311. 1993.

[28] P.Sinha, B.Balas, Y.Ostrovsky, R.Russell. *Face recognition by humans: 20 results all computer vision researchers should know about*. Proceedings of the IEEE, 94, 1948–1962. 2006.

[29] M.S.Keil. *"I Look in Your Eyes, Honey": Internal Face Features Induce Spatial Frequency Preference for Human Face Processing*. PLoS Computational Biology 5(3): e1000329. doi:10.1371/journal.pcbi.1000329. 2009

Books:

[30] Richard O. Duda, Peter E.Hart, David Stork. *Pattern Classification*, 2nd Edition Wiley.

[31] Joan Cabestany, Sergio Bermejo. *Sistemas conexionistas para el tratamiento de la información*, Edicions UPC, Barcelona 2003.

Reference Manuals:

[32] *Intel® Open Source Computer Vision Library. CXCORE, CV, Machine Learning and HighGUI Reference Manuals*, Intel Corporation. PDF Files (2006).

Web Pages:

[33] http://opencvlibrary.sourceforge.net: OpenCV Wiki-pages

[34] http://tech.groups.yahoo.com/group/OpenCV/: OpenCV Open Source Computer Vision Library Community

[35] http://citeseer.ist.psu.edu/burges98tutorial.html: A Tutorial on Support Vector Machines for Pattern Recognition - Burges (ResearchIndex)

[36] http://www.ee.oulu.fi/mvg/page/publications: University of Oulu - Machine Vision Group

[37] http://www.ee.oulu.fi/research/imag/texture/lbp/about/LBP%20Methodology.pdf: University of Oulu - LBP methodology

[38] http://www.humanscan.de/support/downloads/facedb.php : The *BioID* Face Database

[39] http://www.ysbl.york.ac.uk/~garib/mres_course/2005/Lecture5.ppt: Resampling techniques.

[40] http://www.cs.cmu.edu/~awm/tutorials: Support Vector Machines tutorial by Andrew W. Moore.

[41] http://www.svms.org/: Support Vector Machines (SVMs) web site.

[42] http://gps-tsc.upc.es/GTAV/: *Audio Visual Technologies Group* of the *Signal Theory and Communications Department* of the *Technical University of Catalonia*.

[43] http://gps-tsc.upc.es/GTAV/ResearchAreas/UPCFaceDatabase/GTAVFaceDatabase.htm: *Audio Visual Technologies Group* Face Database.

[44] http://www.ee.oulu.fi/mvg/page/lbp_matlab: University of Oulu - New LBP Matlab implementation